PACIFIC EARTHQUAKE ENGINEERING
RESEARCH CENTER

Seismic Evaluation of 550 kV Porcelain Transformer Bearings

Amir S. Gilani
Andrew S. Whittaker
Gregory L. Fenves
Eric Fujisaki

PEER 1999/05
OCTOBER 1999

PACIFIC EARTHQUAKE ENGINEERING
RESEARCH CENTER

Seismic Evaluation of 550 kV Porcelain Transformer Bearings

Amir S. Gilani
Andrew S. Whittaker
Gregory L. Fenves
Eric Fujisaki

PEER 1999/05
OCTOBER 1999

Seismic Evaluation of 550 kV Porcelain Transformer Bushings

Amir S. Gilani
University of California, Berkeley

Andrew S. Whittaker
University of California, Berkeley

Gregory L. Fenves
University of California, Berkeley

Eric Fujisaki
Pacific Gas & Electric Company

This research was sponsored by the Pacific Gas & Electric Company and the California Energy Commission. Additional support was provided by the Pacific Earthquake Engineering Research Center and the National Science Foundation.

PEER Report 1999/05
Pacific Earthquake Engineering Research Center
College of Engineering
University of California, Berkeley

October 1999

ABSTRACT

Three 550 kV porcelain transformer bushings were evaluated for their response to severe earthquake shaking. The first bushing was similar to bushings currently in service in the United States; the other two bushings were modified versions of the first bushing. The modifications to the second and third bushings were intended to enhance seismic performance and included added tiers of springs, increased preload, and stiffer gaskets. The dynamic properties, vibration frequencies, and damping ratios of the bushings were evaluated from the experimental data. Tri-directional earthquake simulator testing was undertaken to investigate the dynamic response of the bushings, to qualify one of the modified bushings for moderate earthquake shaking (per IEEE 693-1997), and to evaluate the response of the other two bushings to extreme shaking effects. For earthquake testing, the bushings were mounted at 20° to the vertical in a stiff support frame. Two sets of spectrum-compatible ground motion records, derived from motions recorded during the 1978 Tabas earthquake in Iran, were used for testing. None of the bushings met the IEEE criteria for Moderate Level qualification. However, the response of the modified bushings was superior to the response of the unmodified bushing.

ACKNOWLEDGMENTS

The work described in this report was funded by the Pacific Gas and Electric (PG&E) Company. This work was supported in part by the Pacific Earthquake Engineering Research Center through the Earthquake Engineering Research Centers program of the National Science Foundation under Award Number EEC-9701568. This financial support is gratefully acknowledged. The transformer bushings were supplied by ABB Power T&D Company, Inc., Components Division of Alamo, Tennessee.

The significant technical contributions of Messrs. Ed Matsuda of PG&E, Mr. Lonnie Elder of ABB, and Mr. Don Clyde of the University of California, Berkeley, made possible the work described in this report. The authors also thank Ms. Janine Hannel for editing this report.

CONTENTS

LIST OF TABLES

LIST OF FIGURES

CHAPTER 1
INTRODUCTION

1.1 Overview

Recent major earthquakes in the United States (Northridge, 1994), Japan (Kobe, 1995) and Turkey (Izmit, 1999) have demonstrated that the reliability of a power transmission and distribution (T&D) system in a region exposed to earthquake shaking is dependent upon the seismic response of its individual components. Porcelain transformer bushings, which are insulated conductors providing electrical connection between a high-voltage line and an oil-filled transformer, have been vulnerable to moderate and severe earthquake shaking (EERI, 1995; Shinozuka, 1995). Bushings are typically mounted on the top of a transformer (see Figure 1-1) using a bolted flange connection.

The research described in this report addresses the vulnerability of high-voltage 550 kV porcelain transformer bushings during moderate earthquake shaking. This work was made possible by a partnership between the Pacific Earthquake Engineering Research (PEER) Center and Pacific Gas & Electric (PG&E) that was formed to investigate the seismic reliability of utility lifelines.

This report documents the seismic response of three 550 kV transformer bushings manufactured by Asea Brown Boveri (ABB) of Alamo, Tennessee. The key objectives of the studies described in the following chapters were to

1. Develop earthquake ground motion records suitable for the seismic evaluation, qualification, and fragility testing of 550 kV bushings.

2. Test three 550 kV bushings on the earthquake simulator at the Pacific Earthquake Engineering Research (PEER) Center using levels of earthquake shaking consistent with those adopted for seismic qualification and fragility testing of electrical equipment.

3. Analyze the data acquired from the earthquake simulator tests to serve four purposes: (a) determine the dynamic properties of the bushings, (b) evaluate the seismic response of the bushings during moderate earthquake shaking, (c) determine the failure mode of two of the bushings subjected to earthquake shaking (fragility testing), and (d) qualify the third 550 kV bushing for moderate earthquake shaking.

4. Draw conclusions about (a) the performance of porcelain transformer bushings, (b) the likely failure modes of a bushing during severe earthquake shaking, (c) the efficacy of the improvements incorporated in the design of 550 kV bushings by the manufacturer, and (d) the utility of the seismic qualification and fragility testing procedures set forth in IEEE 693-1997.

1.2 Seismic Qualification and Fragility Testing

Structural and nonstructural components that do not lend themselves to analysis are often *qualified* for use in specific applications by full-scale testing. Qualification has long been used by the Nuclear Regulatory Commission (NRC) for equipment and hardware (e.g., valves and snubbers)

in nuclear power plants, and by the Departments of Defense and Energy for military hardware. Qualification is a binary decision-making process: equipment or hardware either passes or fails.

The objective of fragility testing is to establish a relation between limiting states of response (e.g., electrical connectivity, gasket failure, and cracking of porcelain) and peak ground acceleration for a selected piece of equipment. This information is then used to develop fragility curves that plot the cumulative probability of reaching a limit state as a function of peak ground acceleration.

In California, electrical equipment is seismically qualified using a standard developed by the Institute of Electrical and Electronic Engineers (IEEE 693-1997). The IEEE standard (IEEE, 1998) entitled *IEEE 693-1997 Recommended Practices for Seismic Design of Substations* details procedures for qualification of electrical substation equipment for different seismic performance levels. The key features of the draft standard as they pertain to this report are described in Section 3.2. Additional information is presented in Appendix A.

1.3 ABB 550 kV Transformer Bushings

One Model 550X2000UW (termed the *unmodified* bushing) and two Model 550SEIS2000-1 (termed the *modified* bushings) 550 kV transformer bushings, manufactured by ABB Power T&D Company, Inc., Components Division were tested as part of the research program described in this report. Figure 1-2 is a photograph of one of the 550kV bushings installed in a mounting frame on the PEER simulator at the University of California at Berkeley.

The *unmodified* bushing is similar to those currently in service at many substations operated by a number of utilities. The modified bushings are prototypes of a new line of 550 kV bushings that incorporate three key changes to the unmodified bushing that are intended to improve seismic performance. The key changes are summarized in Table 1-1.

Table 1-1 Key differences between modified and unmodified bushings

Property	*Unmodified bushing*	*Modified bushings*
Bushing prestressing force	'Standard prestress'	1.4 times 'Standard prestress'
Post-tensioning dome springs	single-tier	multi-tier
Gasket at flange plate-to-porcelain joint	Nitrile rubber	Rubber-impregnated fiber and O-ring seal

A longitudinal section through a typical 550 kV bushing is shown in Figure 1-3. The overall length of the transformer bushing is 256.5 in. (6.5 m). The segment of the bushing above the flange plate (which protrudes above the top of the transformer as seen in Figure 1-1) is 191.5 in. (4.8 m) long and includes three porcelain insulator units (hereafter referred to as UPPER-1, UPPER-2, and UPPER-3), and a metallic dome at the top of the bushing (above porcelain unit UPPER-3). The porcelain units, the cast steel flange, and the metallic dome are separated by gaskets. The segment of the bushing below the steel flange plate includes an extension of the flange plate, one porcelain insulator, and an aluminum lower support. Annular gaskets separate these components. The flange, which is used to connect the bushing to the transformer, is a steel weldment with three lifting lugs to facilitate movement and installation of the bushing.

In cross section, the bushing has an aluminum core, a multi-layered kraft paper condenser wrapped around the core; an annular gap between the porcelain and condenser that is filled with an oil to provide electrical insulation; and a porcelain insulator. The bushing is post-tensioned along its longitudinal axis through the aluminum core. Springs in the metallic dome ensure a uniform distribution of compression around the perimeter of the porcelain units and the gaskets. The weight of the bushing is approximately 3,740 lb (16.6 kN).

The unmodified bushing (Bushing-1) and the first of the two modified bushings (Bushing-2) were designated for fragility testing. No electrical tests were planned for these bushings. ABB did not assign serial numbers to these bushings. The second modified bushing (Bushing-3) was built for seismic qualification testing and passed the requisite electrical tests before shipment to Berkeley. ABB assigned serial number *9C01352502* to this bushing.

1.4 Report Organization

This report is divided into five chapters, references, and one appendix. Following the introduction, Chapter 2 provides information on the simulator used for earthquake testing, the mounting frame designed to support the bushings during testing, and a list of the transducers used to monitor the response of the bushings. Chapter 3 describes the earthquake histories developed for qualification and fragility testing. Chapter 4 provides a summary of the key test results. Chapter 5 includes a summary of the key findings and conclusions drawn from the research project. References are listed following Chapter 5. The IEEE Recommended Practice for earthquake testing of transformer bushings is summarized in Appendix A. Raw data and video images from all earthquake tests were supplied to Pacific Gas & Electric under separate cover.

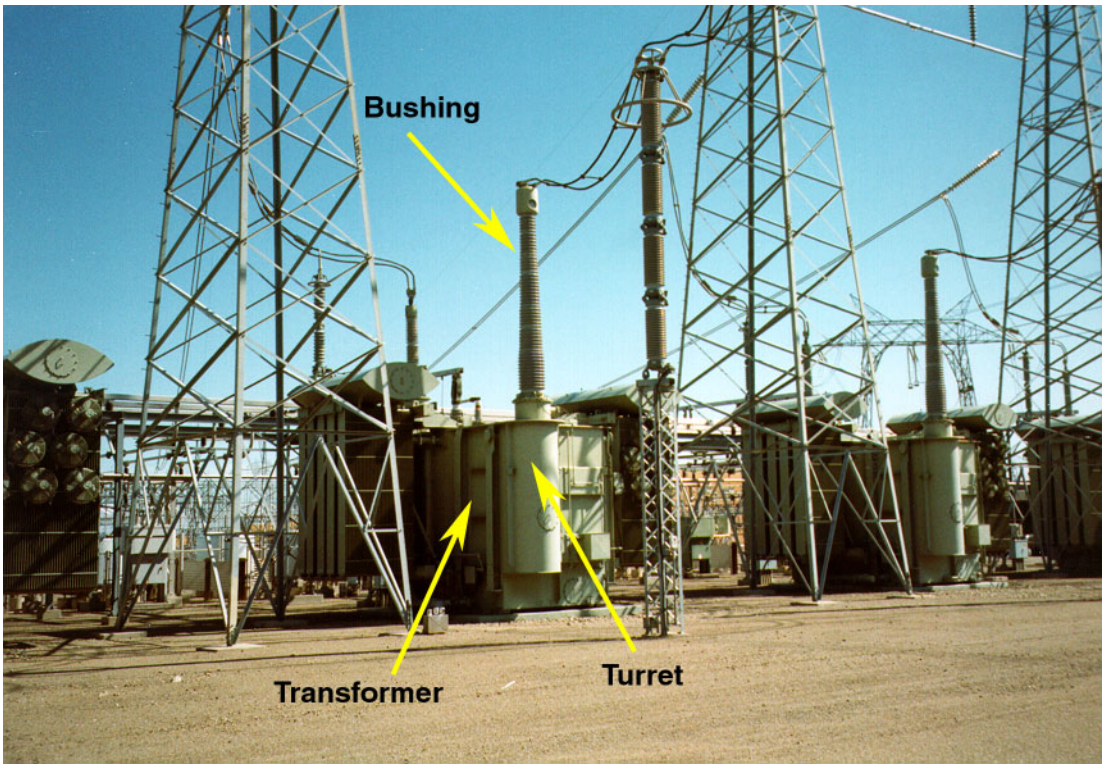

Figure 1-1 Bushing mounted on an oil-filled transformer

Figure 1-2 550 kV bushing installed in mounting frame atop the Berkeley simulator

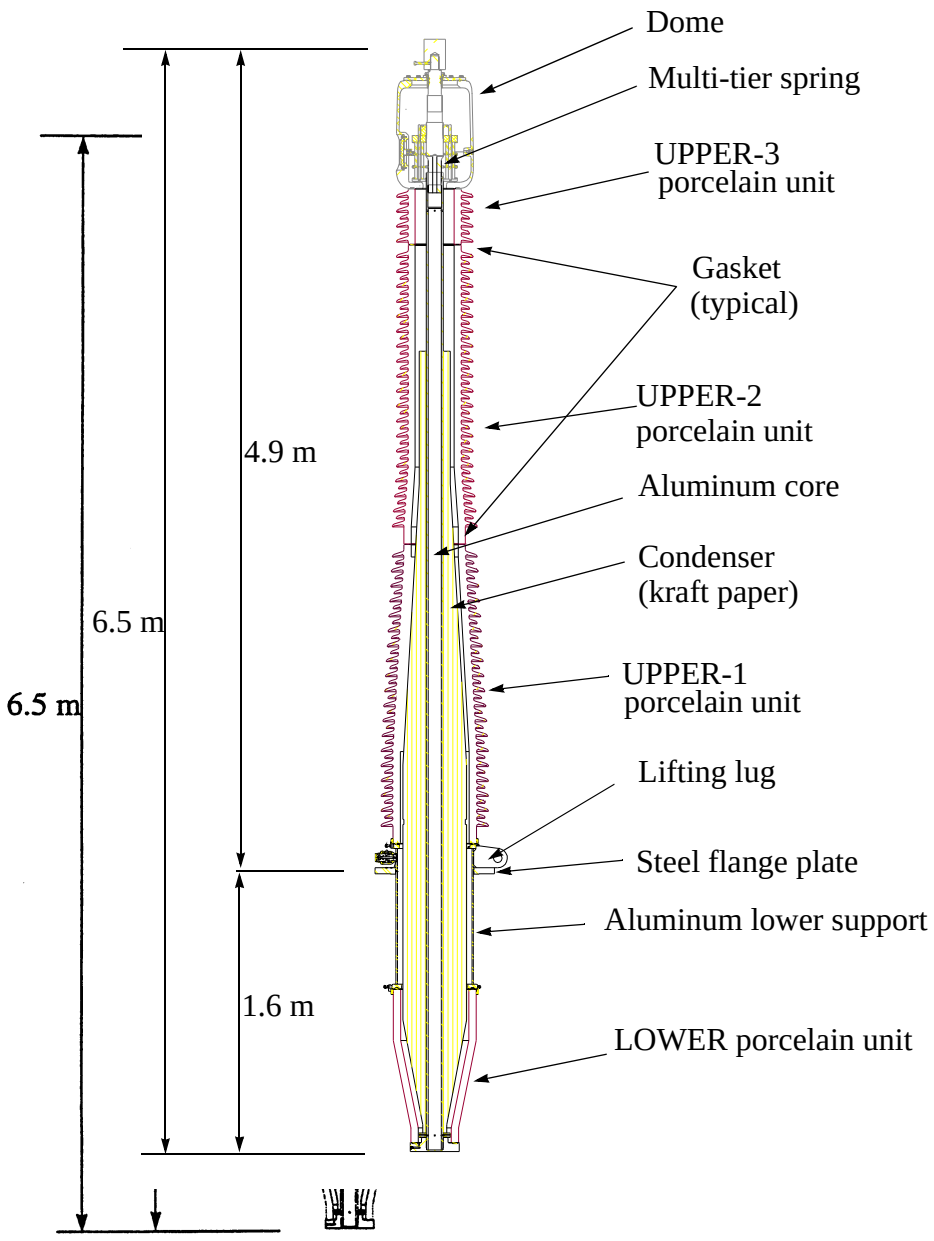

Figure 1-3 Longitudinal section through a modified 550 kV porcelain bushing

CHAPTER 2
EARTHQUAKE SIMULATOR TESTING

2.1 Introduction

Triaxial earthquake simulator testing was used to evaluate the seismic behavior of three 550 kV transformer bushings. The earthquake testing protocol for transformer bushings set forth in IEEE 693-1997 (IEEE, 1998) was adopted for this study. The following sections in this chapter describe the earthquake simulator used for testing the bushings, the *rigid* mounting frame used to support the bushings during testing, and the instrumentation scheme used to monitor the response of the bushings during earthquake testing.

2.2 Earthquake Simulator

The earthquake simulator at the Pacific Earthquake Engineering Research (PEER) Center at the University of California at Berkeley was used for the seismic evaluation and qualification studies described in this report. The simulator, also known as a shaking table, measures 20 ft by 20 ft (6.1 by 6.1 m) in plan; the maximum payload is 140 kips (623 kN). Models up to 40 ft (12.2 m) in height can be tested. The six-degree-of-freedom simulator can be programmed to reproduce any waveform (e.g., sinusoidal, white noise, earthquake history). The maximum stroke and velocity of the simulator are ±5 in. (±127 mm) and 25 in./sec (635 mm/sec), respectively.

2.3 Mounting Frame

IEEE 693-1997 states that bushings rated at 161 kV and above must be qualified using three-component earthquake-simulator testing. Because it is impractical to test bushings mounted on a transformer, IEEE specifies that bushings must be mounted on a rigid stand for earthquake testing and qualification. IEEE also recommends that a transformer bushing be tested at 20 degrees measured from the vertical because a bushing, if so tested and qualified, is assumed to be qualified for use on all transformers with angles from vertical to 20 degrees.

Figure 2-1 is a photograph of the mounting frame used for the earthquake simulator testing. The fully welded mounting frame was specifically designed to support 550 kV bushings, and was constructed of TS-5”x5”x3/8” columns, L-5”x5”x3/4” braces, and a 2-in. (51 mm) thick steel mounting plate (sloping at 20 degrees to the horizontal). The mounting frame was post-tensioned to the earthquake simulator platform using fifteen 1-in. (25 mm) diameter high-strength threaded rods. A special 1.75 in. (44 mm) adaptor plate was designed and fabricated to connect the flange plate of the 550 kV bushings to the support frame. Twelve 1-1/4 in. (32 mm) diameter high-strength bolts were used for the adaptor plate-to-mounting plate connection The flange of the bushing was joined to the adaptor plate with twelve 3/4 in. (19 mm) diameter Grade 2 steel bolts (equivalent to A307 steel) torqued to 100 ft-lb (136 N-m) per the ABB installation specification. The support frame was designed to be extremely stiff to minimize the amplification of the simulator input to the bushing. Table 2-1 reports the computed analytical modal properties of (a) the frame alone and (b) the frame including the mass of the 550 kV bushing.

Table 2-1 Modal properties of mounting frame by analysis

		Frequency (Hz)	
Mode	*Predominant direction*[1]	*Frame only*	*Frame and Bushing*
1	X	78	60
2	Y	72	58
3	Z	88	37
4	θ_z	113	107

1. See Figure 2-2 for coordinate system

2.4 Instrumentation

For seismic testing, IEEE 693-1997 states that porcelain bushings must be instrumented to record (a) maximum vertical and horizontal accelerations at the top of the bushing, at the bushing flange, and at the top of the earthquake simulator platform, (b) maximum displacement of the top of the bushing relative to the flange, and (c) maximum porcelain stresses at the base of the bushing near the flange.

The instrumentation scheme developed for the tests described in this report exceeds the IEEE requirements. Fifty-four channels of data were recorded for each test. Table 2-2 lists the channel number, instrument type, response quantity, coordinate system, and location for each transducer. Figure 2-2 presents information on the instrumentation of the earthquake simulator platform (Figure 2-2a), the bushing and the mounting frame (Figure 2-2b), and the porcelain unit immediately above the flange (UPPER-1) of the bushing (Figure 2-2c). The global (X, Y, Z) and local (*x, y, z*) coordinate systems adopted for the testing program are shown in the figure. Figure 2-3 shows the instrumentation at the base of one of the 550 kV bushings and Figure 2-4 is a photograph of the instrumentation immediately above the flange plate.

Sixteen channels (channels 3 through 18) recorded the acceleration and displacement of the earthquake simulator platform in the global coordinate system. The accelerations of the mounting frame in the local coordinate system (channels 28, 29, and 30) and the absolute displacements of the mounting frame in the global coordinate system (channels 37 and 38) were recorded. The accelerations of the bushing in the local coordinate system (channels 19 through 27) and the absolute displacements of the bushing in the global coordinate system (channels 31 through 36) were measured at the top, midheight, and bottom of the bushing. Four strain gages (channels 39 through 42) monitored the axial strains in the UPPER-1 porcelain unit. Four displacement transducers (channels 43 through 46), located immediately below the gasket, measured the radial slip of the flange plate relative to the support frame. Another four displacement transducers (channels 47 through 50), located immediately above the gasket, measured radial slip of the UPPER-1 porcelain unit relative to the support frame. The relative slip of the porcelain over the flange plate was computed using these eight transducers. Four displacement transducers (channels 51 through 54) recorded UPPER-1 displacements across the gasket, parallel to the axis of the bushing.

Table 2-2 Instrumentation for 550 kV bushing tests

Channel Number	*Transducer*[1]	*Response Quantity*	*Coordinate System and Orientation*	*Transducer Location*
1	-	date	-	-
2	-	time	-	-
3	LVDT	table displacement	global X	simulator platform
4	LVDT	table displacement	global Y	simulator platform
5	LVDT	table displacement	global X	simulator platform
6	LVDT	table displacement	global Y	simulator platform
7	LVDT	table displacement	global Z	simulator platform
8	LVDT	table displacement	global Z	simulator platform
9	LVDT	table displacement	global Z	simulator platform
10	LVDT	table displacement	global Z	simulator platform
11	A	table acceleration	global X	simulator platform
12	A	table acceleration	global X	simulator platform
13	A	table acceleration	global Y	simulator platform
14	A	table acceleration	global Y	simulator platform
15	A	table acceleration	global Z	simulator platform
16	A	table acceleration	global Z	simulator platform
17	A	table acceleration	global Z	simulator platform
18	A	table acceleration	global Z	simulator platform
19	A	bushing acceleration	local x	bottom of bushing
20	A	bushing acceleration	local y	bottom of bushing
21	A	bushing acceleration	local z	bottom of bushing
22	A	bushing acceleration	local x	midheight of bushing
23	A	bushing acceleration	local y	midheight of bushing
24	A	bushing acceleration	local z	midheight of bushing
25	A	bushing acceleration	local x	top of bushing
26	A	bushing acceleration	local y	top of bushing
27	A	bushing acceleration	local z	top of bushing
28	A	frame acceleration	local x	top of mounting frame

Table 2-2 Instrumentation for 550 kV bushing tests

Channel Number	*Transducer*[1]	*Response Quantity*	*Coordinate System and Orientation*	*Transducer Location*
29	A	frame acceleration	local y	top of mounting frame
30	A	frame acceleration	local z	top of mounting frame
31	LP	bushing displacement	global X	bottom of bushing
32	LP	bushing displacement	global Y	bottom of bushing
33	LP	bushing displacement	global X	midheight of bushing
34	LP	bushing displacement	global Y	midheight of bushing
35	LP	bushing displacement	global X	top of bushing
36	LP	bushing displacement	global Y	top of bushing
37	LP	frame displacement	global X	top of mounting frame
38	LP	frame displacement	global Y	top of mounting frame
39	SG	porcelain strain	-	UPPER-1 porcelain unit
40	SG	porcelain strain	-	UPPER-1 porcelain unit
41	SG	porcelain strain	-	UPPER-1 porcelain unit
42	SG	porcelain strain	-	UPPER-1 porcelain unit
43	DCDT	flange plate slip	relative to frame	UPPER-1 porcelain unit
44	DCDT	flange plate slip	relative to frame	UPPER-1 porcelain unit
45	DCDT	flange plate slip	relative to frame	UPPER-1 porcelain unit
46	DCDT	flange plate slip	relative to frame	UPPER-1 porcelain unit
47	DCDT	UPPER-1 slip	relative to frame	UPPER-1 porcelain unit
48	DCDT	UPPER-1 slip	relative to frame	UPPER-1 porcelain unit
49	DCDT	UPPER-1 slip	relative to frame	UPPER-1 porcelain unit
50	DCDT	UPPER-1 slip	relative to frame	UPPER-1 porcelain unit
51	DCDT	longitudinal uplift	relative to frame	UPPER-1 porcelain unit
52	DCDT	longitudinal uplift	relative to frame	UPPER-1 porcelain unit
53	DCDT	longitudinal uplift	relative to frame	UPPER-1 porcelain unit
54	DCDT	longitudinal uplift	relative to frame	UPPER-1 porcelain unit

1. A = accelerometer; LVDT = displacement transducer; LP = linear potentiometer; SG = strain gage; DCDT = displacement transducer

Figure 2-1 550 kV bushing mounting frame

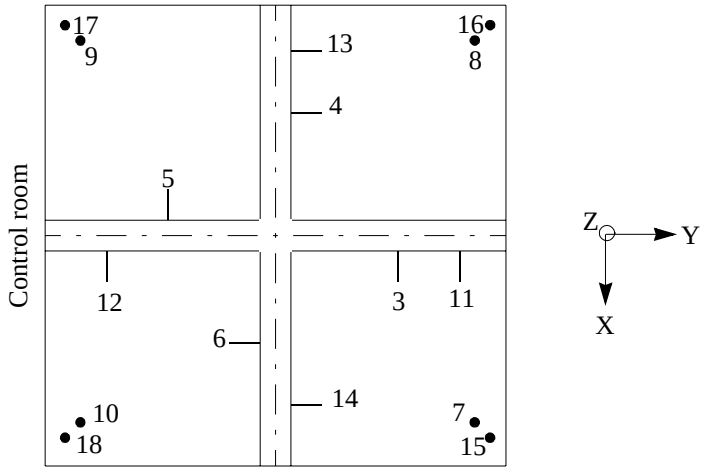

(a) Earthquake simulator (view from beneath)

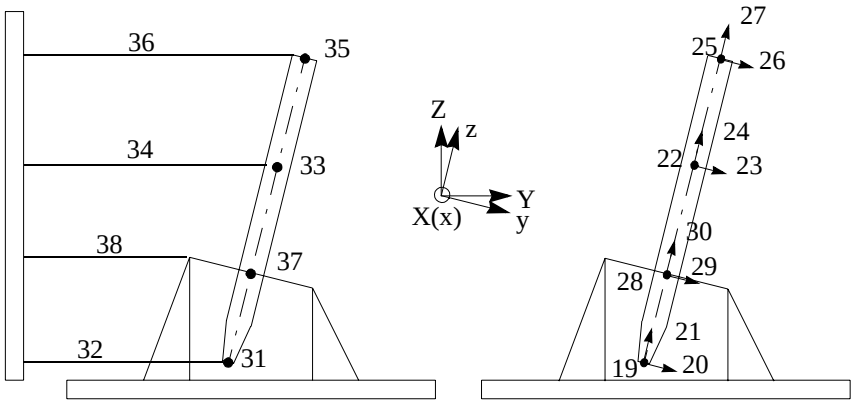

(b) Bushing and mounting frame

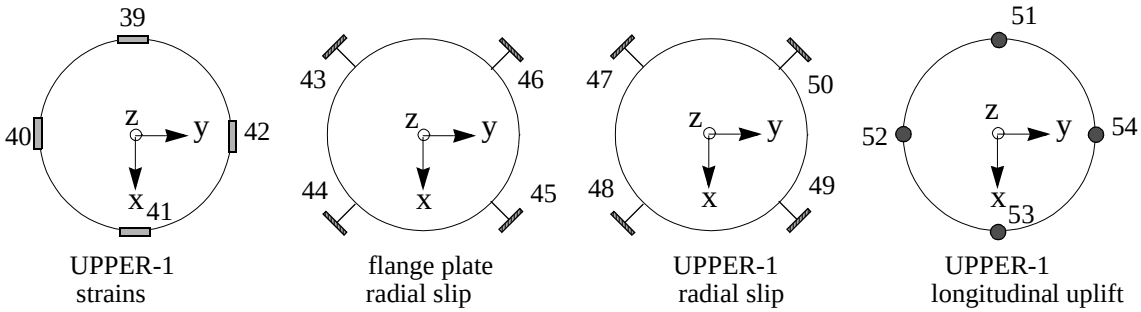

(c) UPPER-1 porcelain unit and flange plate

Figure 2-2 Instrumentation for 550 kV bushings

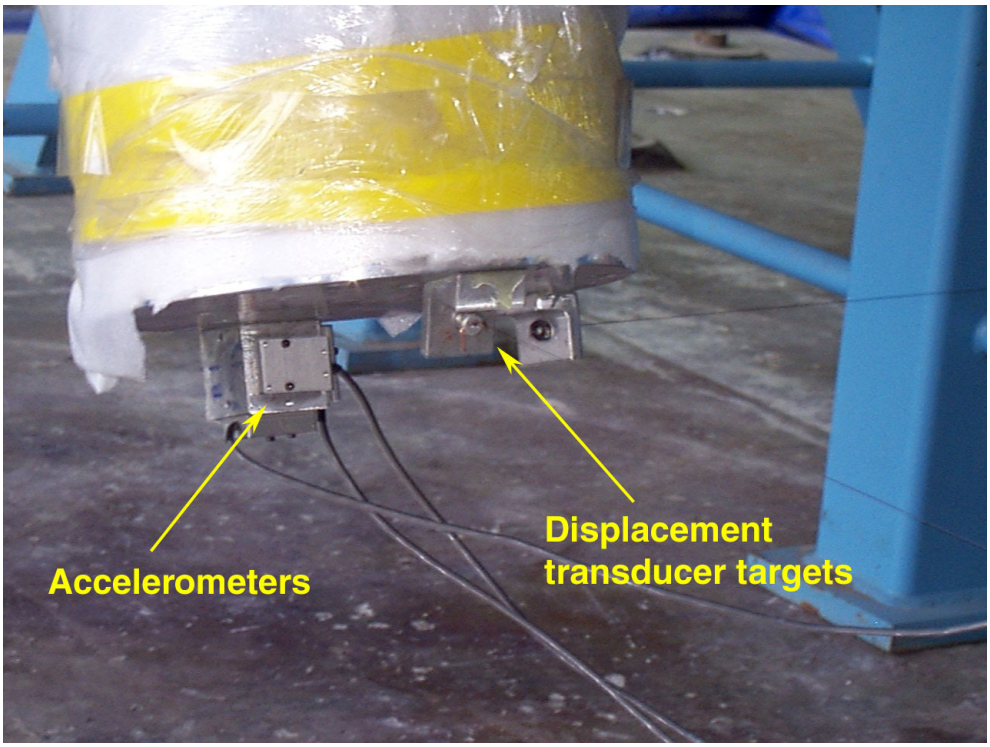

Figure 2-3 Instrumentation at the base of one of the 550 kV bushings

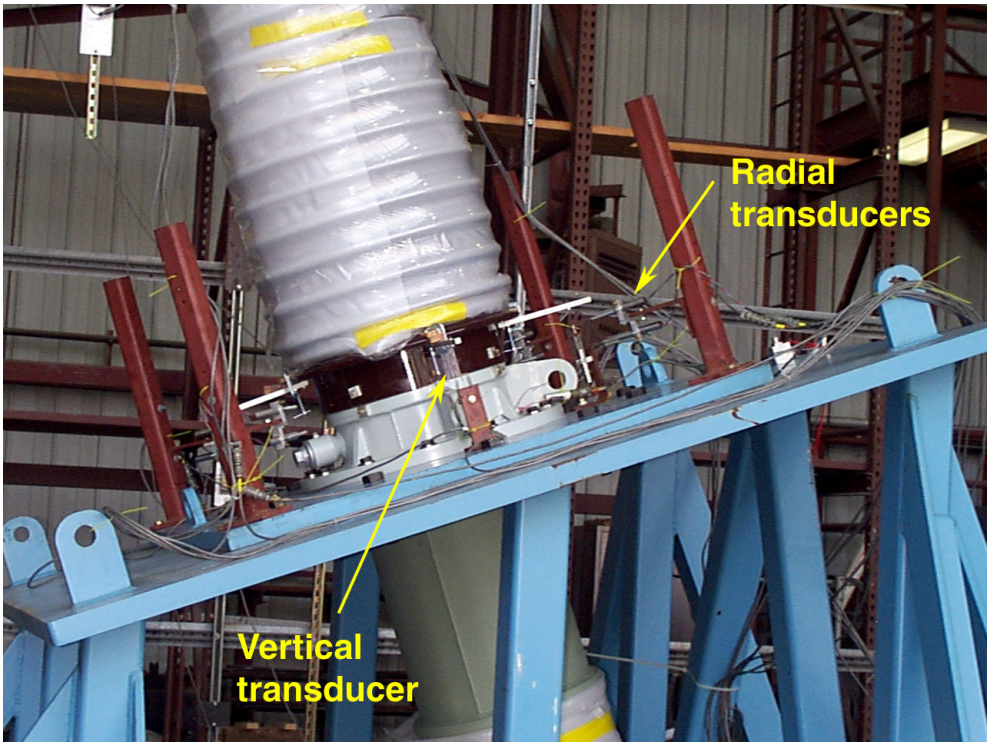

Figure 2-4 Instrumentation of an UPPER-1 porcelain unit

CHAPTER 3
QUALIFICATION AND FRAGILITY TESTING

3.1 Introduction

Recorded earthquake ground motion histories were used to evaluate the seismic response of the three 550 kV transformer bushings (hereafter termed Bushing-1, Bushing-2, and Bushing-3). The following section describes the requirements of IEEE 693-1997 (IEEE, 1998) for the qualification of transformer bushings and the procedures used to develop earthquake histories for testing.

3.2 IEEE 693-1997 Requirements for Bushing Qualification

Three types of earthquake-simulator testing are identified in IEEE 693-1997 for the seismic qualification of transformer bushings: (a) earthquake ground motions, (b) resonant frequency search, and (c) sine-beat testing. Earthquake ground motion tests (termed *time-history shake table tests* in IEEE) and resonant frequency tests are mandatory. Information on these two types of tests follow.

3.2.1 Resonant search tests

Sine-sweep or broadband white noise tests are used to establish the dynamic characteristics (natural frequencies and damping ratios) of a bushing. These so-called *resonant search* tests are undertaken using uni-directional excitation along each global axis of the earthquake simulator platform. If only broadband white noise tests are performed, the amplitude of the white noise must not be less than 0.25g. If only sine-sweep tests are used, IEEE 693-1997 specifies that the resonant search be conducted at a rate not exceeding one octave per minute in the range for which the equipment has resonant frequencies but at least at 1 Hz; frequency searching above 33 Hz is not required. Because both sine-sweep and white-noise tests were used in this testing program to identify the modal properties of the transformer bushings, the recommendations of IEEE 693-1997 were not followed exactly.

The history for the banded white-noise tests was prepared using a random signal generator. The sine sweep history was developed using a rate of two octaves per minute. (At two octaves per minute, the input frequency doubles every 30 seconds.) A continuous frequency function was used to develop the sine-sweep function

$$x(t) = x_0 \sin\left(2\pi\left[\frac{30}{\log 2}\right]2^{t/30}\right) \tag{3-1}$$

where x is the displacement, and x_0 is the maximum displacement. For both sine-sweep and white-noise tests, a simulator input acceleration of 0.1g was used.

3.2.2 Earthquake test response spectrum

IEEE 693-1997 identifies several response spectra of identical shape but different amplitudes for the qualification of transformer bushings. These spectra are described below; a more detailed description is presented in Appendix A.

Test Response Spectrum (TRS). For earthquake simulator testing, IEEE 693-1997 states that the TRS for each horizontal earthquake motion must match or exceed the target spectrum and that the TRS for vertical earthquake motion be no less than 80 percent of target spectrum. IEEE 693-1997 recommends that 2-percent damping be used for spectral matching and requires at least 20 seconds of strong motion shaking be present in each earthquake record. Earthquake motions can be established using either synthetic or recorded histories. Recorded motions formed the basis of the earthquake histories used to test the 550 kV bushings.

Performance Level (PL). IEEE 693-1997 represents a PL for substation equipment by a response spectrum. The PL represents the expected level of performance when a piece of equipment is qualified to the RRS and meets the requirements for allowable stress design. The two PLs relevant to California are *Moderate* and *High*. The Moderate PL was selected by PG&E, ABB, and PEER for the studies reported herein. Equipment that is shown to perform acceptably in ground shaking consistent with the Moderate Seismic Performance Level (see Table 3-1) is said to be seismically qualified to the Moderate Level.

Required Response Spectrum (RRS). It is often neither practical nor cost effective to test components to the Moderate PL. As such, IEEE 693-1997 permits equipment to be tested using a reduced level of shaking called the RRS. The shapes of the RRS and the PL are identical, but the ordinates of the PL are twice (referred to as performance factor in IEEE 693-1997) that of the RRS. Equipment tested or analyzed using the RRS is expected to have acceptable performance at the PL. This assumption is checked by measuring the stresses obtained from testing at the RRS, and (a) comparing the stresses to 50 percent (equal to the inverse of the performance factor) of the ultimate strength of the porcelain (assumed to be brittle) or cast aluminum components and (b) using a factor of safety against yield combined with an allowance for ductility of steel and other ductile materials.

Test Response Spectra for Mounted Equipment (TRSME). To account for the amplification of earthquake motion due to the influence of the transformer body and local flexibility of the transformer near the bushing mount, IEEE 693-1997 states that the input motion *as measured at the bushing flange* shall match a spectrum with ordinates twice that of the RRS, termed herein as the TRSME. For this level of shaking, IEEE 693-1997 states that the stresses in the porcelain components must be less than 50 percent of the ultimate stress, and the factor of safety against oil leakage must be greater than or equal to 2.0.

An alternate approach that is identified in Annex D5.1(d) of IEEE 693-1997 was used for the studies reported herein. Namely, earthquake histories with spectral ordinates twice those of the TRSME were used for testing: the target peak horizontal acceleration at the bushing flange was 1.0g. Porcelain stresses at this level of earthquake shaking were required to be less than or equal to the ultimate value, and there was to be no evidence of oil leakage. The spectrum for this motion is shown in Figure 3-2 and is the same as the Moderate PL spectrum.

The key requirements of IEEE 693-1997 for qualification and fragility testing of bushings are summarized in Table 3-1.

Table 3-1 IEEE earthquake-history testing requirements for Moderate Level qualification

Peak Ground Acceleration	*Comments*
0.5g	Moderate Seismic Performance Level (PL) for substation equipment
0.25g	Required Response Spectrum (RRS) for Moderate Seismic Performance Level for substation equipment
0.5g	Test Response Spectrum for mounted equipment (TRSME) for Moderate Seismic Performance Level.
1.0g	Response spectrum for checking porcelain stresses and oil leakage for bushings mounted on transformers.

3.2.3 Earthquake ground motions

The earthquake histories used for the qualification and fragility testing of the 550 kV bushings were developed using the three-component set of near-fault earthquake motions recorded during the 1978 Tabas earthquake. Figures 3-3 through 3-5 present the acceleration history, power spectrum, and pseudo-acceleration response spectra for the three components of the Tabas record. The amplitude of each history (X-, Y-, and Z-) record was normalized to a peak acceleration of 1.0g. The power spectrum for each history has moderate bandwidth. The 2-percent and 5-percent damped IEEE spectra for Moderate Level qualification, anchored to a peak ground acceleration of 1.0g are also shown in the figures. The response-spectrum ordinates for each normalized earthquake history exceed the target IEEE values for frequencies greater than 2 to 3 Hz and drop below the target values for frequencies less than 2 Hz.

To obtain IEEE 693-1997 spectrum-compatible normalized histories, the original Tabas acceleration records were modified using a non-stationary response-spectrum matching technique developed by Abrahamson (Abrahamson, 1996). In traditional spectrum-matching routines, adjustments are performed in the frequency domain. Specifically, the original acceleration record is transformed into the frequency domain, the amplitude of the Fourier spectrum is adjusted at each frequency to match the target value, and the record is then transformed back into the time domain. Two key disadvantages of the frequency-domain method are that the modified earthquake history rarely resembles the original earthquake history, and that frequency leakage often makes convergence to the target spectrum difficult. Abrahamson's time-domain method is based on the algorithm proposed by Lilhanad and Tseng (1988) wherein short-duration wavelets are added to the original earthquake history at optimal times in the history to match the spectral amplitude at each frequency to the target value. The modified history generally resembles the original earthquake history and frequency leakage is negligible.

The testing of 196 kV ABB bushings (Gilani, et al., 1998) at Berkeley utilized spectrum-compatible earthquake histories developed using the Abrahamson technique. The resulting spectra matched the target spectrum across a broad frequency range (0.1 Hz to 100 Hz). Because the maximum displacement and velocity of the simulator platform are 5 in. (127 mm) and 25 in./

sec (635 mm/sec), respectively, the spectrum-compatible motions were high-pass filtered (removal of low-frequency content) to reduce the peak displacements and velocities of the simulator platform. However, the resulting power spectra of the filtered histories were narrow-banded, and not representative of strong earthquake ground motion.

A different strategy was used to develop earthquake histories for the studies reported herein. This strategy combined the Abrahamson spectrum-matching algorithm and frequency-domain trapezoidal high-pass filters. Input ground motions to the simulator were developed in a three-step process as follows. First, the original earthquake history was high-pass filtered to remove low frequency content (see Table 3-2) such that the maximum displacement and velocity of the filtered history were approximately equal to 5 in. (127 mm) and 25 in./sec (635 mm/sec), respectively. (All content below the cut-off frequency was eliminated; all content above the corner frequency was retained; and content between these frequencies was multiplied by a linearly increasing value that ranged from zero at the cut-off frequency to unity at the corner frequency. The cut-off frequencies were much smaller than the resonant frequency of the 550 kV bushings [known to range between 6 Hz and 9 Hz]. Removal of such low-frequency components from the input signals to the simulator is known to have a negligible impact on the dynamic response of the bushings.) Second, the filtered earthquake history from step one was matched to the target spectrum for frequencies greater than the corner frequency of the trapezoidal filter using the Abrahamson algorithm. Third, the spectrum compatible motions from step two were high-pass filtered to exactly limit the maximum displacement and velocity to 5 in. (127 mm) and 25 in./ sec (635 mm/sec), respectively.

Two independent sets of three earthquake histories (Tabas-A and Tabas-B) were generated using the above procedure. Tabas-A was used for all simulations up to and including the Moderate Level qualification for which the target simulator acceleration was 1.0g (see Table 3-2). Tabas-B was used for all other tests up to those corresponding to High Level qualification for which the target acceleration was 2.0g. Table 3-2 summarizes the step-one filter frequencies used to generate the Tabas-A and Tabas-B histories. Figures 3-6 through 3-8 present the acceleration history, power spectrum, and response spectra for the three spectrum-compatible Tabas-A records. Figures 3-9 through 3-11 present the same information for the three spectrum-compatible Tabas-B records.

Table 3-2 High-pass filter frequencies for earthquake histories

		Filter frequencies (Hz)	
Set	*Component*	*Cut-off*	*Corner*
Tabas-A	*X*	1.0	1.5
	Y	1.0	1.5
	Z	1.0	1.5
Tabas-B	*X*	2.0	2.5
	Y	2.2	2.5
	Z	2.2	2.5

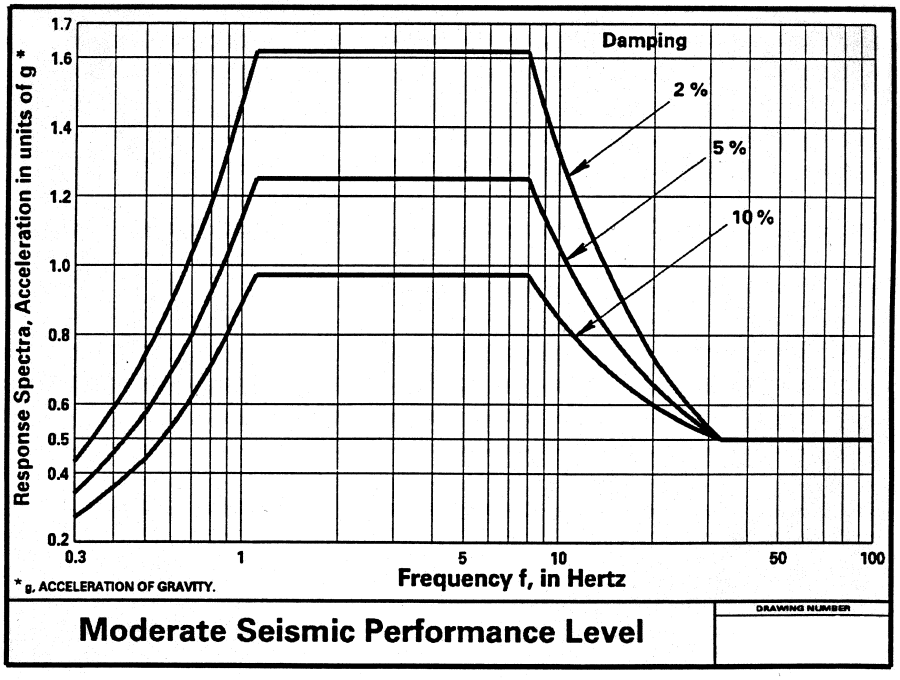

Figure 3-1 Spectra for the Moderate Seismic Performance Level (IEEE, 1998)

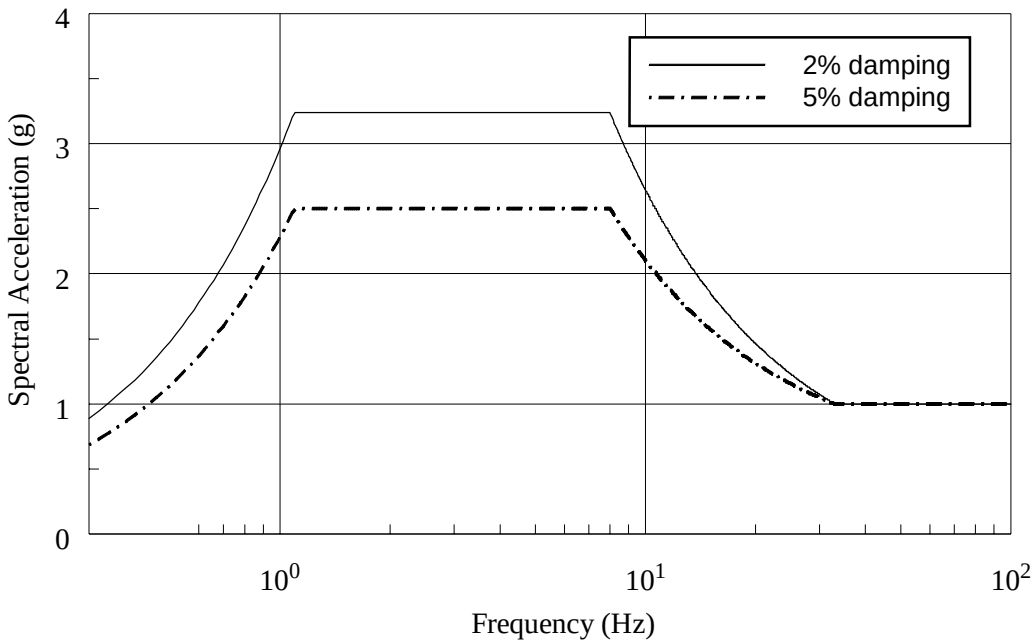

Figure 3-2 Test Response Spectra at bushing flange for Moderate PL

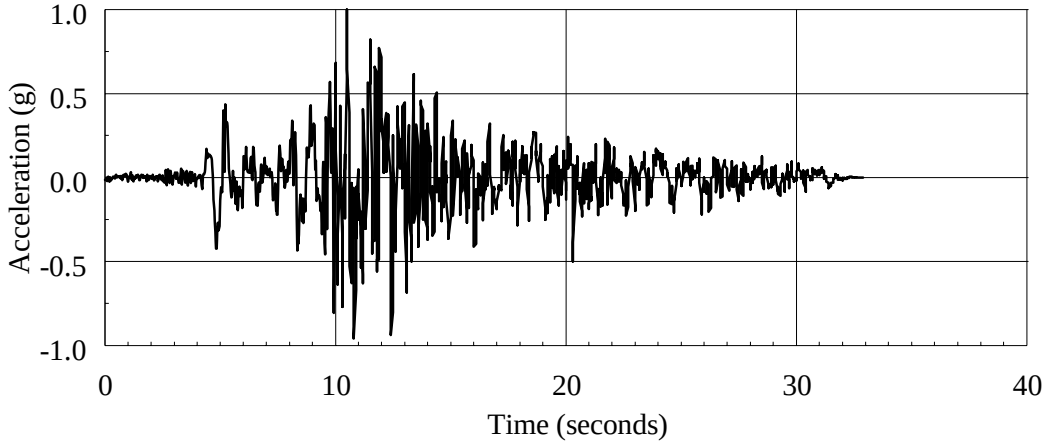

a. Normalized acceleration history

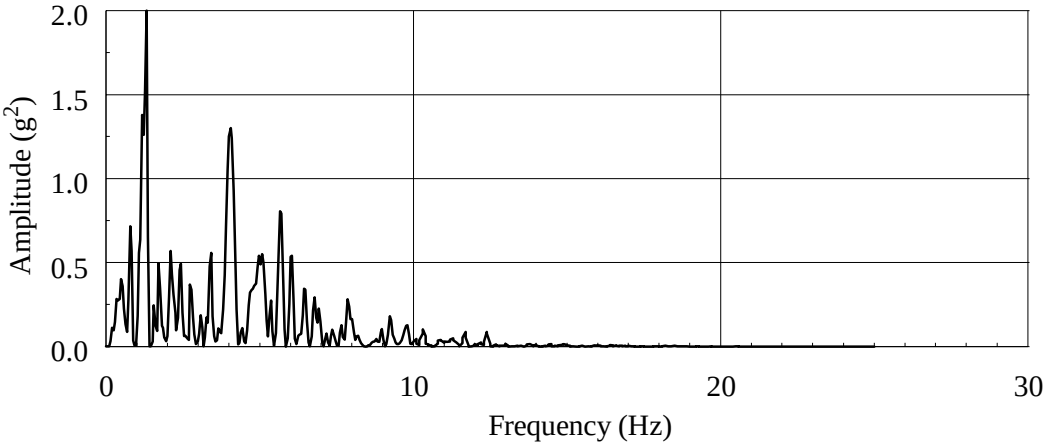

b. Power spectrum

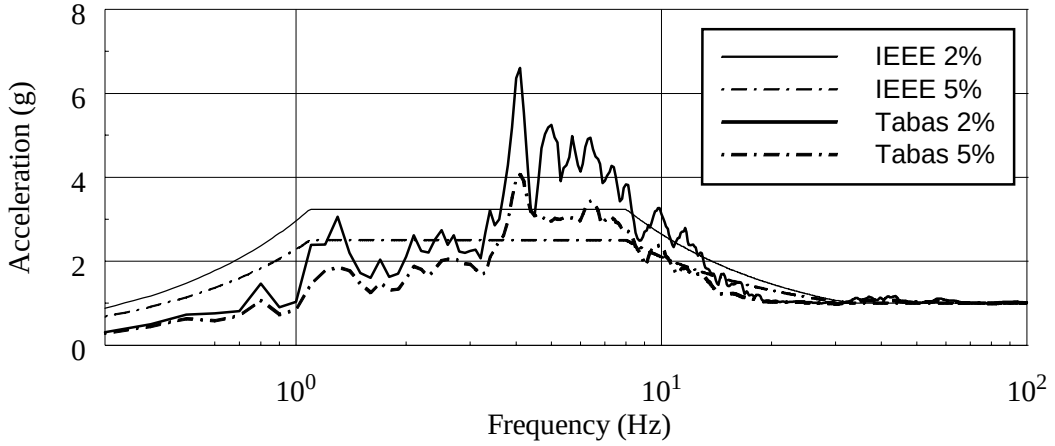

c. Response spectrum

Figure 3-3 Normalized acceleration history, power spectrum, and response spectra for the longitudinal (X-) component of the original Tabas record

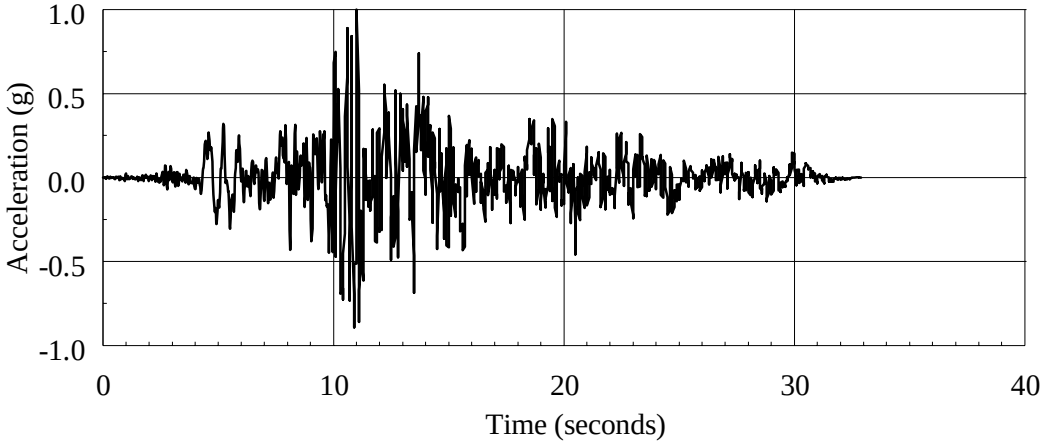

a. Normalized acceleration history

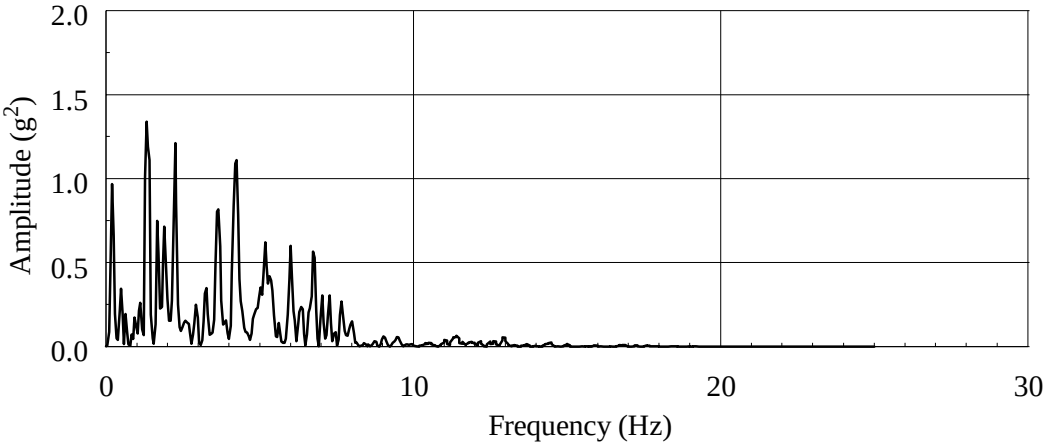

b. Power spectrum

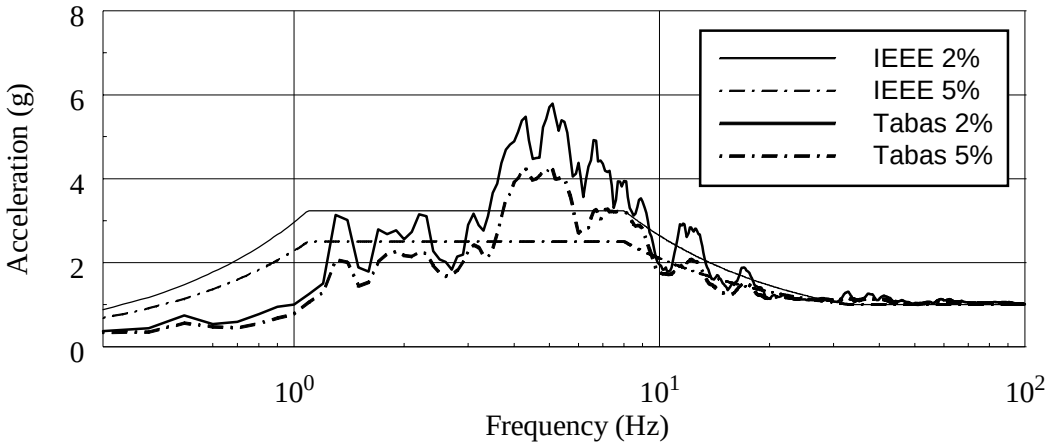

c. Response spectrum

Figure 3-4 Normalized acceleration history, power spectrum, and response spectra for the lateral (Y-) component of the Tabas record

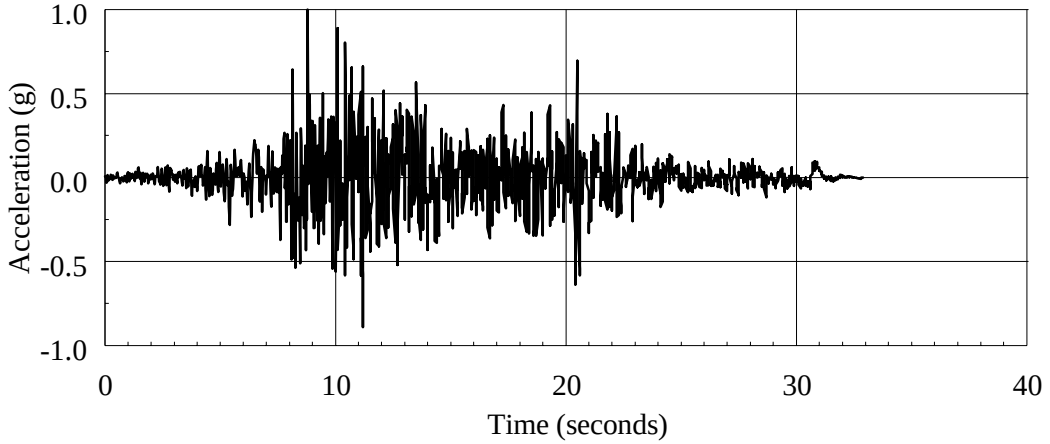

a. Normalized acceleration history

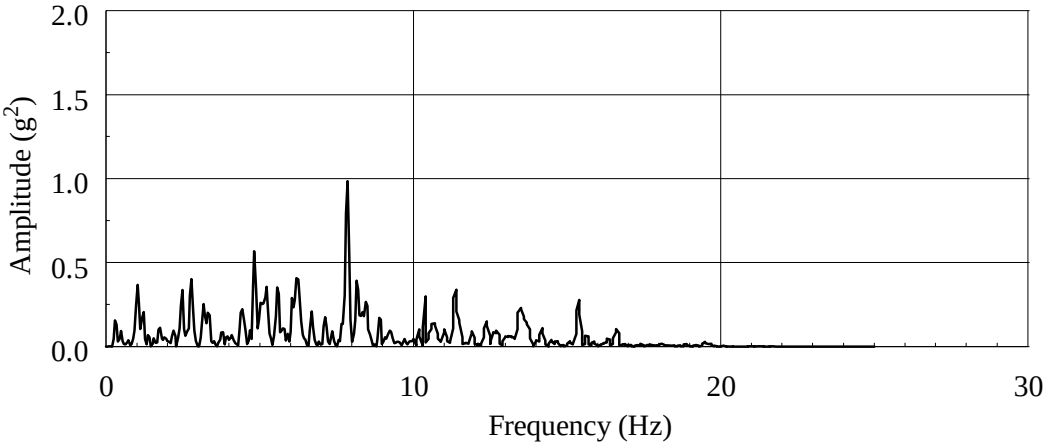

b. Power spectrum

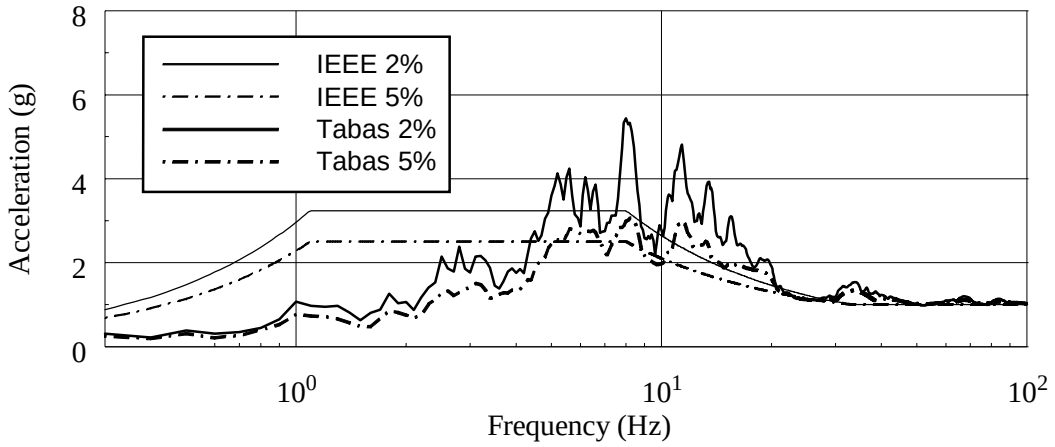

c. Response spectrum

Figure 3-5 Normalized acceleration history, power spectrum, and response spectra for the vertical (Z-) component of the original Tabas record

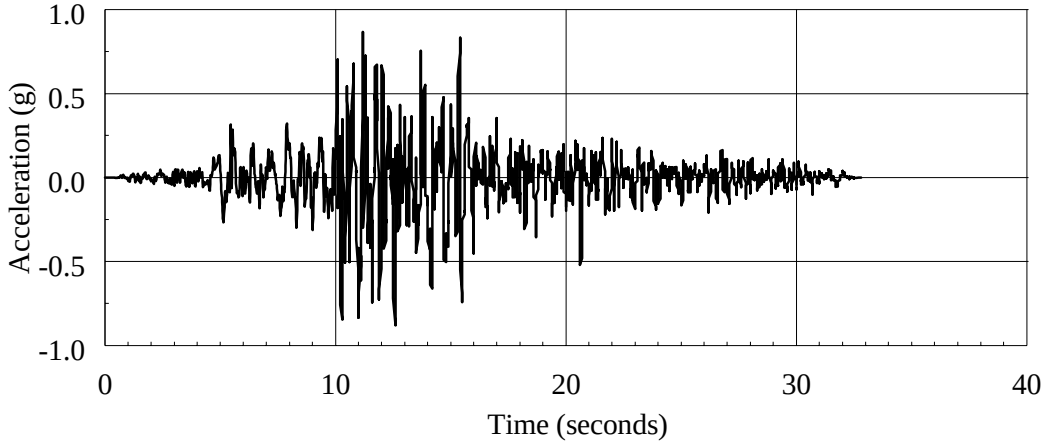

a. Acceleration history

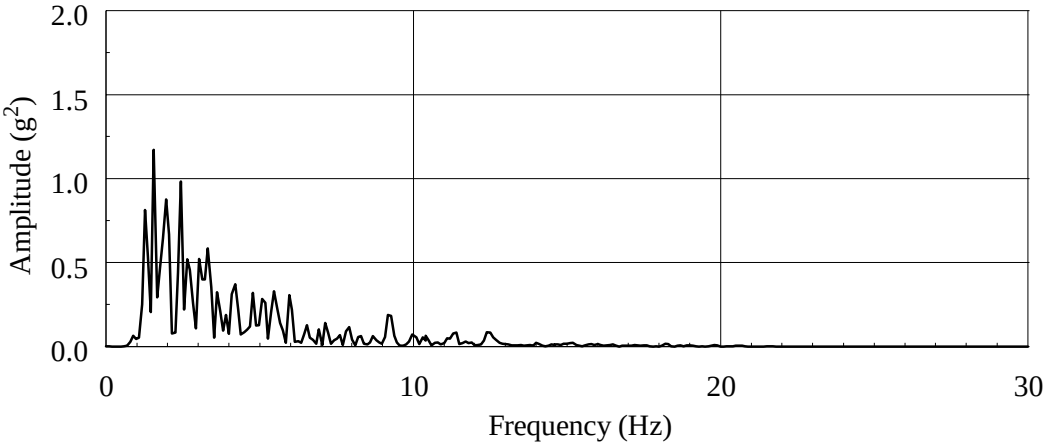

b. Power spectrum

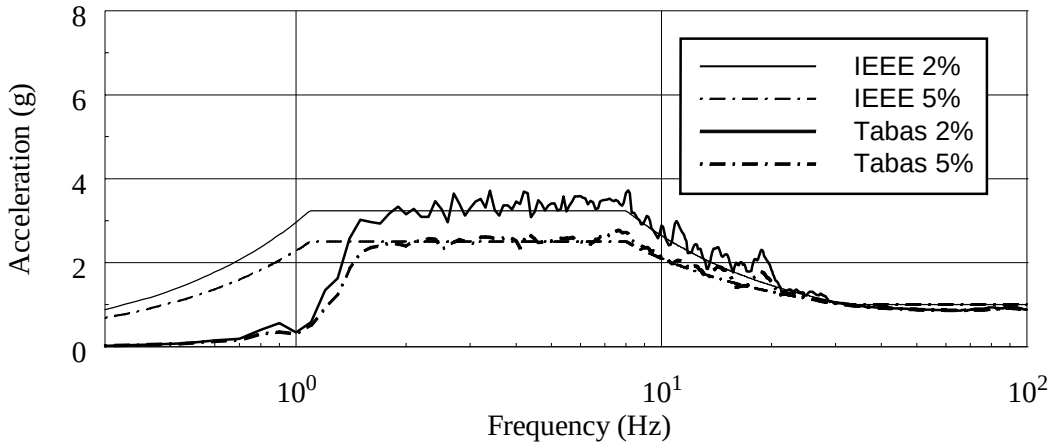

c. Response spectrum

Figure 3-6 Acceleration history, power spectrum, and response spectra for the longitudinal (*X*-) component of the Tabas-A record

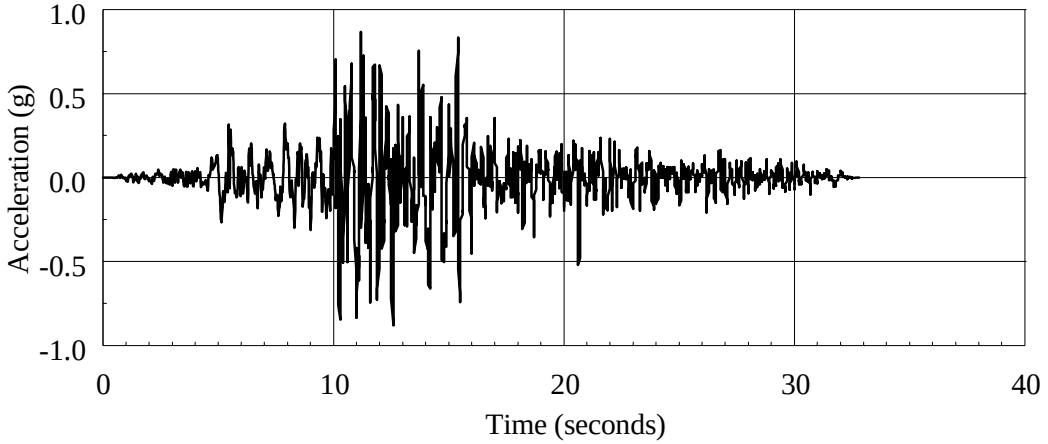

a. Acceleration history

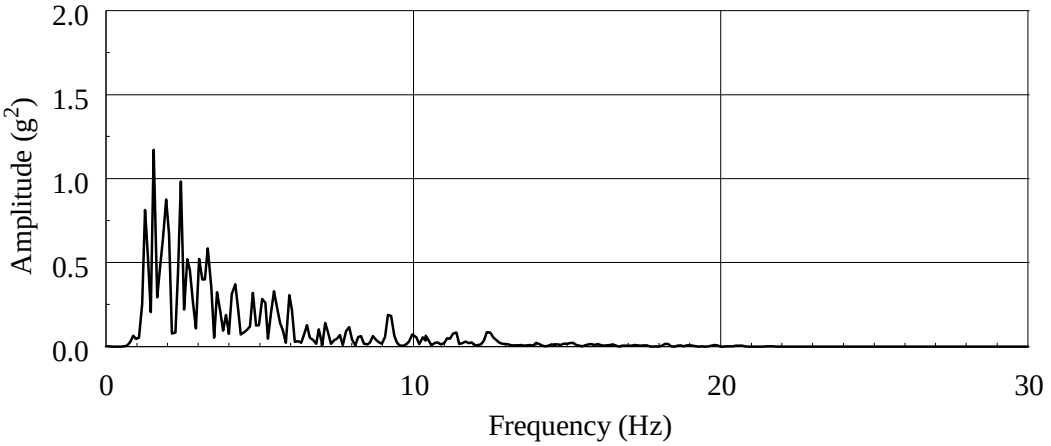

b. Power spectrum

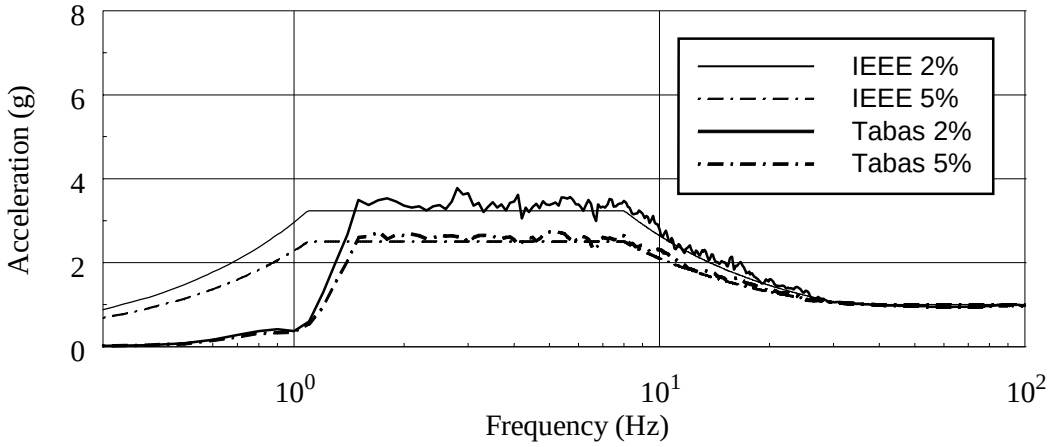

c. Response spectrum

Figure 3-7 Acceleration history, power spectrum, and response spectra for the lateral (*Y*-) component of the Tabas-A record

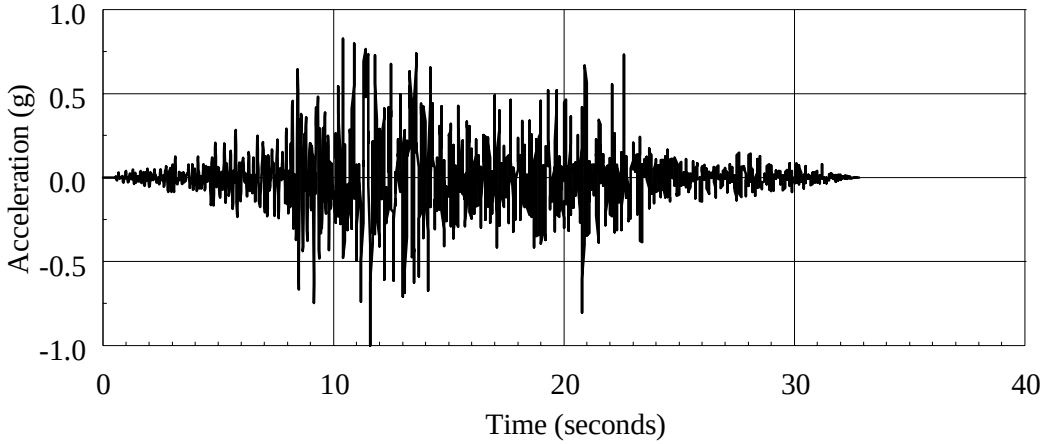

a. Acceleration history

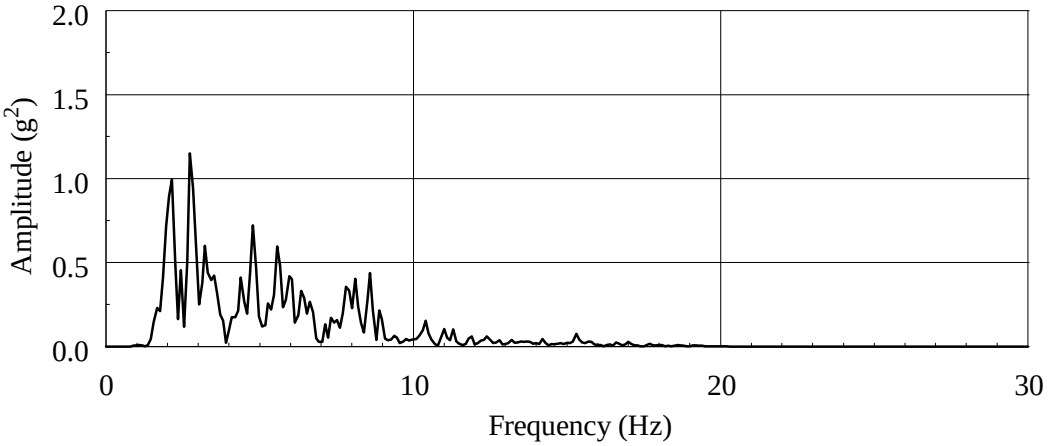

b. Power spectrum

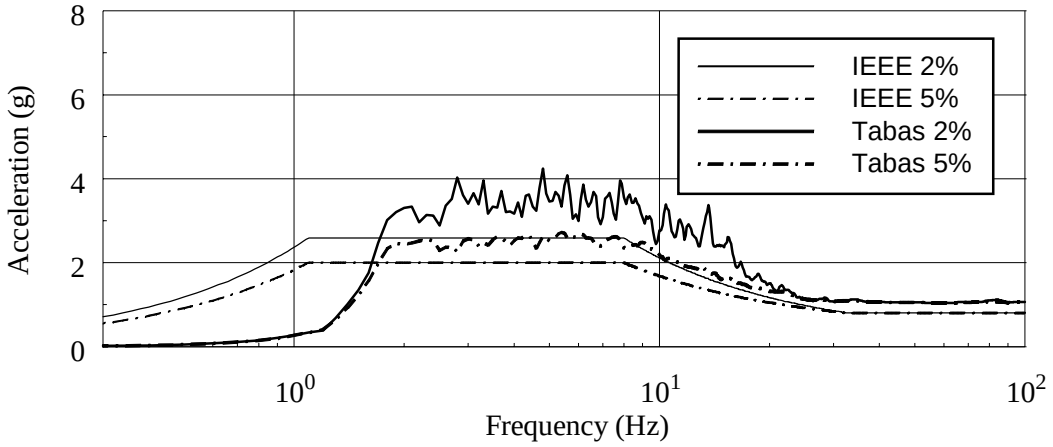

c. Response spectrum

Figure 3-8 Acceleration history, power spectrum, and response spectra for the vertical (*Z*-) component of the Tabas-A record

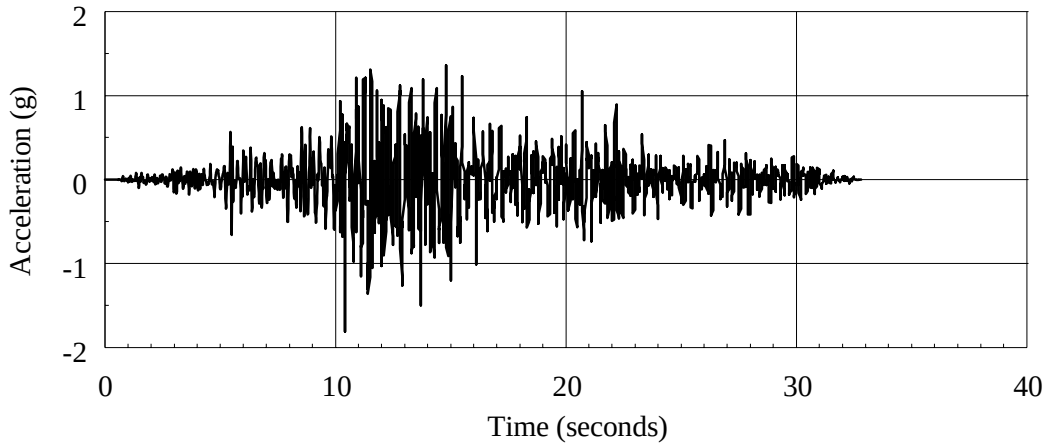

a. Acceleration history

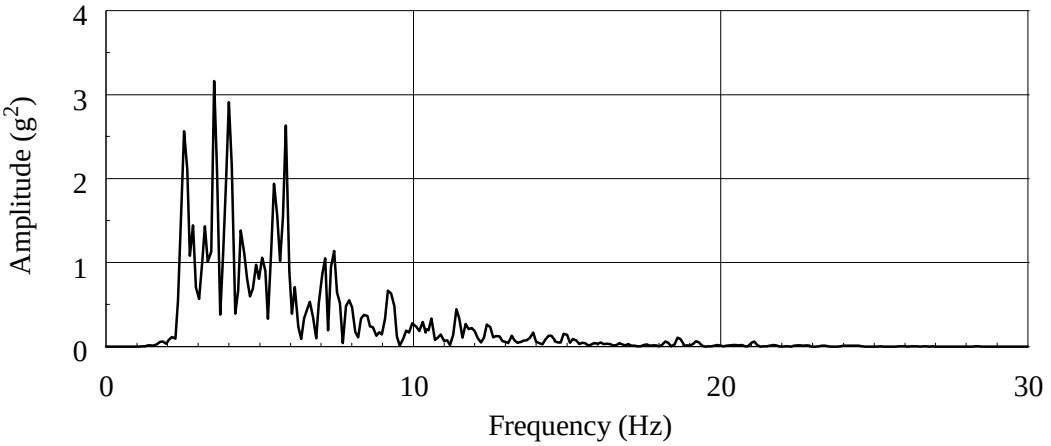

b. Power spectrum

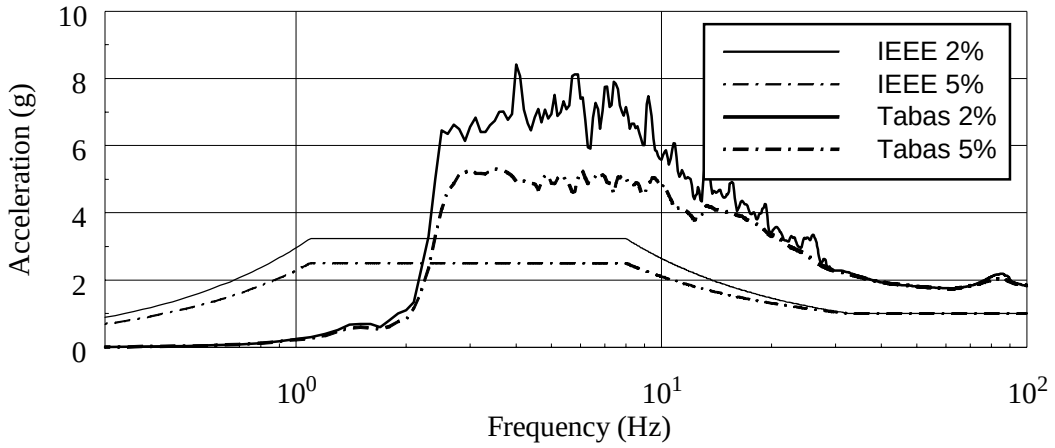

c. Response spectrum

Figure 3-9 Acceleration history, power spectrum, and response spectra for the longitudinal (*X*-) component of the Tabas-B record

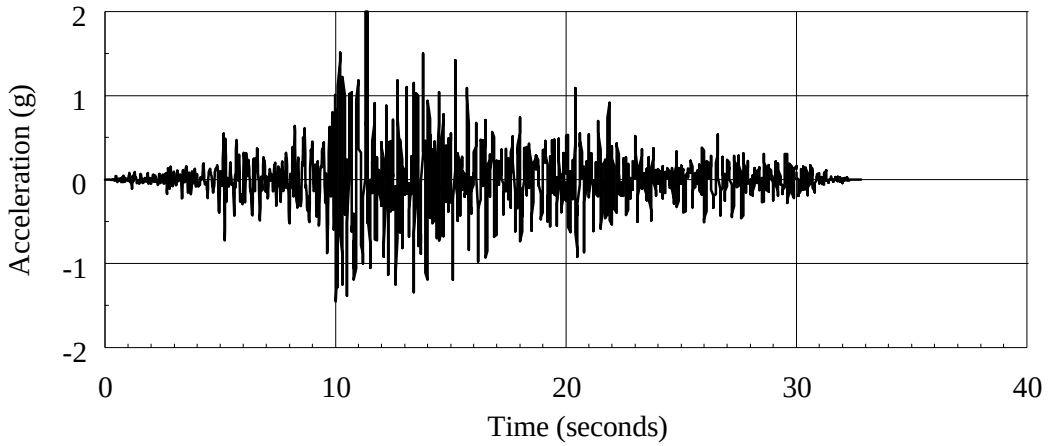

a. Acceleration history

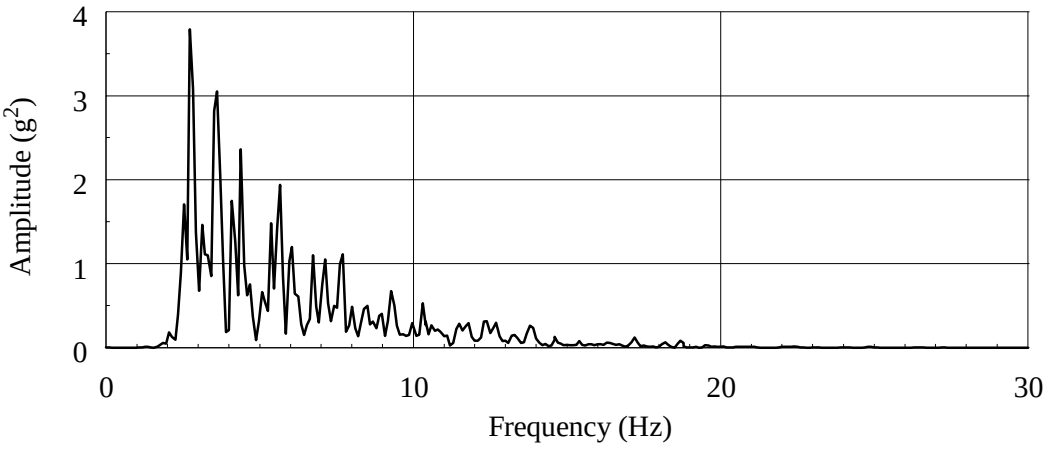

b. Power spectrum

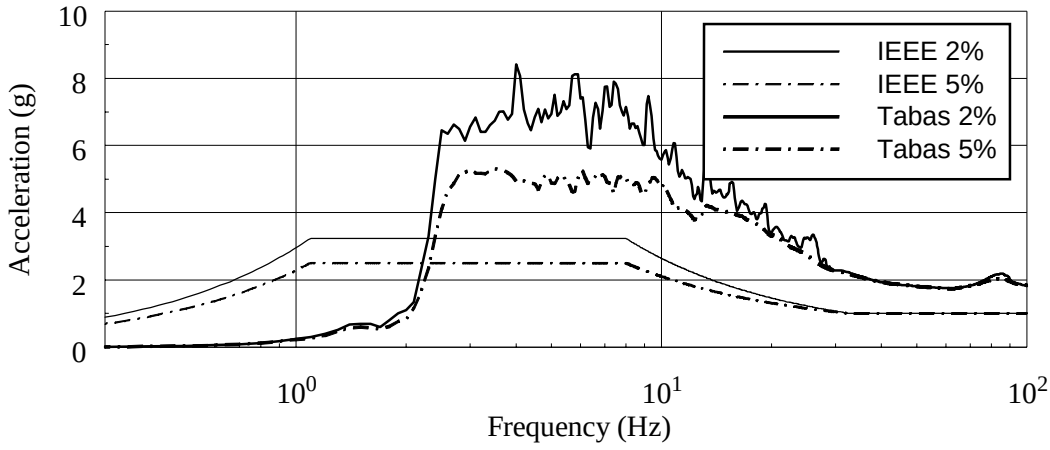

c. Response spectrum

Figure 3-10 Acceleration history, power spectrum, and response spectra for the lateral (*Y*-) component of the Tabas-B record

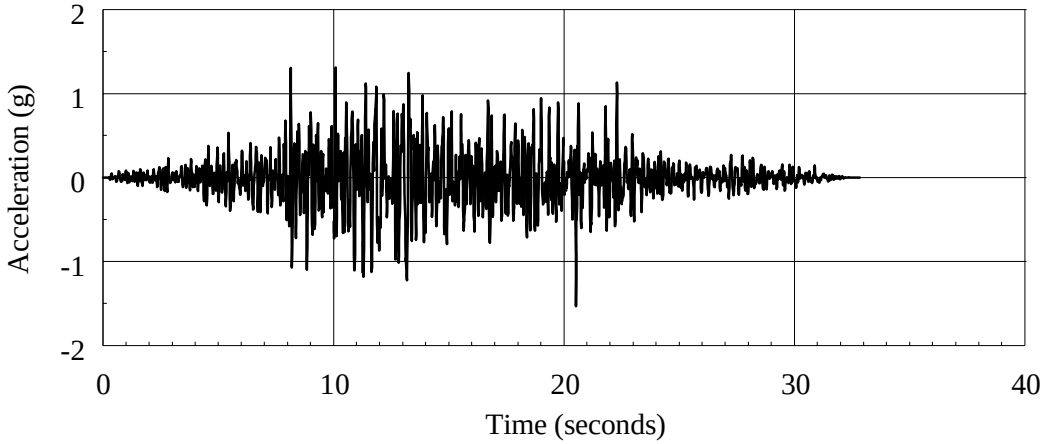

a. Acceleration history

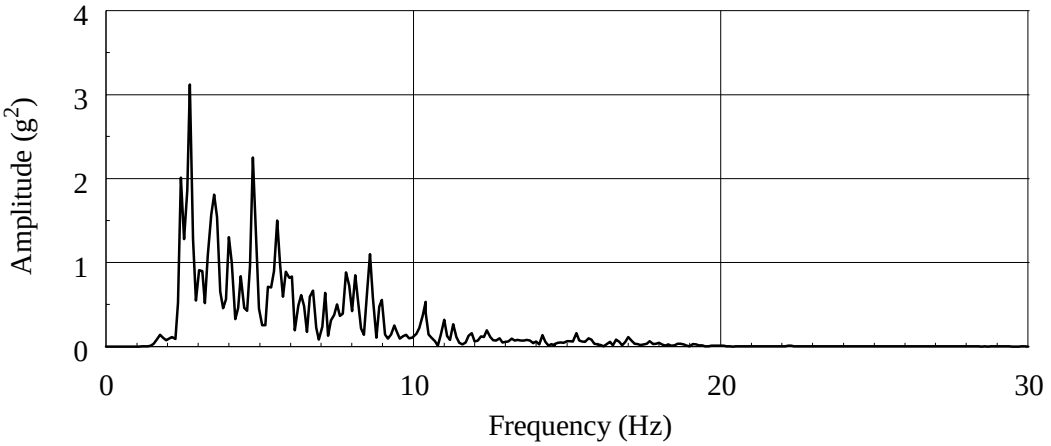

b. Power spectrum

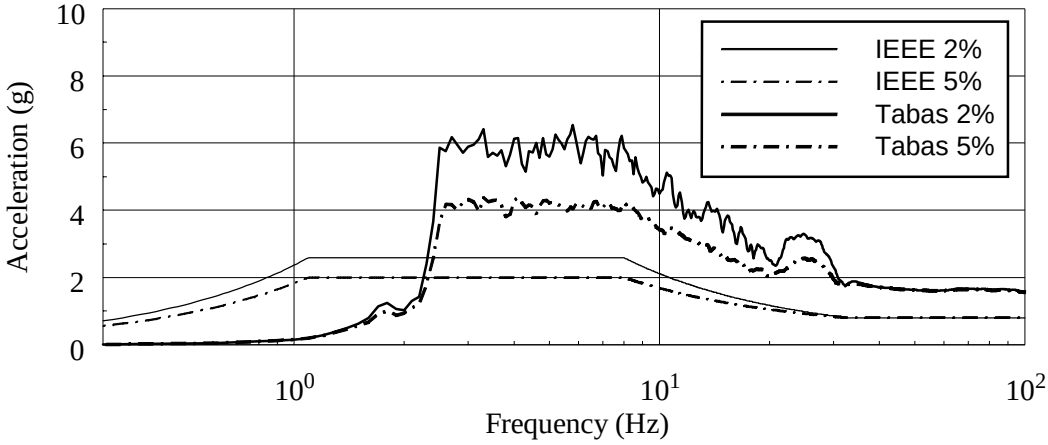

c. Response spectrum

Figure 3-11 Acceleration history, power spectrum, and response spectra for the vertical (*Z*-) component of the Tabas-B record

CHAPTER 4
SUMMARY OF EXPERIMENTAL DATA

4.1 Overview

The objectives of the testing program were to evaluate the seismic behavior of 550 kV transformer bushings by testing Bushing-1 and Bushing-2 to failure, to qualify Bushing-3 to the Moderate Level, and to evaluate the efficacy of manufacturer-detailed modifications to 550 kV bushings (Bushing-2 and Bushing-3). The key modifications are listed in Table 1-1. For seismic testing, each bushing was installed in the rigid mounting frame described in Section 2.3. A photograph of one of the bushings installed in the mounting frame is presented in Figure 1-2.

The following sections summarize the dynamic properties and the seismic response of the bushings. Section 4.4 discusses the qualification of Bushing-3. Section 4.5 presents fragility data for Bushing-1 and Bushing-2, and critiques the IEEE 693-1997 procedures for fragility testing of substation equipment.

4.2 Dynamic Properties of 550 kV Bushings

Sine-sweep and white-noise tests were used to calculate the modal frequencies and damping ratios for each bushing. Matlab (Mathworks, 1999) was used to process the experimental data. The data was zero-corrected and low-pass filtered with a corner and cut-off frequencies of 30 Hz. Figures 4-1 to 4-3 show the transfer functions between the upper tip of the bushing and the mounting frame in the three local directions (*x, y, z*) for Bushing-1, Bushing-2, and Bushing-3, respectively. The resonant frequency in the local *x*- and *y*-directions is approximately 8 Hz. Damping ratios of approximately 4 percent of critical were obtained using the half-power bandwidth method.

Table 4-1 summarizes the measured dynamic properties of the bushings. Modal data could not be determined for the local *z*-direction. The modal frequencies differ slightly in *x*- and *y*- directions due to the unsymmetric distribution of lifting lugs immediately above the flange plate.

Table 4-1 Modal properties of bushings from sine-sweep tests

	Frequency (Hz)		*Damping Ratio (% critical)*	
Bushing	*x-direction*	*y-direction*	*x-direction*	*y-direction*
1	8.2	7.9	4	4
2	8.0	8.2	4	4
3	8.0	7.8	4	4

4.3 Earthquake Testing of Bushing-1, Bushing-2, and Bushing-3

4.3.1 Introduction

The list of earthquake tests and key observations for Bushing-1, Bushing-2, and Bushing-3 are listed in Tables 4-2 to 4-4, respectively. After each earthquake test, the response data were analyzed, the bushing was inspected for damage and oil seepage, and the bolts joining the bushing flange plate to the adaptor plate, and the adaptor plate to the mounting plate, were checked for tightness. All bolts were found to be tight for all tests.

Table 4-2 Summary of earthquake testing of Bushing-1

Test No.	*Test date*	*Identification*[1]	*PGA*[2]	*Comments*
1	03/29/99	WN-X	0.1g	
2	03/29/99	WN-Y	0.1g	
3	03/29/99	WN-Z	0.1g	
4	03/29/99	SS-X	0.1g	
5	03/29/99	SS-Y	0.1g	
6	03/29/99	SS-Z	0.1g	
7	03/29/99	Tabas-A	0.1g	
8	03/30/99	Tabas-A	0.2g	
9	03/30/99	Tabas-A	0.3g	
10	03/30/99	Tabas-A	0.5g	Oil leak at the gasket connection[3].
11	03/30/99	Tabas-A	0.5g	Repeat test to investigate whether oil will lubricate gasket and facilitate slip of porcelain.
12	03/30/99	Tabas-A	0.7g	Oil leak and slip of porcelain above gasket.
13	03/31/99	SS-X	0.1g	Install manufacturer’s shipping ring around gasket connection.
14	03/31/99	SS-Y	0.1g	
15	03/31/99	SS-Z	0.1g	
16	03/31/99	Tabas-A	0.7g	Oil leak at gasket connection
17	03/31/99	Tabas-A	1.0g	Large slip of porcelain over gasket; rotation of shipping ring; see Figure 4-4.

1. WN = white noise, SS = sine sweep; -X, -Y, and -Z denote direction of testing in global coordinate system; Tabas-A = spectrum-compatible Tabas-A earthquake histories; Tabas-B = spectrum-compatible Tabas-B earthquake histories
2. PGA = target peak acceleration of the simulator platform
3. Connection of UPPER-1 porcelain unit to the flange plate

Table 4-3 Summary of earthquake testing of Bushing-2

Test No.	*Test date*	*Identification*[1]	*PGA*[2]	*Comments*
1	04/05/99	WN-X	0.1g	
2	04/05/99	WN-Y	0.1g	
3	04/05/99	WN-Z	0.1g	
4	04/05/99	SS-X	0.1g	
5	04/05/99	SS-Y	0.1g	
6	04/05/99	SS-Z	0.1g	
7	04/05/99	Tabas-A	0.1g	
8	04/05/99	Tabas-A	0.2g	
9	04/05/99	Tabas-A	0.3g	
10	04/05/99	Tabas-A	0.5g	
11	04/05/99	Tabas-A	0.7g	
12	04/05/99	Tabas-A	1.0g	
13	04/05/99	Tabas-B	1.2g	Oil leak at the gasket connection[3]; large slip of UPPER-1 porcelain unit over the flange plate; gasket visible; see Figure 4-5.

1. WN = white noise, SS = sine sweep; -X, -Y, and -Z denote direction of testing in global coordinate system; Tabas-A = spectrum-compatible Tabas-A earthquake histories; Tabas-B = spectrum-compatible Tabas-B earthquake histories
2. PGA = target peak acceleration of the simulator platform
3. Connection of UPPER-1 porcelain unit to the flange plate

The following subsections present peak responses of the mounting frame and the bushings; data related to the qualification and fragility testing of Bushing-1, Bushing-2, and Bushing-3; and local response characteristics of the bushings measured at the junction of the UPPER-1 porcelain unit and the flange plate.

4.3.2 Peak Responses

The transducer response histories were processed using the computer program Matlab (Mathworks, 1999). Experimental histories were low-passed filtered using a rectangular filter with a cut-off frequency of 30 Hz and then zero-corrected if necessary.

The peak acceleration responses of the mounting frame and the bushings are presented in Tables 4-5 and 4-6, respectively. Only the peak responses at the upper tip of each bushing are reported; the maximum accelerations at the base of the bushings were always less than those at the upper tip.

Table 4-4 Summary of earthquake testing for Bushing-3

Test No.	*Test date*	*Identification*[1]	*PGA*[2]	*Comments*
1	04/20/99	SS-X	0.1g	
2	04/20/99	SS-Y	0.1g	
3	04/20/99	SS-Z	0.1g	
4	04/20/99	Tabas-A	1.0g	Slight slip of porcelain; no evidence of oil leak. spectral amplitude lower than target value at bushing frequency of approximately 8 Hz; adjust simulator span setting and retest.
5	04/20/99	Tabas-A	1.0g	Noticeable slip of porcelain over the gasket connection[3]; gasket visible; significant oil leakage; see Figures 4-6 and 4-7.

1. WN = white noise, SS = sine sweep; -X, -Y, and -Z denote direction of testing in global coordinate system; Tabas-A = spectrum-compatible Tabas-A earthquake histories; Tabas-B = spectrum-compatible Tabas-B earthquake histories
2. PGA = target peak acceleration of the simulator platform
3. Connection of UPPER-1 porcelain unit to the flange plate

The peak displacement responses of the bushings relative to the mounting frame are presented in Table 4-7. Only the peak responses in the global X-direction and global Y-direction at the upper tip of each bushing are reported; the maximum displacements at the base of the bushings were always less than those at the upper tip.

A total of sixteen transducers measured porcelain strain (channels 39 through 42), radial motion of the flange plate with respect to mounting frame (channels 43 through 46), radial motion of the UPPER-1 porcelain unit with respect to mounting frame (channels 47 through 50), and local vertical motion of the UPPER-1 porcelain unit with respect to the flange plate (channels 51 through 54). Maximum values, computed as the peak value of the four transducers, for porcelain strain, local UPPER-1 radial motion, and local UPPER-1 vertical motion, are presented in Table 4-8.

4.3.3 Response of the Mounting Frame

The mounting frame was designed to be *rigid* and thus not amplify the motions of the earthquake simulator. Figure 4-8 shows the mounting frame-to-earthquake simulator transfer functions (in the X-, Y-, and Z-directions) calculated from the sine-sweep tests of Bushing-1 (Test Numbers 4 through 6). The mounting-frame accelerations were transformed into the global coordinate system for these calculations. If the mounting frame were truly rigid, the transfer function would be flat with a value equal to 1.0 across the entire frequency range. The transfer functions show little amplification of motion in the frequency range of 0 to 10 Hz, but significant amplification of

Table 4-5 Peak accelerations of the mounting frame

				Peak Acceleration (g)		
Bushing	*Test No.*	*Identification*[1]	*PGA*[2]	*x-direction*[3]	*y-direction*[3]	*z- direction*[3]
1	7	Tabas-A	0.1g	0.21	0.33	0.16
1	8	Tabas-A	0.2g	0.37	0.43	0.24
1	9	Tabas-A	0.3g	0.51	0.47	0.37
1	10	Tabas-A	0.5g	0.65	0.65	0.49
1	11	Tabas-A	0.5g	0.69	0.65	0.47
1	12	Tabas-A	0.7g	0.92	0.79	0.72
1	16	Tabas-A	0.7g	0.84	0.86	0.72
1	17	Tabas-A	1.0g	1.23	1.00	0.96
2	7	Tabas-A	0.1g	0.21	0.30	0.17
2	8	Tabas-A	0.2g	0.38	0.46	0.24
2	9	Tabas-A	0.3g	0.57	0.57	0.29
2	10	Tabas-A	0.5g	0.79	0.65	0.46
2	11	Tabas-A	0.7g	1.00	0.75	0.66
2	12	Tabas-A	1.0g	1.18	1.09	0.99
2	13	Tabas-B	1.2g	1.22	1.26	0.86
3	4	Tabas-A	1.0g	1.32	1.03	0.89
3	5	Tabas-A	1.0g	1.45	1.65	1.33

1. Tabas-A = spectrum-compatible Tabas-A earthquake histories; Tabas-B = spectrum-compatible Tabas-B earthquake histories
2. PGA = target peak acceleration of the simulator platform
3. Local coordinate system

horizontal motion for frequencies between 10 and 20 Hz. For reference, the fundamental frequency of the bushing in the *x*- and *y*- directions was approximately 8 Hz. For such a frequency the amplitude of the transfer functions range in value between 0.8 and 1.2. Accordingly, the mounting frame can be assumed to be *rigid* for the purpose of the experiments described below.

The amplification of horizontal motion above 10 Hz is due to rotational accelerations of the simulator platform which produce translational accelerations in the mounting frame. The rotational accelerations of the simulator platform are related to the oil-column frequencies of the vertical actuators that support the platform: the pitch and roll frequencies of the simulator are in the range of 13 to 18 Hz.

Table 4-6 Peak acceleration responses of the upper tip of the bushings

				Peak Acceleration (g)		
Bushing	*Test No.*	*Identification*[1]	*PGA*[2]	*x-direction*[3]	*y-direction*[3]	*Maximum*[4]
1	7	Tabas-A	0.1g	1.00	1.12	1.12
1	8	Tabas-A	0.2g	1.54	1.64	1.87
1	9	Tabas-A	0.3g	1.48	1.68	2.10
1	10	Tabas-A	0.5g	1.95	1.80	2.12
1	11	Tabas-A	0.5g	1.94	1.93	2.22
1	12	Tabas-A	0.7g	2.43	2.18	2.52
1	16	Tabas-A	0.7g	2.30	2.33	2.36
1	17	Tabas-A	1.0g	2.64	2.93	2.96
2	7	Tabas-A	0.1g	0.99	1.07	1.32
2	8	Tabas-A	0.2g	1.51	1.60	1.98
2	9	Tabas-A	0.3g	1.61	2.08	2.36
2	10	Tabas-A	0.5g	2.24	2.39	2.62
2	11	Tabas-A	0.7g	2.68	2.86	2.96
2	12	Tabas-A	1.0g	3.69	4.04	4.04
2	13	Tabas-B	1.2g	4.09	6.40	6.46
3	4	Tabas-A	1.0g	3.56	3.81	3.91
3	5	Tabas-A	1.0g	3.92	4.13	4.17

1. Tabas-A = spectrum-compatible Tabas-A earthquake histories; Tabas-B = spectrum-compatible Tabas-B earthquake histories
2. PGA = target peak acceleration of the simulator platform
3. Local coordinate system
4. Maximum vector value calculated at each time step in the response history

4.3.4 Response of Bushing-1

The global response of Bushing-1 was assessed by analysis of data from Test Number 17 (Tabas-A, target PGA equal to 1.0g). Figure 4-9 presents the translation histories in the global X- and Y-directions of the upper tip of Bushing-1 relative to the mounting frame. The maximum relative displacement between the bushing tip and the mounting frame was 2.20 in. (56 mm). The maximum total acceleration at the upper tip of the bushing was approximately 3.0g. Acceleration response spectra for Bushing-1 in the local coordinate system, generated using measured

Table 4-7 Peak relative tip displacement of the bushing relative to the mounting frame

				Peak relative displacement (in.)		
Bushing	*Test No.*	*Identification*[1]	*PGA*[2]	*X-direction*[3]	*Y-direction*[3]	*Maximum*[4]
1	7	Tabas-A	0.1g	0.20	0.32	0.32
1	8	Tabas-A	0.2g	0.23	0.31	0.32
1	9	Tabas-A	0.3g	0.26	0.39	0.40
1	10	Tabas-A	0.5g	0.46	0.54	0.57
1	11	Tabas-A	0.5g	0.47	0.67	0.69
1	12	Tabas-A	0.7g	0.93	0.95	1.11
1	16	Tabas-A	0.7g	0.78	0.88	0.94
1	17	Tabas-A	1.0g	1.70	1.51	2.20
2	7	Tabas-A	0.1g	0.17	0.23	0.25
2	8	Tabas-A	0.2g	0.23	0.30	0.35
2	9	Tabas-A	0.3g	0.24	0.38	0.41
2	10	Tabas-A	0.5g	0.37	0.47	0.47
2	11	Tabas-A	0.7g	0.50	0.58	0.64
2	12	Tabas-A	1.0g	0.89	1.14	1.14
2	13	Tabas-B	1.2g	0.97	1.67	1.68
3	4	Tabas-A	1.0g	0.91	1.29	1.35
3	5	Tabas-A	1.0g	1.44	2.15	2.40

1. Tabas-A = spectrum-compatible Tabas-A earthquake histories; Tabas-B = spectrum-compatible Tabas-B earthquake histories
2. PGA = target peak acceleration of the simulator platform
3. Global coordinate system
4. Maximum vector value calculated at each step in the response history

acceleration histories at the flange plate are shown in Figure 4-10. The zero-period accelerations for these spectra are given in Table 4-5. For information, the 2-percent and 5-percent damped IEEE 693-1997 response spectra for Moderate Level qualification (see row 5 of Table 3-1) are also shown in this figure.

Figure 4-11a shows the relation between the average vertical displacement in the local *z*-direction and rocking about the local *y*-axis. The average vertical displacement in the *z*-direction was calculated as one-half of the sum of the channel 51 and channel 53 displacements. Rocking about the local *y*-axis was calculated as the difference between the channel 51 and 53 displacements divided by the 36-in. (914 mm) distance between these transducers. Figure 4-11b shows the relation between the average vertical displacement in the local *z*-direction and rocking about the local *x*-axis. The average vertical displacement in the *z*-direction was calculated as one-half of the

Table 4-8 Peak local responses of UPPER-1 porcelain units

				Maximum response[3]		
Test Number	*Bushing*	*Identification*[1]	*PGA*[2]	*Porcelain strain (με)*	*Radial displacement (inches)*	*Vertical displacement (inches)*
1	7	Tabas-A	0.1g	14	0.010	0.005
1	8	Tabas-A	0.2g	22	0.014	0.009
1	9	Tabas-A	0.3g	27	0.018	0.013
1	10	Tabas-A	0.5g	36	0.036	0.024
1	11	Tabas-A	0.5g	33	0.051	0.028
1	12	Tabas-A	0.7g	47	0.261	0.053
1	16	Tabas-A	0.7g	67	0.040	0.040
1	17	Tabas-A	1.0g	100	0.410	0.090
2	7	Tabas-A	0.1g	15	0.007	0.004
2	8	Tabas-A	0.2g	19	0.011	0.007
2	9	Tabas-A	0.3g	22	0.012	0.010
2	10	Tabas-A	0.5g	39	0.015	0.014
2	11	Tabas-A	0.7g	31	0.020	0.018
2	12	Tabas-A	1.0g	74	0.041	0.036
2	13	Tabas-B	1.2g	140	0.520	0.100
3	4	Tabas-A	1.0g	76	0.060	0.040
3	5	Tabas-A	1.0g	490	1.100	0.126

1. Tabas-A = spectrum-compatible Tabas-A earthquake histories; Tabas-B = spectrum-compatible Tabas-B earthquake histories
2. PGA = target peak acceleration of the simulator platform
3. Local coordinate system; maximum displacement relative to flange plate for each test after zero-correction

sum of the channel 52 and channel 54 displacements; the rocking about the local *x*-axis was calculated as the difference between the channel 52 and 54 displacements divided by the 36-in. (914 mm) distance between these transducers. The maximum uplift at the edge of porcelain unit (listed in Table 4-8) can be computed by adding the product of the rocking angle and the radius of the UPPER-1 porcelain unit, at the flange plate, to the average longitudinal displacement.

Figure 4-12 presents the zero-corrected displacement orbit of the center of the bushing, measured at the height of the radial displacement transducers, relative to the flange plate. The coordinates (*x*,*y*) of the UPPER-1 porcelain unit at the start of the test (corresponding to prior slip of the unit) were (0.12, 0.20) inch. The predominant relative displacement of the bushing lies along an axis at

45 degrees to the local *x*-axis and *y*-axis of the bushing. It is noted that both the shear deformation in the gasket and the slip of UPPER-1 porcelain over the gasket contribute to the displacement orbit. At the conclusion of the test, the coordinates of the unit were (0.12, 0.32) in., corresponding to a 0.35 in. (9 mm) of total slip.

4.3.5 Response of Bushing-2

The global response of Bushing-2 was assessed by analysis of data from Test Number 13 (Tabas-B, target PGA equal to 1.2g). Figure 4-13 presents the translation histories in the global X- and Y-directions of the upper tip of Bushing-2 relative to the mounting frame. The maximum relative displacement between the bushing tip and the mounting frame was 1.68 in. (43 mm). The maximum total acceleration at the upper tip of the bushing exceeded 6.4g. Acceleration response spectra for Bushing-2 in the local coordinate system, generated using measured acceleration histories of the flange plate are shown in Figure 4-14. The zero-period accelerations for these spectra are given in Table 4-5. For information, the 2-percent and 5-percent damped IEEE 693-1997 response spectra for Moderate Level qualification (see row 5 of Table 3-1) are also shown in this figure.

Figure 4-15a shows the relation between the average vertical displacement in the local *z*-direction and rocking about the local *y*-axis. Figure 4-15b shows the relation between the average vertical displacement in the local *z*-direction and rocking about the local *x*-axis. Rocking of the UPPER-1 porcelain unit was accompanied by translation in the local *z*-direction. Such translation of 0.03 inch (0.8 mm) likely led to oil leakage.

Figure 4-16 presents the zero-corrected displacement orbit of the center of the bushing, measured at the height of the radial displacement transducers, relative to the flange plate. The coordinates (*x*,*y*) of the UPPER-1 porcelain unit at the start of the test (corresponding to prior slip of the unit) were (0.06, 0.06) inch. The predominant relative displacement of the bushing lies along the local *y*-axis of the bushing. It is noted that both the shear deformation in the gasket and the slip of UPPER-1 porcelain over the gasket contribute to the displacement orbit. At the conclusion of the test, the coordinates of the unit were (0.10, 0.58) in., corresponding to a 0.59 in. (15 mm) of total slip.

4.3.6 Response of Bushing-3

The global response of Bushing-3 was assessed by analysis of data from Test Number 5 (Tabas-A, target PGA equal to 1.0g). Figure 4-17 presents the translation histories in the global X- and Y-directions of the upper tip of Bushing-3 relative to the mounting frame. The maximum relative displacement between the bushing tip and the mounting frame was 2.40 in. (61 mm). The maximum total acceleration at the upper tip of the bushing was approximately equal to 4.2g. Acceleration response spectra for Bushing-3 in the local coordinate system, generated using measured acceleration histories of the flange plate are shown in Figure 4-18. The zero-period accelerations for these spectra are given in Table 4-5. For information, the 2-percent and 5-percent damped IEEE 693-1997 response spectra for Moderate Level qualification (see row 5 of Table 3-1) are also shown in this figure.

Figure 4-19a shows the relation between the average vertical displacement in the local *z*-direction and rocking about the local *y*-axis. Figure 4-19b shows the relation between the average vertical displacement in the local *z*-direction and rocking about the local *x*-axis. Rocking of the UPPER-1 porcelain unit was accompanied by translation in the local *z*-direction. Such translation of 0.07 in. (1.8 mm) likely led to oil leakage.

Figure 4-20 presents the displacement orbit of the center of the bushing, measured at the height of the radial displacement transducers, relative to the flange plate. The coordinates (*x*,*y*) of the UPPER-1 porcelain unit at the start of the test (corresponding to prior slip of the unit) were (0.01, 0.03) inch. The predominant relative displacement of the bushing lies along an axis at 45 degrees to the local *x*-axis and *y*-axis of the bushing. It is noted that both the shear deformation in the gasket and the slip of UPPER-1 porcelain over the gasket contribute to the displacement orbit. At the conclusion of the test, the coordinates of the unit were (0.72, 0.81) in., corresponding to a 1.1 in. (28 mm) of total slip.

4.4 Seismic Qualification of Bushing-3

To satisfy the IEEE 693-1997 requirements for Moderate Level qualification, the measured peak horizontal acceleration at the bushing flange is required to be 0.50g (see Appendix A). For this level of shaking, IEEE 693-1997 states that the stresses in the porcelain components must be less than 50 percent of the ultimate stress, and the factor of safety against oil leakage must be greater than or equal to 2.0. An alternative approach that is identified in Annex D5.1(d) of IEEE 693-1997 was used to evaluate qualification of Bushings. Namely, earthquake histories with spectral ordinates twice those of the Test Response Spectrum were used for testing: the target peak horizontal acceleration at the bushing flange was 1.0g. Porcelain stresses at this level of earthquake shaking were required to be less than or equal to the ultimate value, and there was to be no evidence of oil leakage. Similarly, qualification of transformer bushings at the High Level requires the use of earthquake histories with spectral ordinates twice those of the target spectrum described in the previous paragraph. Using a target peak acceleration for these histories of 2.0g, a bushing would be qualified at the High Level if the porcelain stresses were less than the ultimate value and there was no evidence of oil leakage.

Bushing-3 was built for the purpose of qualification to the Moderate Level. The bushing passed the requisite IEEE electrical tests prior to shipment to Berkeley for testing. Table 4-4 lists the tests of Bushing-3. Bushing-3 leaked oil and its UPPER-1 porcelain unit slipped significantly during Test Number 5 (see Figures 4-6 and 4-7). As such, data from Test Number 4 was used to judge the response of Bushing-3. The peak accelerations of the mounting frame during this test were 1.32g, 1.03g, and 0.89g, in the local *x*-, *y*-, and *z*-directions, respectively (see Table 4-5). Figure 4-21 presents 5-percent damped spectra evaluated using the *x*- and *y*-histories of the mounting plate of Test Number 4.

The peak input accelerations of the mounting plate exceed the zero-period accelerations of the IEEE spectrum (1.0g, 1.0g, and 0.8g, in the local *x*-, *y*-, and *z*-directions, respectively). The local *x*-direction spectral acceleration at the fundamental frequency of the bushing (8 Hz) exceeds the target IEEE spectral value of 2.5g by approximately 15 percent (see Figure 4-21a). The local *y*-

direction spectral acceleration at a frequency of 8 Hz is less than 80 percent of the target value (see Figure 4-21b). For qualification, the spectral accelerations in both principal directions must exceed the target IEEE values. As such, Bushing-3 did not meet the IEEE 693-1997 standards for qualification at the Moderate Level.

4.5 Fragility Testing of Bushings

4.5.1 Introduction

Fragility curves for electrical equipment are often developed using information from testing programs such as the program described in this report. Such curves typically relate the cumulative probability of exceeding a limit state to a ground motion parameter such as spectral acceleration or peak ground acceleration and serve to partly account for randomness and uncertainty in both seismic demand and component capacity. Seismic demand and component capacity are typically assumed to be random variables that conform to either a normal or log-normal distribution. Component performance can then be described by a log-normal distribution and the component fragility curve is given by a log-normal cumulative probability density function.

Peak ground acceleration is a poor seismic demand parameter because acceleration alone is a poor descriptor of the damage potential of an earthquake history. Spectral acceleration at the fundamental frequency of the bushing is an improved demand parameter but unless the installed configuration exactly replicates the tested configuration, spectral capacities measured in the laboratory are likely unreliable. (For example, the 550-kV bushings tested on the Berkeley simulator had no top-mounted terminal and were attached to a stiff mounting frame. In the field, such bushings are often equipped with terminals of significant weight, the terminals are connected to other substation equipment, and the bushings are mounted on transformers with flexible turrets. Such differences between the tested and installed configurations can substantially modify the dynamic characteristics of the bushings.) An average value of spectral acceleration over a broad range of frequencies would provide a better estimate of bushing capacity (resistance to either porcelain-unit slip or oil leakage) than a single value of spectral acceleration.

4.5.2 Fragility Data for Peak Ground (Input) Acceleration

Each value of peak acceleration listed below was taken as the greater of the maximum accelerations of the mounting frame along the local *x*- and *y*-axes for the test immediately prior to that test in which the specified limit state was exceeded. For example, if a bushing was subjected to increasing levels of ground shaking with each test in the fragility sequence, and if the bushing exceeded a limit state in Test 100, fragility data would be collected from Test 99. If during Test 99, the maximum local *x*- and *y*- accelerations of the mounting frame were 0.5g and 0.4g, respectively, the fragility data point would be taken as 0.5g. Although the utility of such an approach is questionable unless the reported acceleration is a principal acceleration and the limit state is exceeded due to shaking along the principal acceleration axis, this procedure is conventional and is therefore adopted herein.

If the limiting state of bushing response is oil leakage, Bushing-1 reached this limit state at a peak horizontal acceleration (in the local coordinate system) of 0.51g. (Bushing-1 leaked oil during Test Number 10 and fragility data are calculated using data from Test Number 9.) Bushing-2 and Bushing-3 reached this limit state at peak accelerations of 1.18g and 1.32g, respectively. If the limiting state of response is slip of the porcelain unit above the flange plate, Bushing-1 reached this limit state at a peak horizontal acceleration (in the local coordinate system) of 0.69g. Bushing-2 and Bushing-3 reached this limit state at peak accelerations of 1.18 and 1.32g, respectively.

Figure 4-21 illustrates this process for Test Number 4 of Bushing-3. The 5-percent damped spectra in parts (a) and (b) of this figure were generated using the acceleration histories of the mounting plate in the local *x*- and *y*-directions. The maximum accelerations of the mounting frame were 1.32 g and 1.03 g in the local *x*- and *y*-directions, respectively (see Table 4-5).

4.5.3 Fragility Data for Spectral Acceleration

Each value of spectral acceleration listed below was taken as the greater of the two spectral accelerations calculated using the acceleration histories of the mounting plate in the local *x*- and *y*-directions. If 5-percent damped spectral acceleration at the fundamental frequency of the bushing (=8 Hz) is used as the seismic demand parameter and if the limiting state of response is oil leakage, Bushing-1 reached this limit state at a spectral acceleration (in the local coordinate system) of 1.18g. Bushing-2 and Bushing-3 reached this limit state at spectral accelerations of 2.79g and 2.92g, respectively. If the limiting state of response is slip of the porcelain unit above the flange plate, Bushing-1 reached this limit state at a spectral acceleration (in the local coordinate system) of 1.53g. Bushing-2 and Bushing-3 reached this limit state at spectral accelerations of 2.79g and 2.92g, respectively.

Figure 4-21 illustrates this calculation for Test Number 4 of Bushing-3. At a frequency of 8 Hz (see vertical dash-dot line in the figure), the spectral accelerations in the local *x*- and *y*-directions were 2.92g and 1.88g, respectively.

4.5.4 Fragility Data for Average Spectral Acceleration

Average spectral acceleration over a range of frequencies including the fundamental frequency of the bushing will provide fragility data for a range of bushing-support conditions. If the test configuration includes a near-rigid mounting frame, the frequency range should be less than and equal to the fundamental frequency of the bushing. The spectral response should not vary widely over the selected frequency range otherwise the reported value may be substantially unconservative for a number of support conditions. A frequency range of 4 Hz to 8 Hz was selected to calculate the average spectral acceleration for these studies. If the limiting state of response is oil leakage, Bushing-1 reached this limit state at an average spectral acceleration (in the local coordinate system) of 0.99g. Bushing-2 and Bushing-3 reached this limit state at a average spectral accelerations of 2.85g and 2.94g, respectively. If the limiting state of response is slip of the porcelain unit above the flange plate, Bushing-1 reached this limit state at a average spectral acceleration (in the local coordinate system) of 1.48g. Bushing-2 and Bushing-3 reached this limit state at average spectral accelerations of 2.85g and 2.94g, respectively.

Figure 4-21 illustrates the above process for Test Number 4 of Bushing-3. In the frequency range of 4 Hz to 8 Hz, the average spectral accelerations in the local *x*- and *y*-directions were 2.94g and 2.39g, respectively (see the horizontal dashed line in each figure). In the local *x*- and *y*-directions, the spectral accelerations at a frequency of 8 Hz are equal to or less than the average spectral accelerations by factors of 1.0 and 0.8, respectively.

4.5.5 Fragility Estimates from Principal Acceleration Data

The fragility data presented in the preceding sections listed peak values and made use of measured acceleration histories in the local *x*- and *y*-directions of the 550 kV bushings. Although the approach adopted above constitutes conventional practice, it may be inappropriate for several reasons. First, if damage (oil leakage, slippage) is maximized along an axis that is rotated from the coordinate system from which the fragility data (maximum acceleration, spectral acceleration) were calculated, do the reported values correctly characterize the response of the bushing? Second, should principal acceleration data be used instead of acceleration data from the local coordinate system? Third, should maximum or minimum values be reported?

The following paragraphs present fragility data calculated using acceleration histories from coordinate systems (Axis 1, Axis 2) that are rotated from the local *x*- and *y*-directions. Such data are presented to foster discussion on the utility of the IEEE 693-1997 procedures for equipment fragility testing and qualification. No recommendations for changing the current IEEE procedures are made at this time.

Accelerations along axes rotated from the local x- and y-directions were calculated using the following transformation:

$$\begin{bmatrix} a_1 \\ a_2 \end{bmatrix} = \begin{bmatrix} \cos\theta & \sin\theta \\ -\sin\theta & \cos\theta \end{bmatrix} \begin{bmatrix} a_x \\ a_y \end{bmatrix} \tag{4-1}$$

where a_1 and a_2 are the accelerations along Axis 1 and Axis 2, respectively; θ is the angle of rotation from the horizontal (*x*) axis (measured in the *x*-*y* plane); and a_x and a_y are the accelerations along the local *x*- and *y*-axes. Table 4-9 lists peak and spectral acceleration data for 10-degree increments of axis rotation for Test Number 4 of Bushing-3. Figure 4-22 presents 5-percent damped acceleration response spectra for 10-degree increments of axis rotation for Test Number 4 of Bushing-3. For reference, Bushing-3 slipped in a direction at 45 degrees to the local coordinate system (see Figure 4-20 for Test Number 5).

In the unrotated coordinate system, the *fragility* peak acceleration of Bushing-3 was 1.32g. In the direction of slip, the maximum peak acceleration of 1.50g is greater than the *fragility* peak acceleration by 15 percent. The minimum value of peak acceleration was 0.92g, 70 percent of the *fragility* value in the unrotated coordinate system.

Columns 4 and 5 of Table 4-9 list 5-percent damped spectral accelerations at a frequency of 8 Hz. The *fragility* spectral acceleration of Bushing-3 was 2.92g. The maximum and minimum values of spectral acceleration listed in columns 4 and 5 are 112 percent and 62 percent of the *fragility* spectral acceleration. Figure 4-22 shows the variations in spectral response along Axes 1 and 2 as a function of the rotation angle θ.

Mean values of spectral acceleration in the frequency range of 4 to 8 Hz are listed in columns 6 and 7 of Table 4-9. Such a frequency range would cover a broad range of support conditions for a bushing with a fundamental frequency of 8 Hz. The maximum and minimum values of spectral acceleration listed in these columns are 110 percent and 70 percent of the *fragility* spectral acceleration. In this frequency range, the ordinates of the response spectra (see Figure 4-21) vary widely and the use of mean spectral values might be unconservative.

Variations in spectral response over a frequency range could be addressed through the use of mean-minus-one-standard-deviation values of spectral acceleration. For Test Number 4, these values of spectral acceleration range between 80 and 90 percent of mean values, and the maximum and minimum values are 93 percent and 59 percent of the *fragility* spectral acceleration of 2.92g.

4.5.6 Summary

Conventional procedures for reporting fragility data for substation equipment such as transformer may be neither appropriate nor conservative. The fragility data reported above were based on earthquake simulator testing of a bushing installed in a *rigid* mounting frame. This configuration is likely not representative of a field installation because (a) bushings are often mounted on flexible components, (b) terminals of significant weight are often attached to the upper tip of the bushing, and (c) the terminals are connected to other substation equipment. Such differences could substantially modify both the modal properties of the bushing and the critical loading environment.

Putting aside these shortcomings, the fragility data presented in the previous sections are substantially scattered. Maximum and minimum values for different fragility parameters are summarized in Table 4-10. Use of the minimum values for the fragility parameters will be conservative but will likely be misleading. Improved strategies for characterizing the fragility of substation equipment are obviously needed.

Table 4-9 Fragility data for Bushing-3, Tabas-A, Test Number 4

	PGA *[g]*[1]		*PSa(f=8Hz,ξ=0.05)* *[g]*[2]		*PSa(4<f<8Hz,ξ=0.05)*$_{\mu}$ *[g]*[3]		*PSa(4<f<8Hz,ξ=0.05)*$_{\mu-1\sigma}$ *[g]*[4]	
θ[5]	*Axis 1*	*Axis 2*	*Axis 1*	*Axis 2*	*Axis 1*	*Axis 2*	*Axis 1*	*Axis 2*
0	1.32	1.03	2.92	1.88	2.94	2.39	2.65	2.10
10	1.40	1.00	3.13	1.83	3.11	2.21	2.70	1.89
20	1.45	0.95	3.25	1.89	3.20	2.10	2.71	1.78
30	1.50	0.92	3.27	1.94	3.22	2.06	2.66	1.72
40	1.51	0.98	3.19	1.95	3.17	2.13	2.58	1.82
50	1.48	1.00	3.02	2.15	3.06	2.29	2.46	2.03
60	1.40	1.09	2.75	2.29	2.91	2.46	2.34	2.21
70	1.28	1.16	2.40	2.39	2.73	2.60	2.25	2.37
80	1.15	1.26	2.13	2.65	2.56	2.74	2.21	2.52
90	1.03	1.32	1.88	2.92	2.39	2.94	2.10	2.65

1. Peak acceleration of mounting plate along axes of rotated (*Axis 1, Axis 2*) coordinate system
2. Spectral acceleration at frequency of 8 Hz and damping ratio of 5 percent, along axes of rotated (*Axis 1, Axis 2*) coordinate system
3. Mean spectral acceleration over frequency range of 4 Hz to 8 Hz and damping ratio of 5 percent, along axes of rotated (*Axis 1, Axis 2*) coordinate system
4. Mean minus one standard deviation spectral acceleration over frequency range of 4 Hz to 8 Hz and damping ratio of 5 percent, along axes of rotated (*Axis 1, Axis 2*) coordinate system
5. Counter-clockwise angle of rotation of local (*x,y*) coordinate system into (*Axis 1, Axis 2*) coordinate system

Table 4-10 Summary of fragility data for Bushing-3 from Test Number 4

	PGA *[g]*[1]	*PSa(f=8Hz,ξ=0.05)* *[g]*[2]
Maximum	1.52	3.27
Minimum	0.92	1.83

1. Peak acceleration of mounting plate along all axes of rotated (*Axis 1, Axis 2*) coordinate system
2. Spectral acceleration at frequency of 8 Hz and damping ratio of 5 percent, along all axes of rotated (*Axis 1, Axis 2*) coordinate system

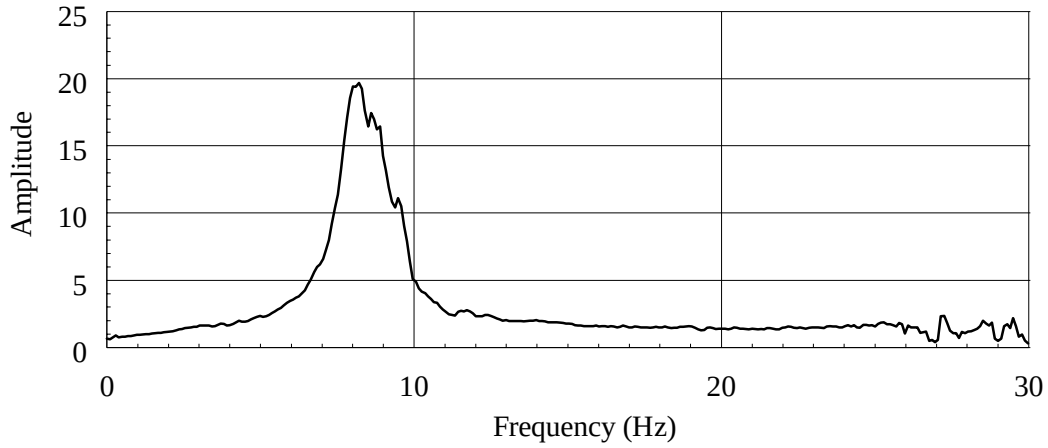

a. *x*-direction

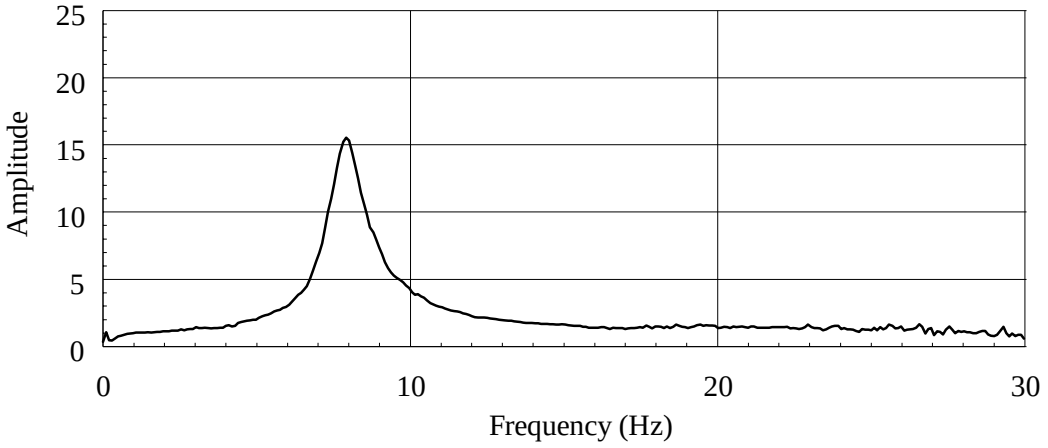

b. *y*-direction

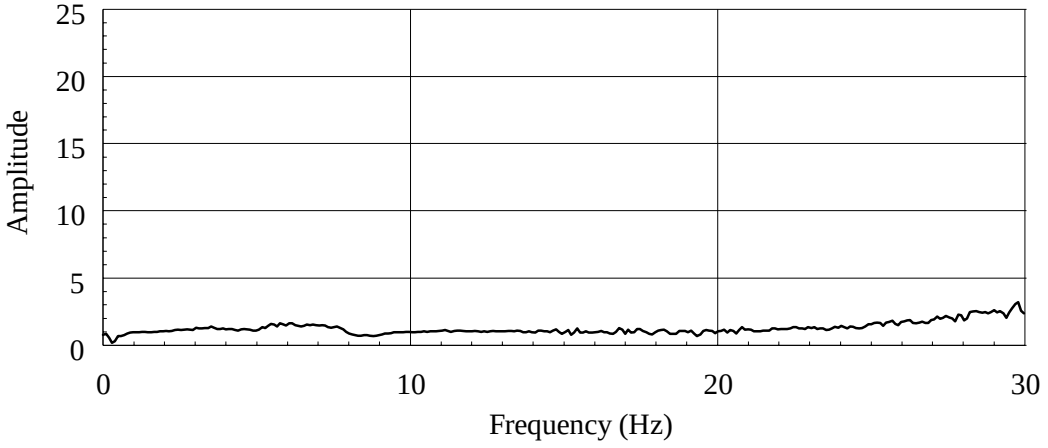

c. *z*-direction

Figure 4-1 Bushing-1 upper tip to mounting frame transfer functions

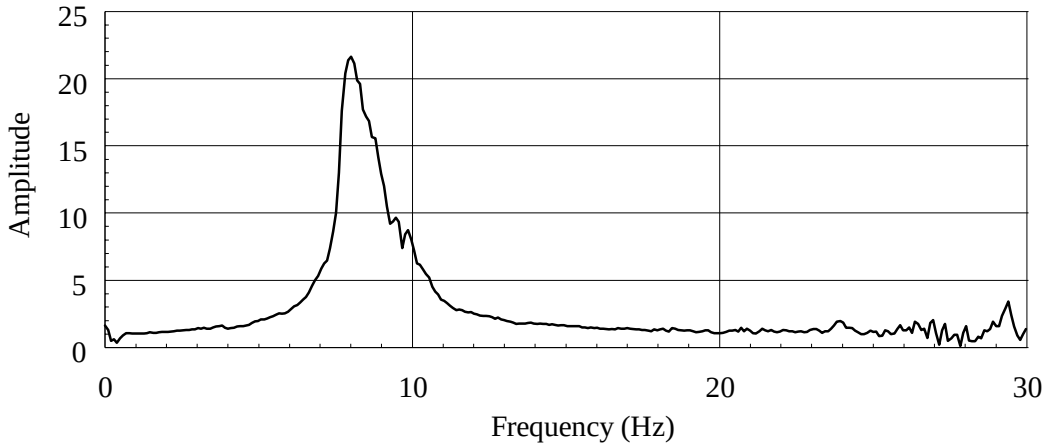

a. *x*-direction

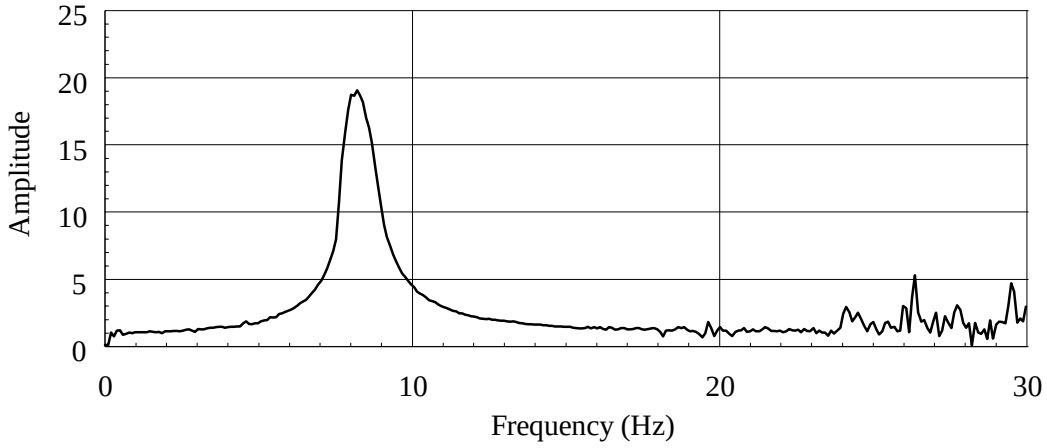

b. *y*-direction

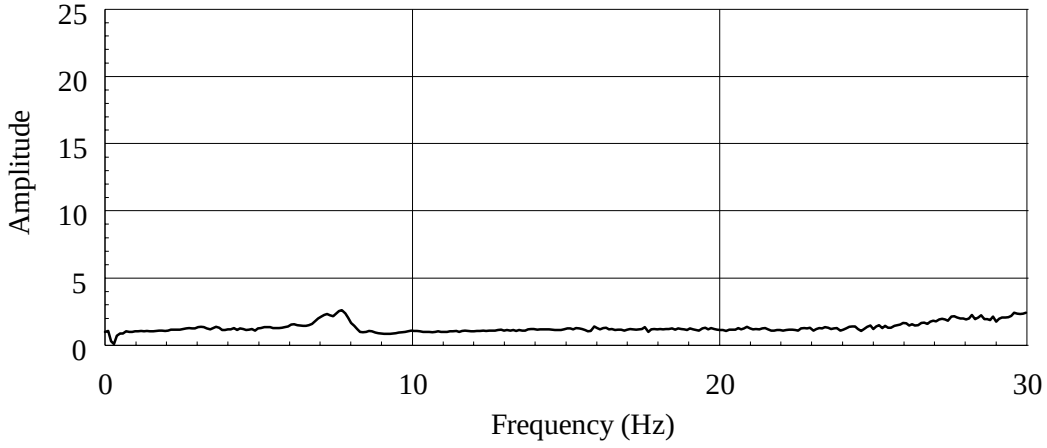

c. *z*-direction

Figure 4-2 Bushing-2 upper tip to mounting frame transfer functions

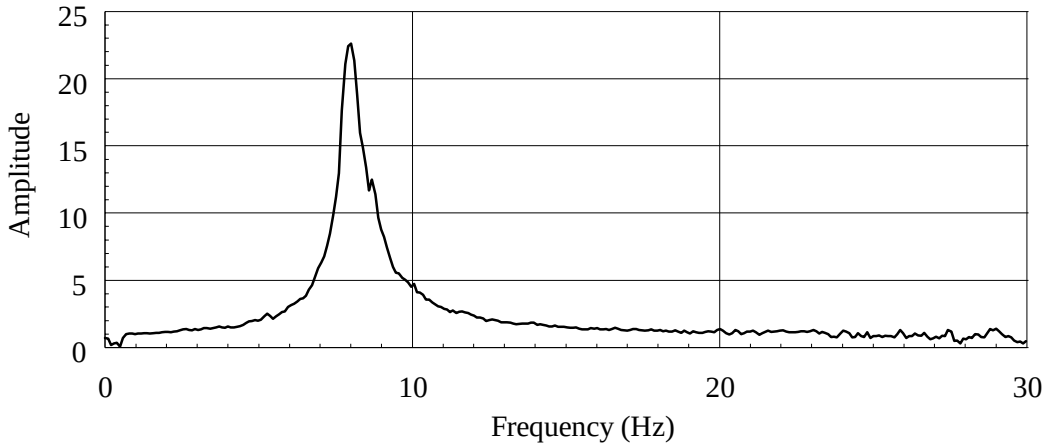

a. *x*-direction

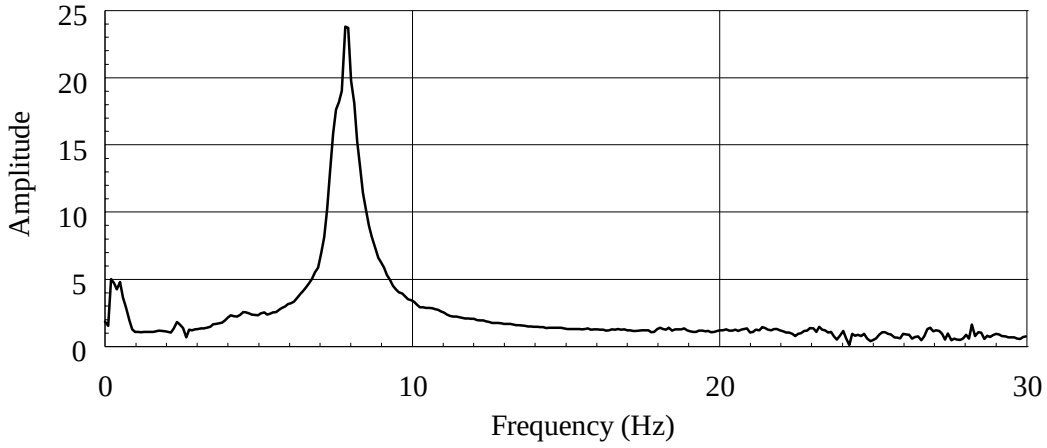

b. *y*-direction

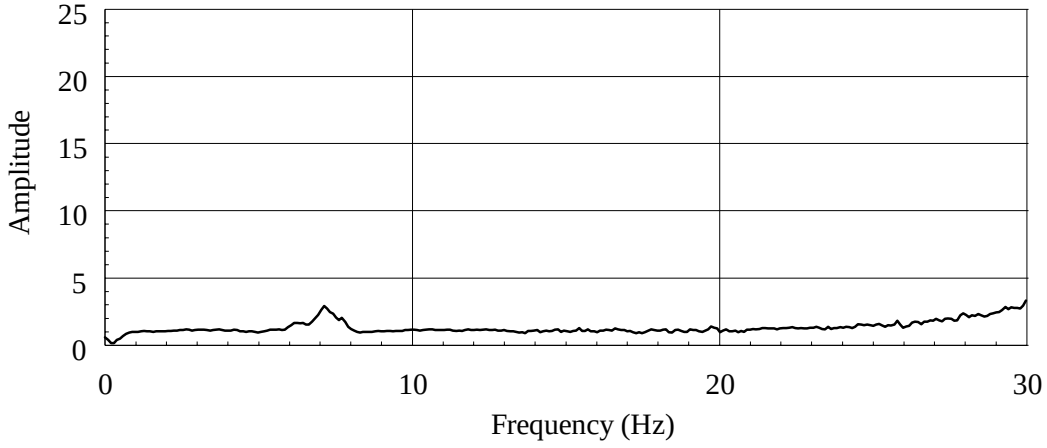

c. *z*-direction

Figure 4-3 Bushing-3 upper tip to mounting frame transfer functions

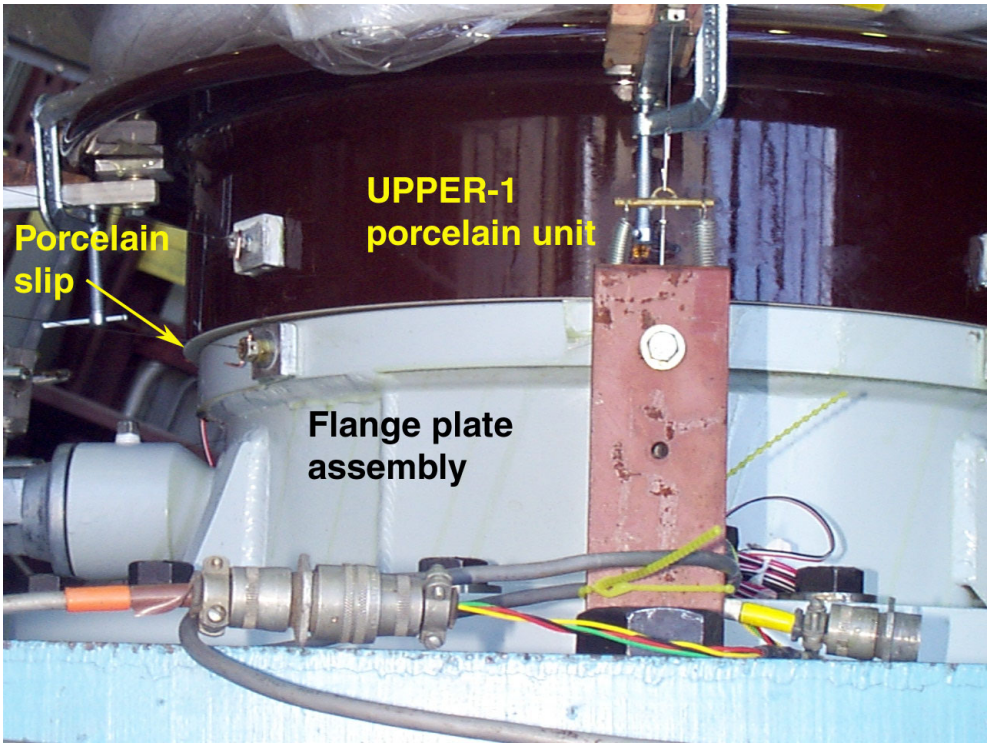

Figure 4-4 Bushing-1 following Test Number 12 showing UPPER-1 porcelain unit slip

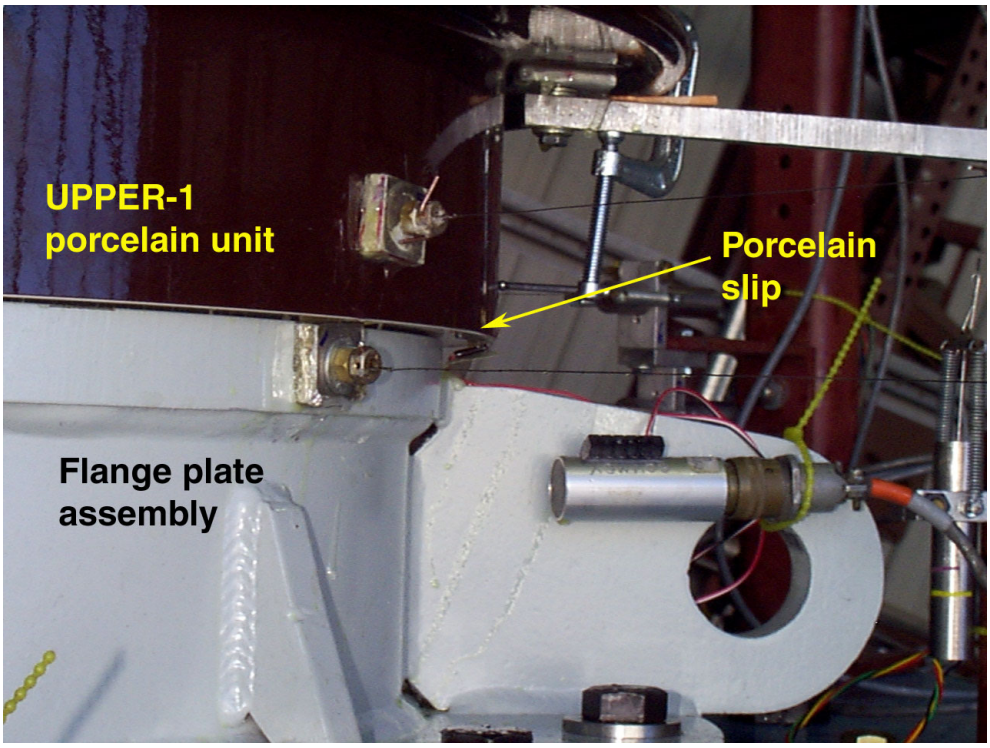

Figure 4-5 Bushing-2 following Test Number 13 showing UPPER-1 porcelain unit slip

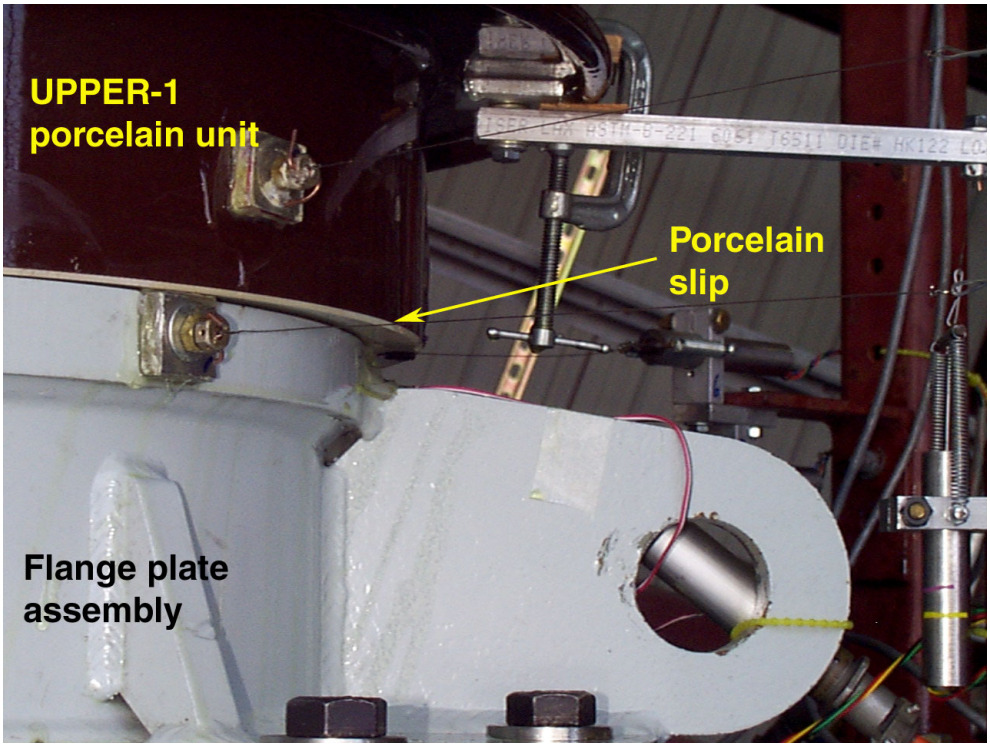

Figure 4-6 Bushing-3 following Test Number 5 showing UPPER-1 porcelain unit slip

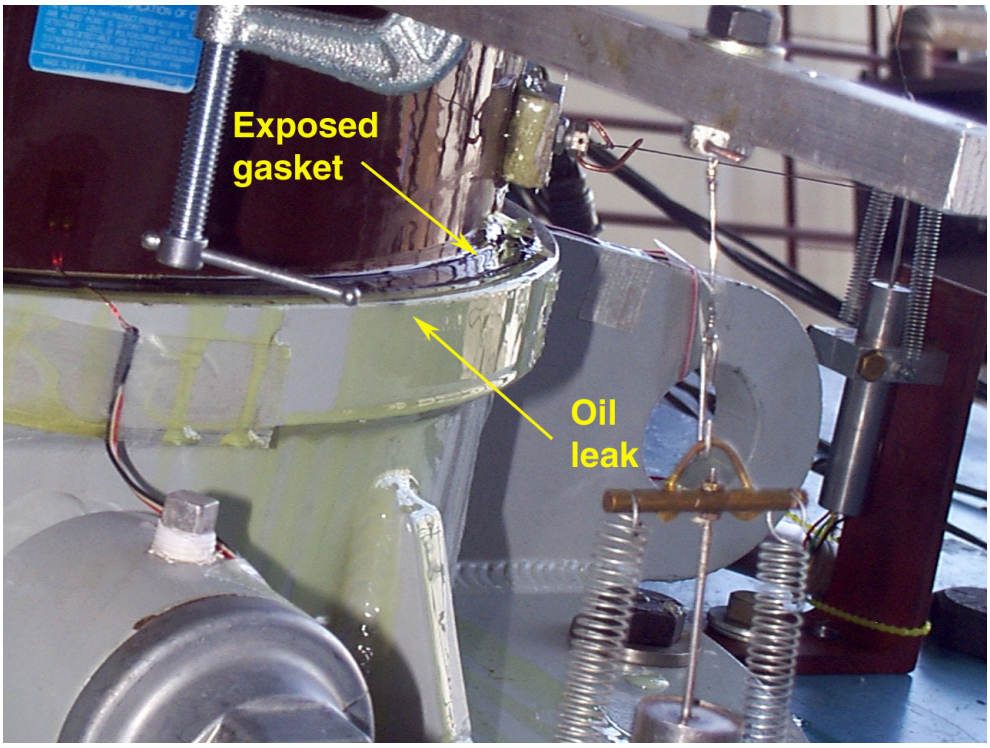

Figure 4-7 Bushing-3 following Test Number 5 showing the exposed gasket

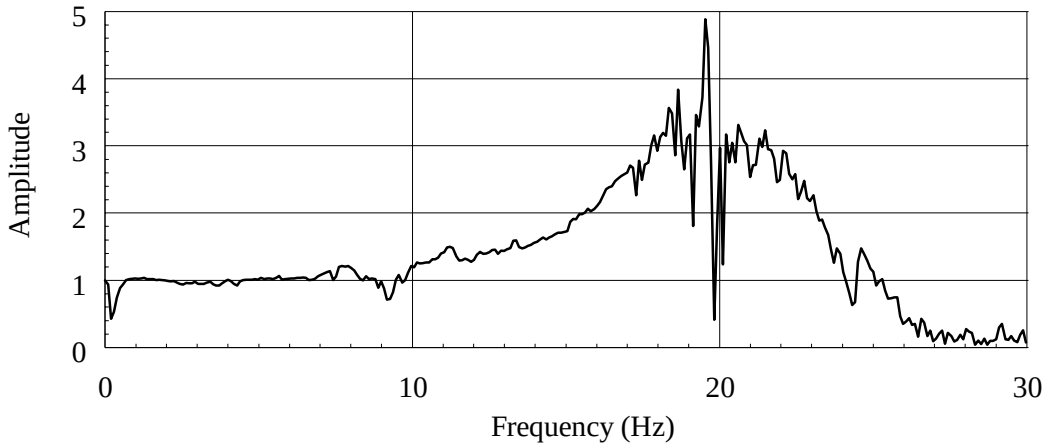

a. X-direction

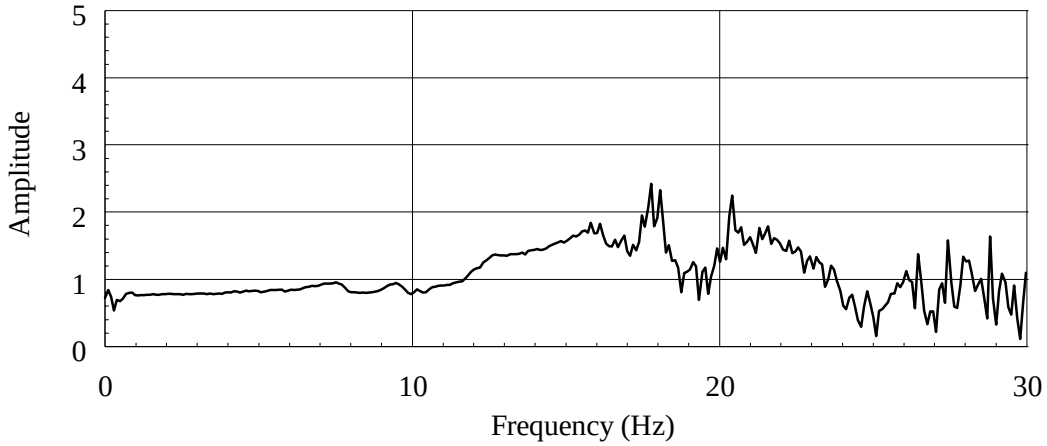

b. Y-direction

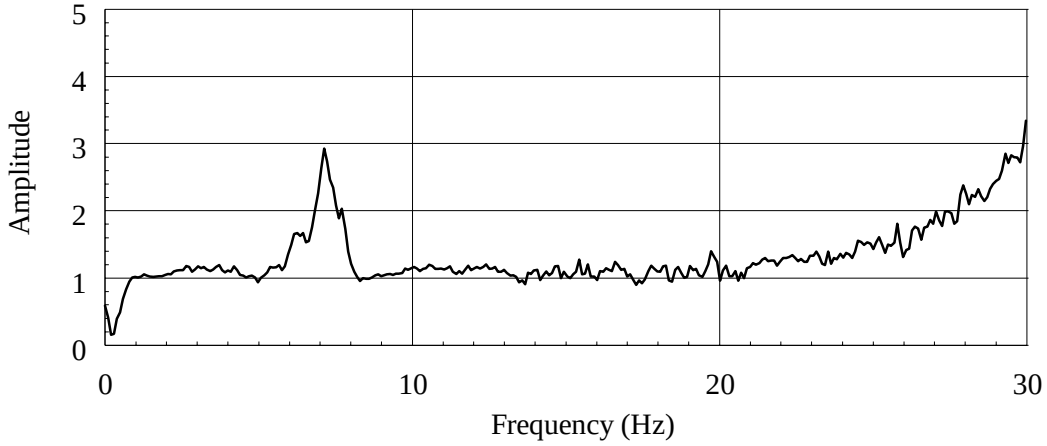

c. Z-direction

Figure 4-8 Mounting frame to earthquake simulator transfer functions

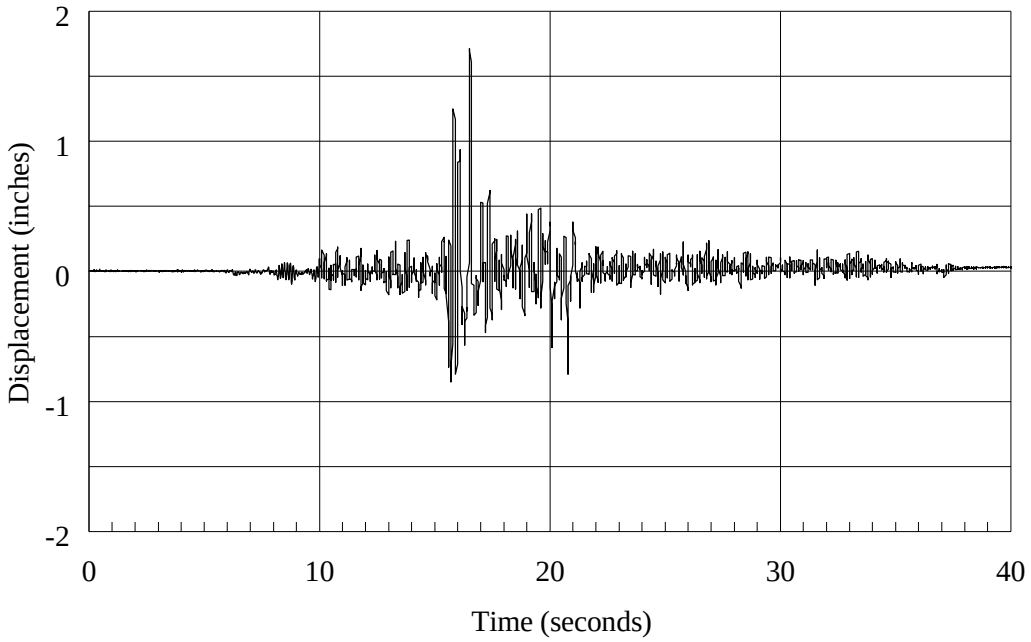

a. X-direction

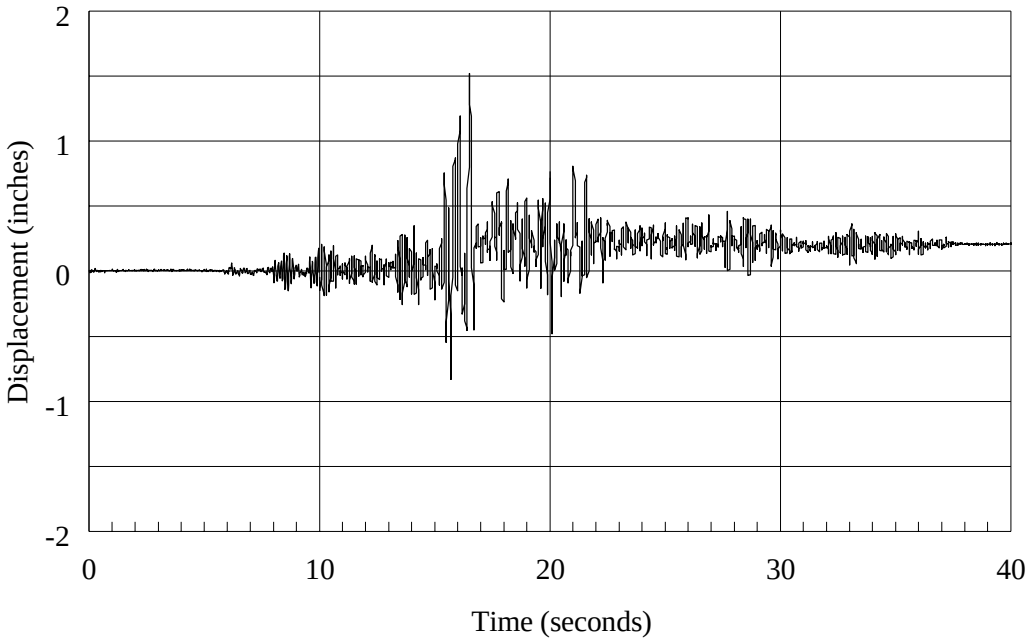

b. Y-direction

Figure 4-9 Relative displacement response of upper tip of Bushing-1, Test Number 17, Tabas-A, target PGA = 1.0g

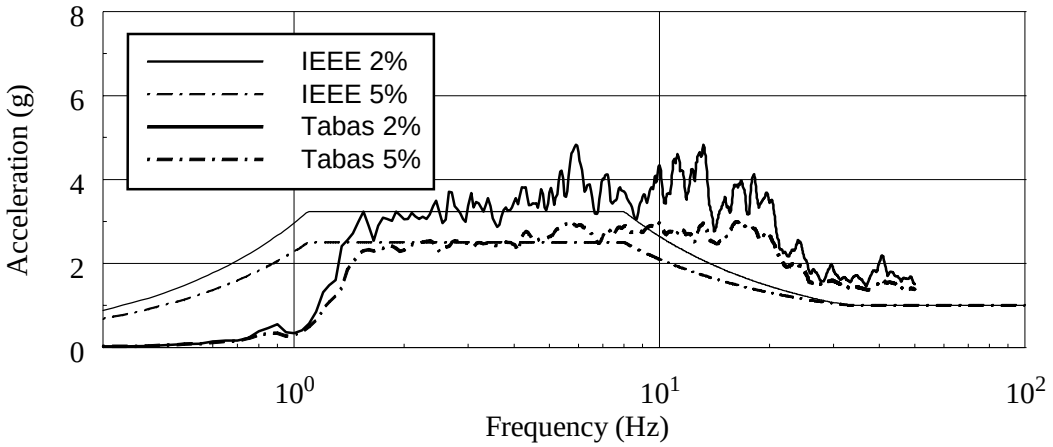

a. *x*-direction

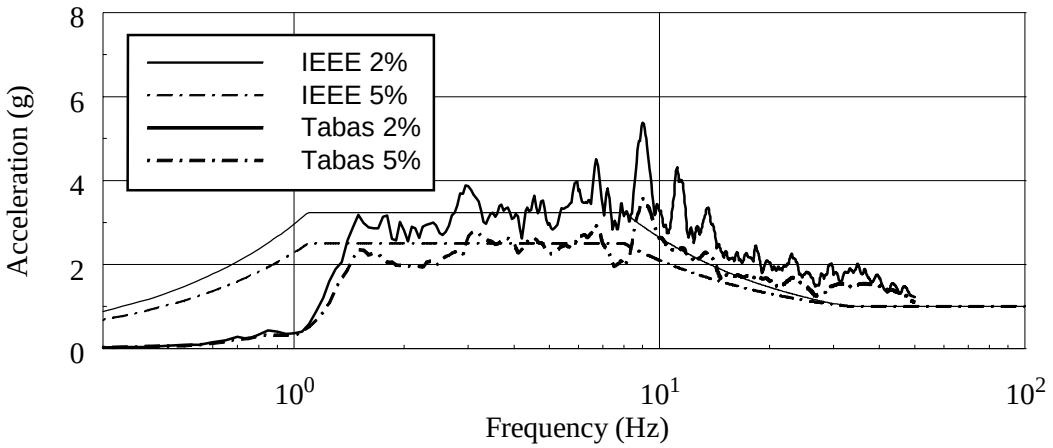

b. *y*-direction

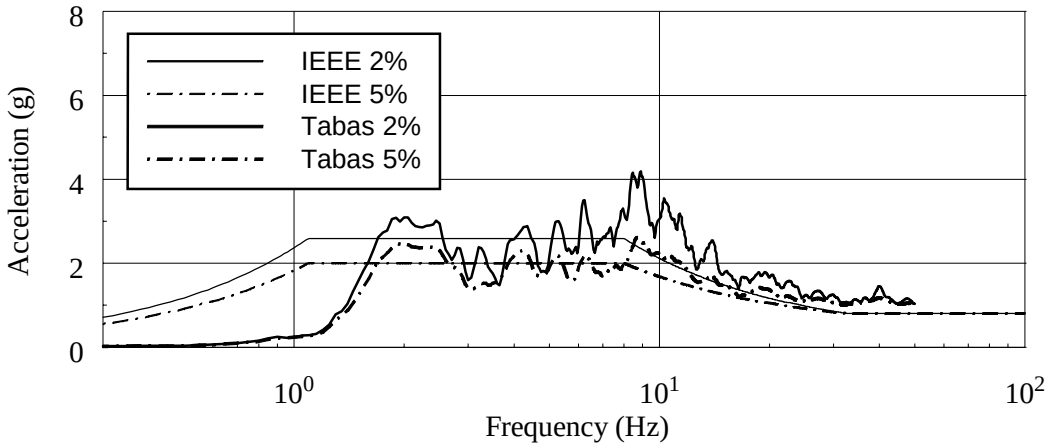

c. *z*-direction

Figure 4-10 Acceleration response spectra calculated using measured mounting frame acceleration histories for Bushing-1, Test Number 17, Tabas-A, target peak acceleration = 1.0g

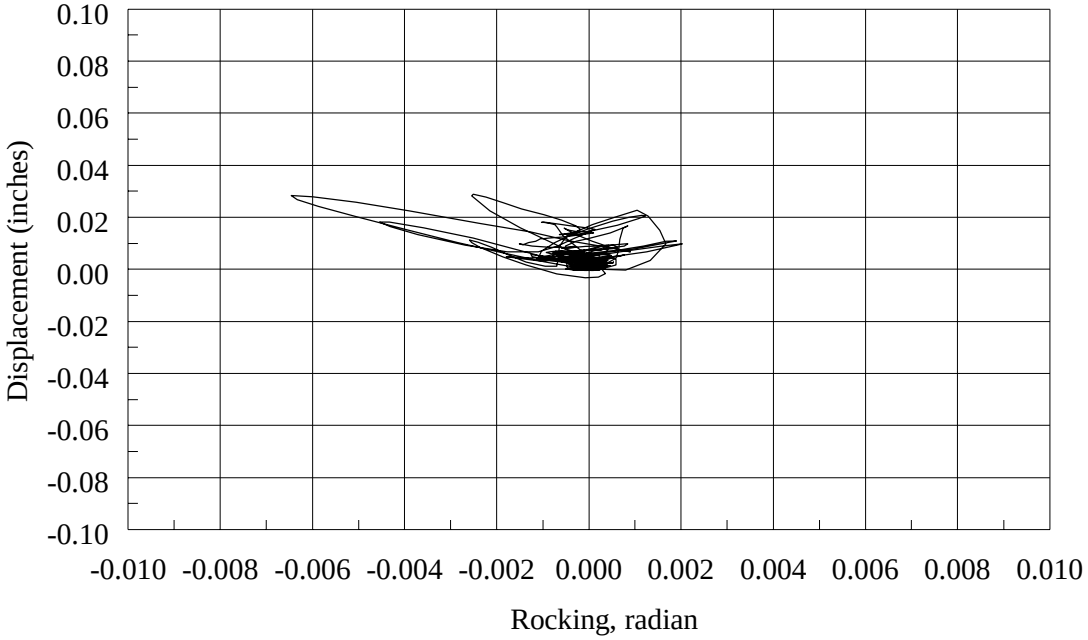

a. rocking about *y*-axis*s*

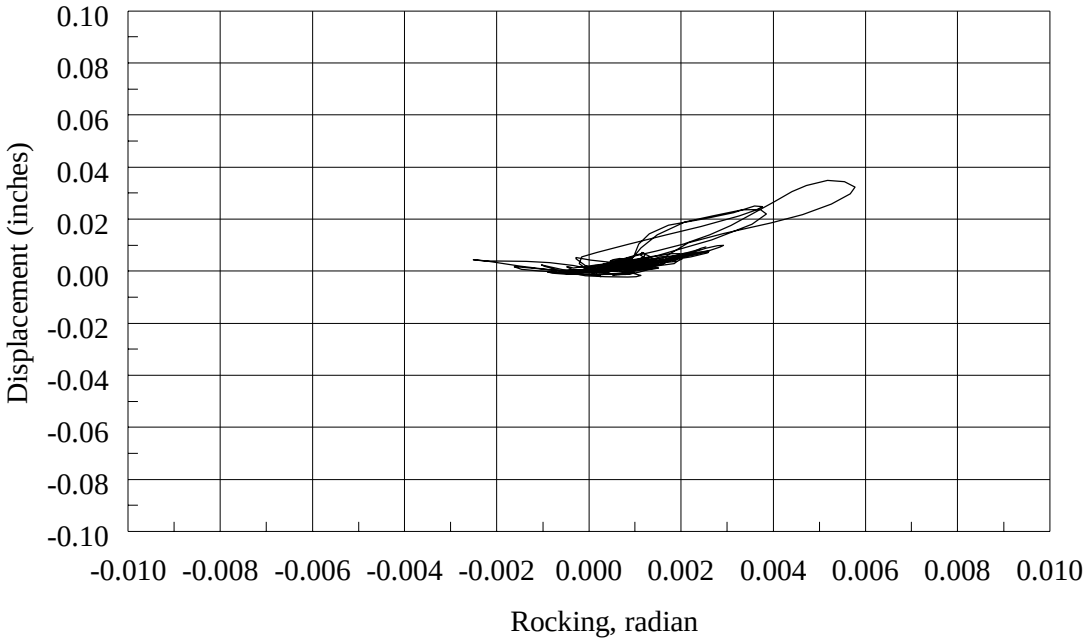

b. rocking about *x*-axis

Figure 4-11 Average relative vertical displacement versus rocking response of Bushing-1, Test Number 17, Tabas-A, target PGA = 1.0g

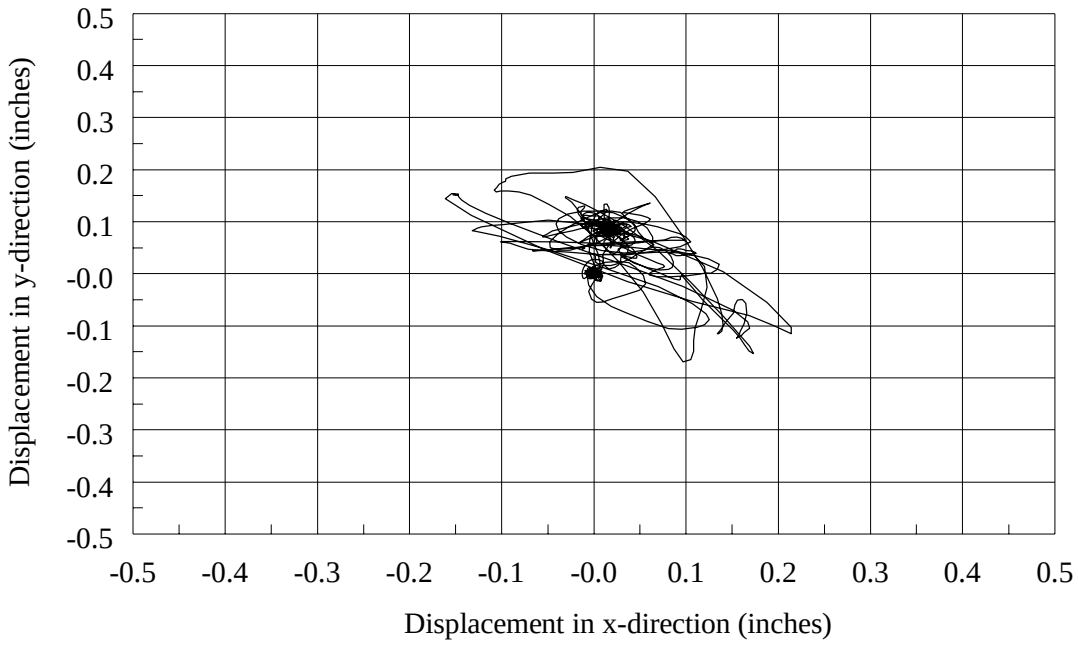

Figure 4-12 Orbit of relative displacement of UPPER-1 porcelain unit over gasket for Bushing-1, Test Number 17, Tabas-A, target PGA = 1.0g

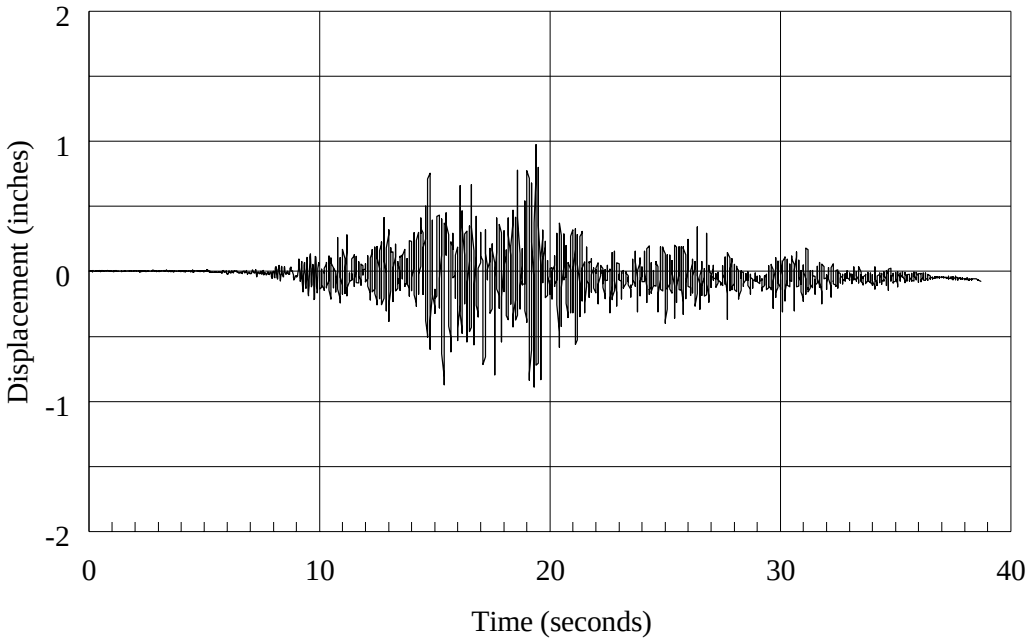

a. X-direction

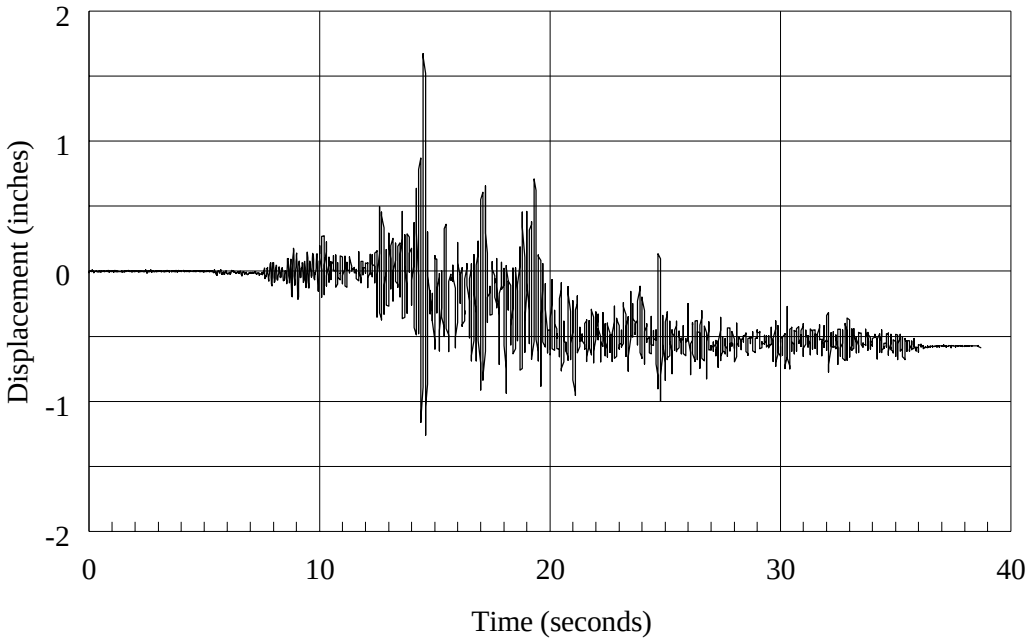

b. Y-direction

Figure 4-13 Relative displacement response of upper tip of Bushing-2, Test Number 13, Tabas-B, target PGA = 1.2g

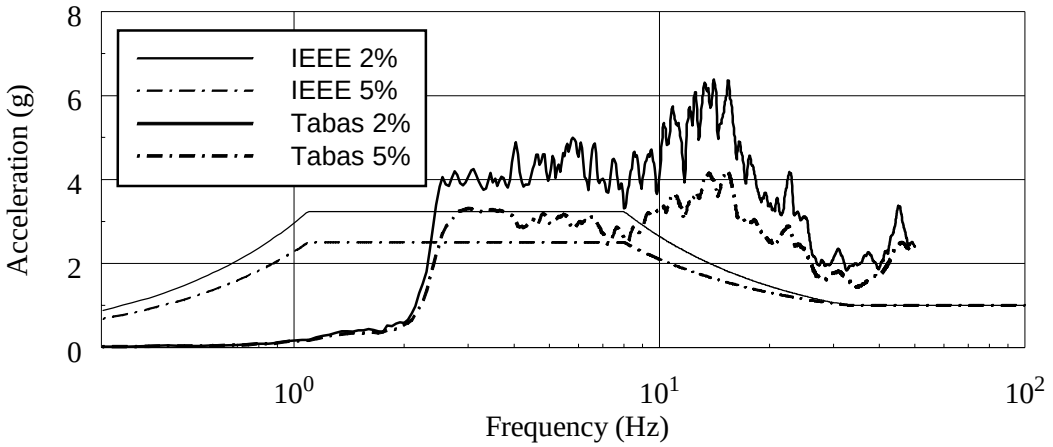

a. *x*-direction

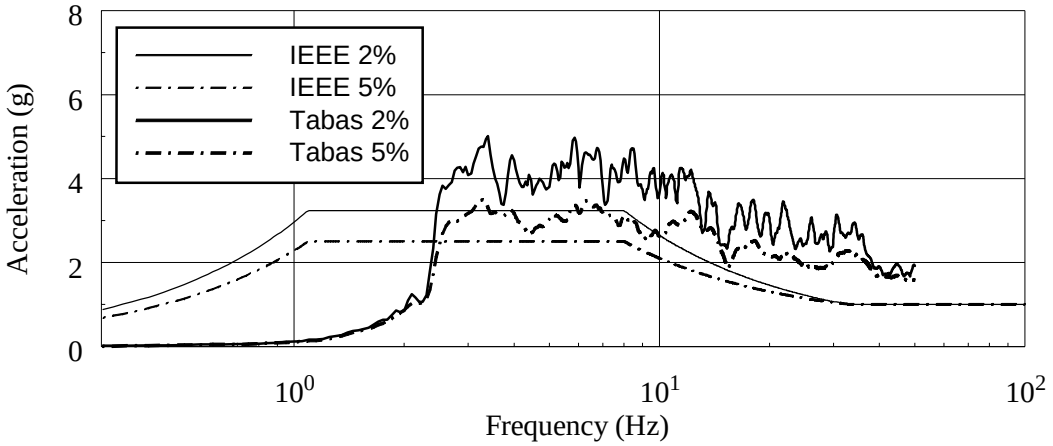

b. *y*-direction

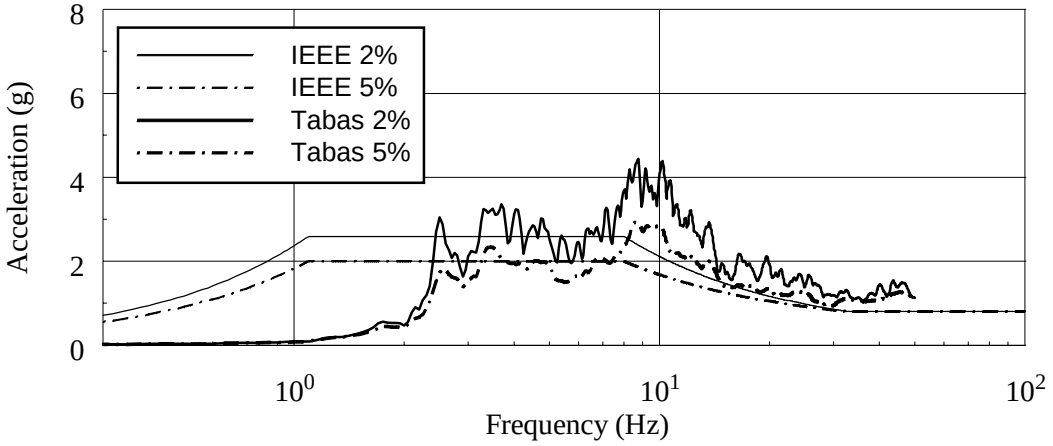

c. *z*-direction

Figure 4-14 Acceleration response spectra calculated using measured mounting frame acceleration histories for Bushing-2, Test Number 13, Tabas-B, target peak acceleration = 1.2g

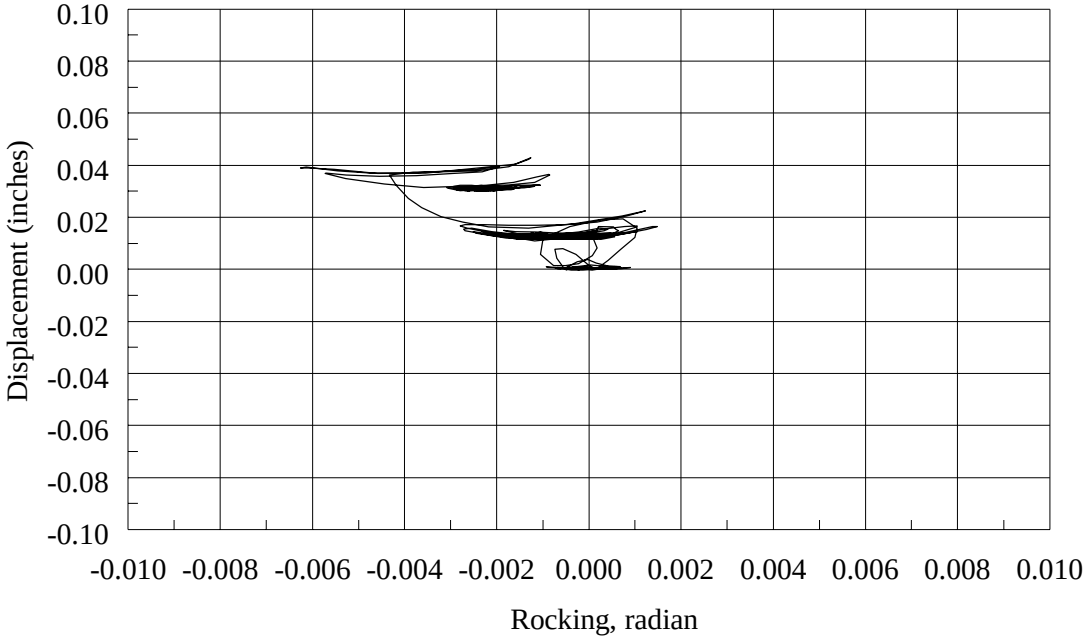

a. rocking about *y*-axis

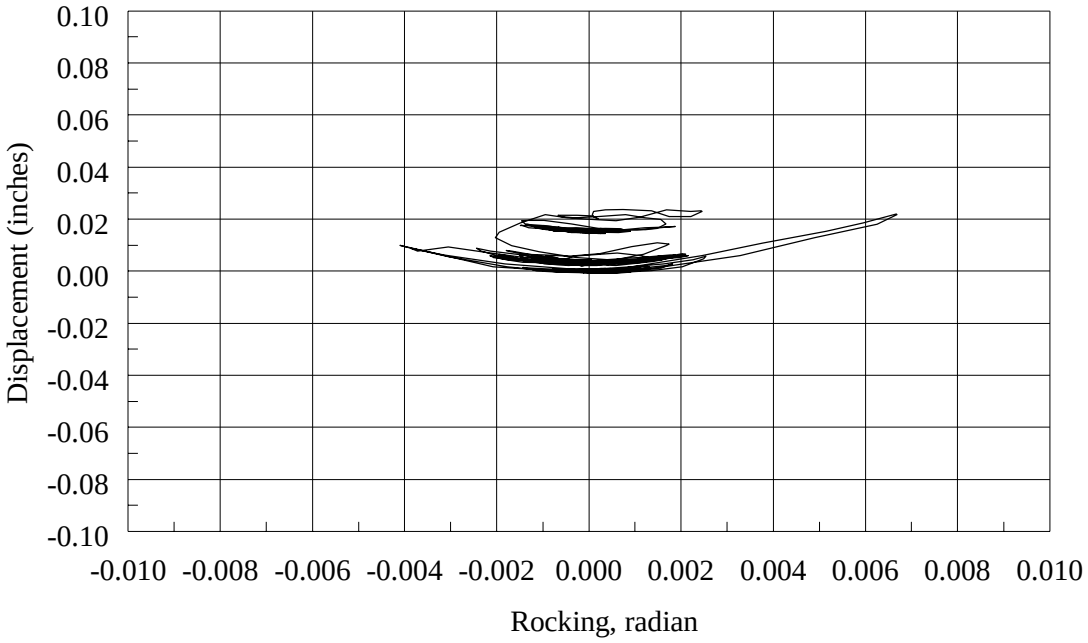

b. rocking about *x*-axis

Figure 4-15 Average relative vertical displacement versus rocking response of Bushing-2, Test Number 13, Tabas-B, target PGA = 1.2g

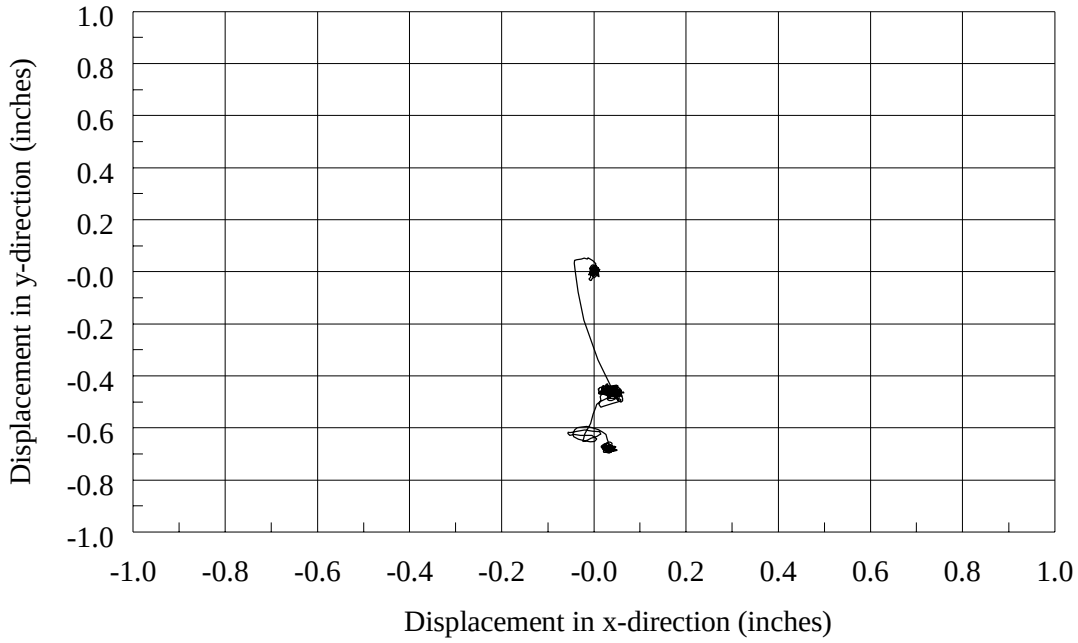

Figure 4-16 Orbit of relative displacement of UPPER-1 porcelain unit over gasket for Bushing-2, Test Number 13, Tabas-B, target PGA = 1.2g

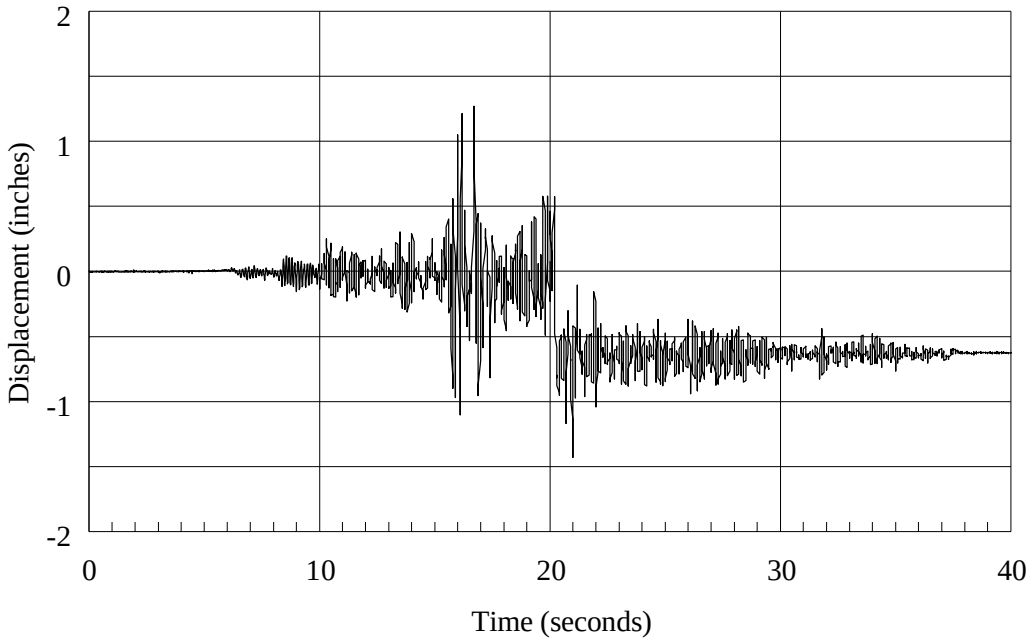

a. X-direction

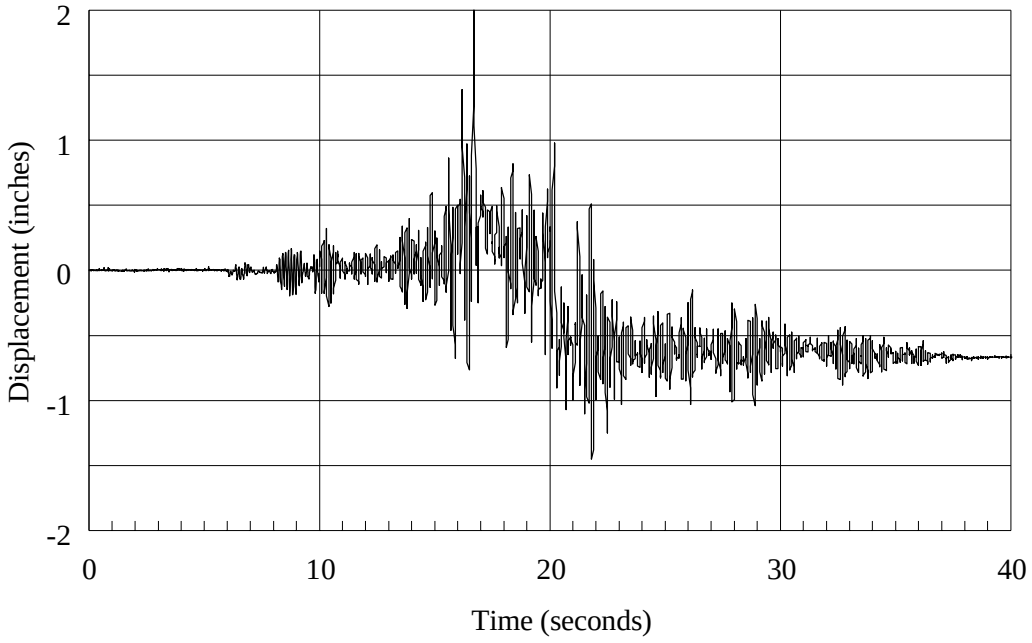

b. Y-direction

Figure 4-17 Relative displacement response of upper tip of Bushing-3, Test Number 5, Tabas-A, target PGA = 1.0g

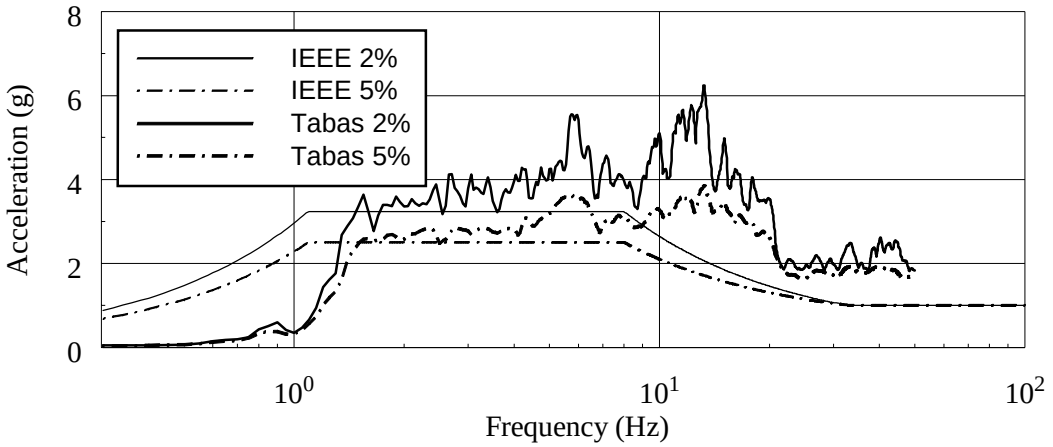

a. *x*-direction

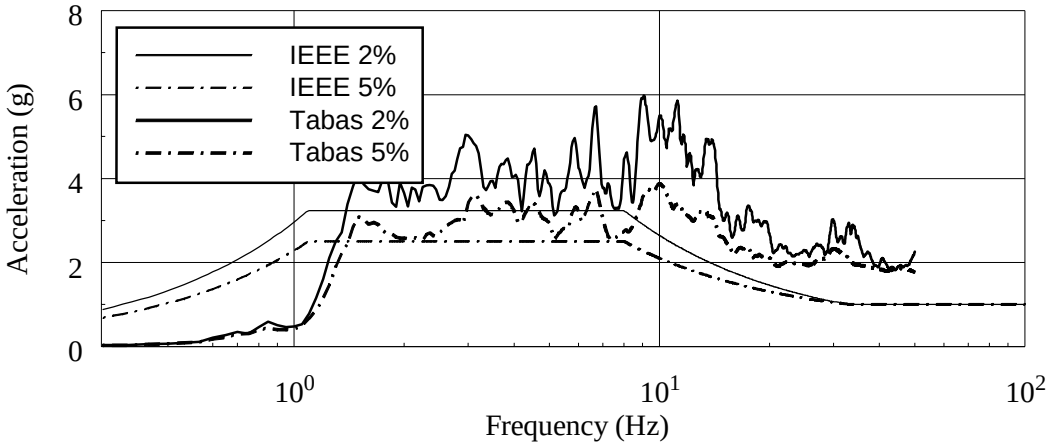

b. *y*-direction

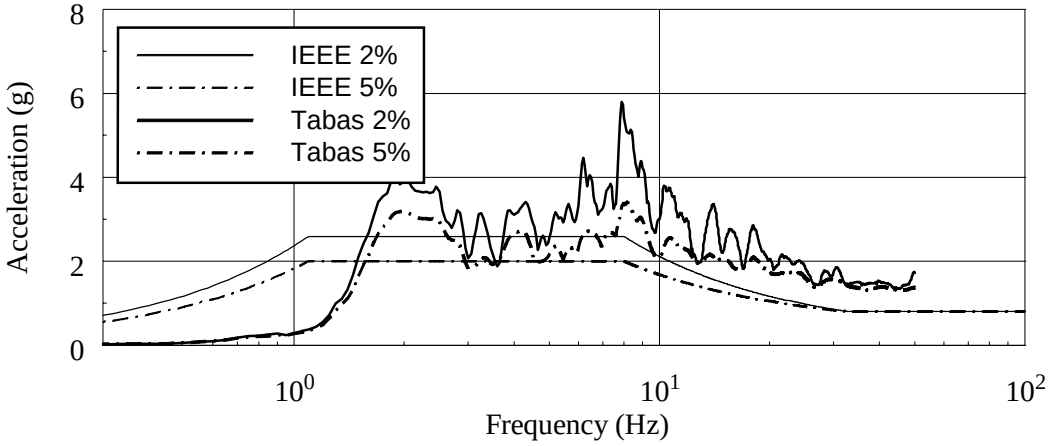

c. *z*-direction

Figure 4-18 Acceleration response spectra calculated using measured mounting frame acceleration histories for Bushing-3, Test Number 5, Tabas-A, target peak acceleration = 1.0g

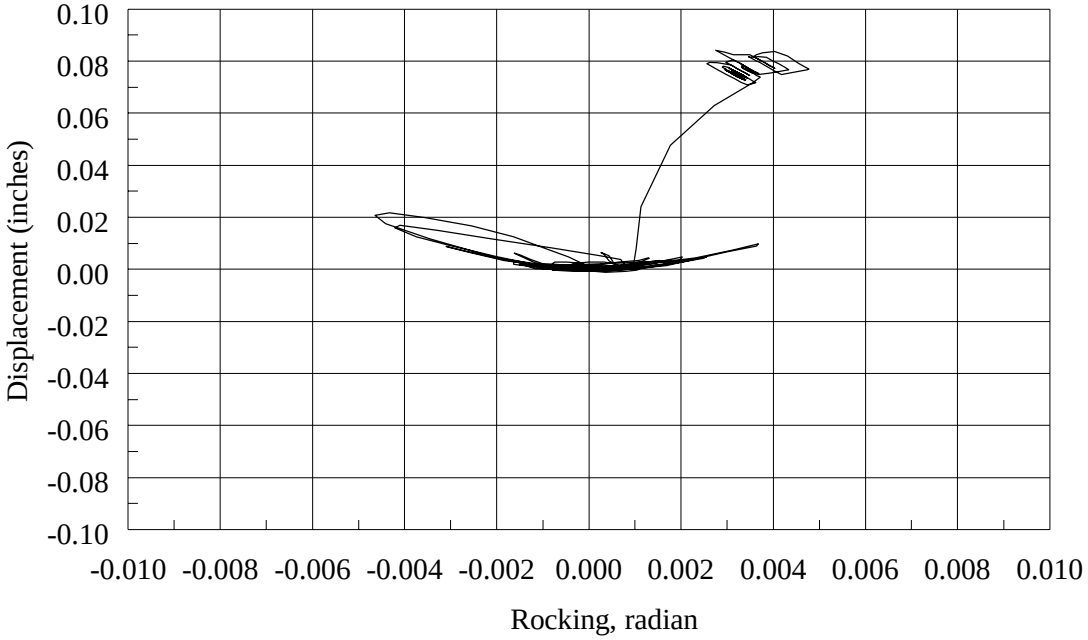

a. rocking about *y*-axis

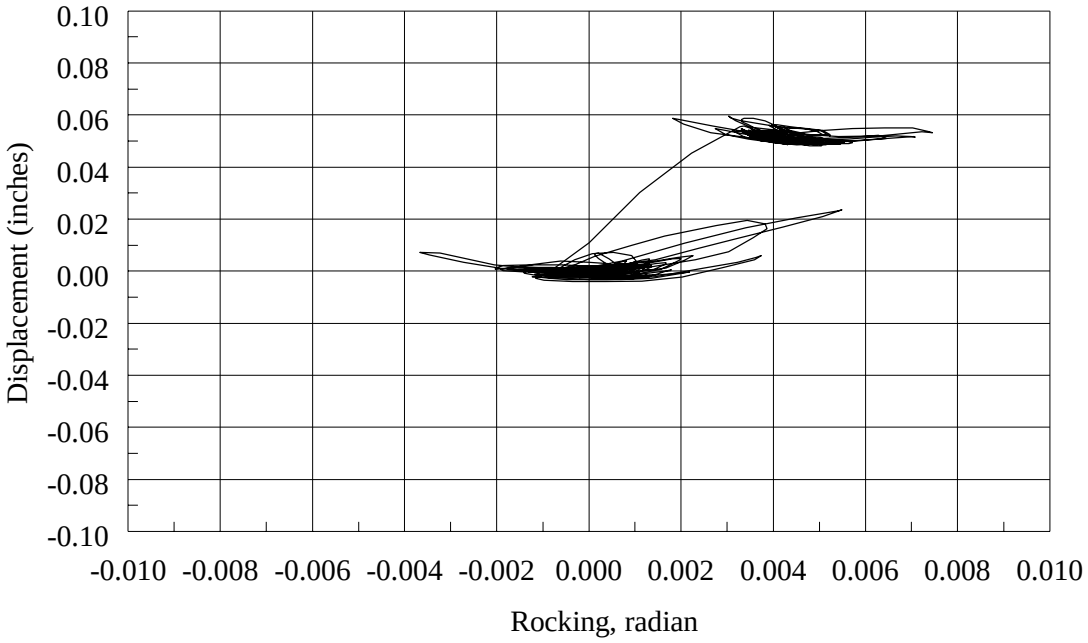

b. rocking about *x*-axis

Figure 4-19 Average relative vertical displacement versus rocking response of Bushing-3, Test Number 5, Tabas-A, target PGA = 1.0g

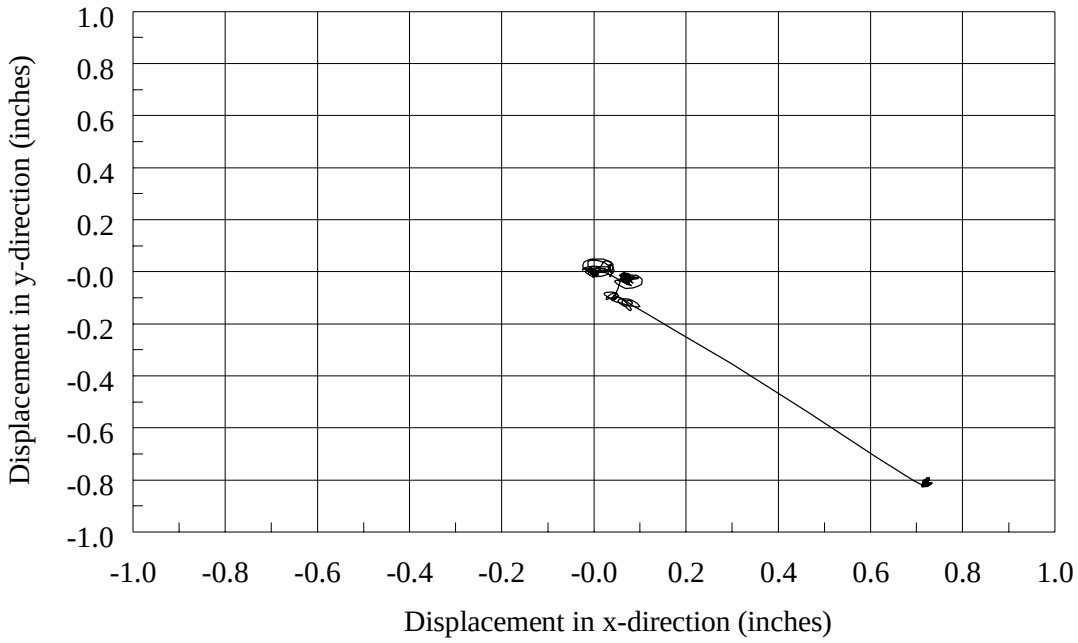

Figure 4-20 Orbit of relative displacement of UPPER-1 porcelain unit over gasket for Bushing-3, Test Number 5, Tabas-A, target PGA = 1.0g

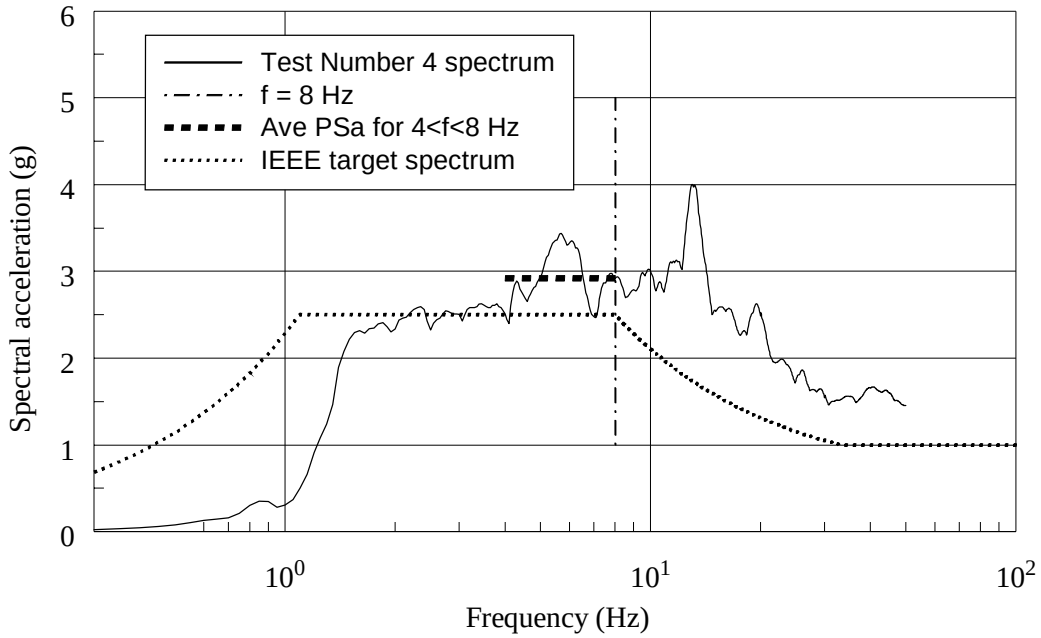

a. local *x*-direction

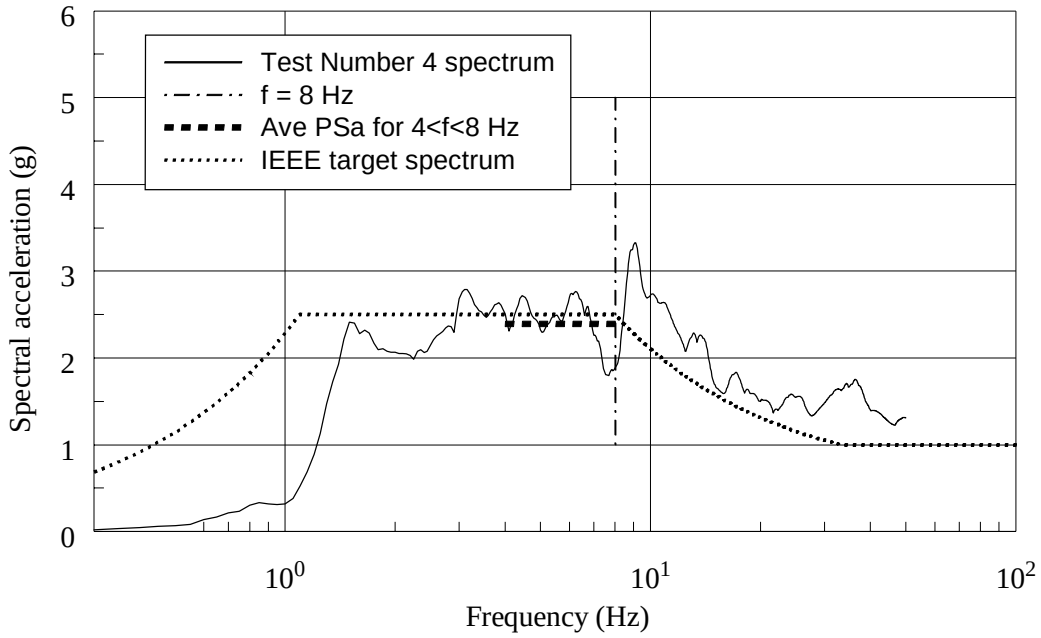

b. local *y*-direction

Figure 4-21 Fragility data for Bushing-3, Tabas-A, Test Number 4

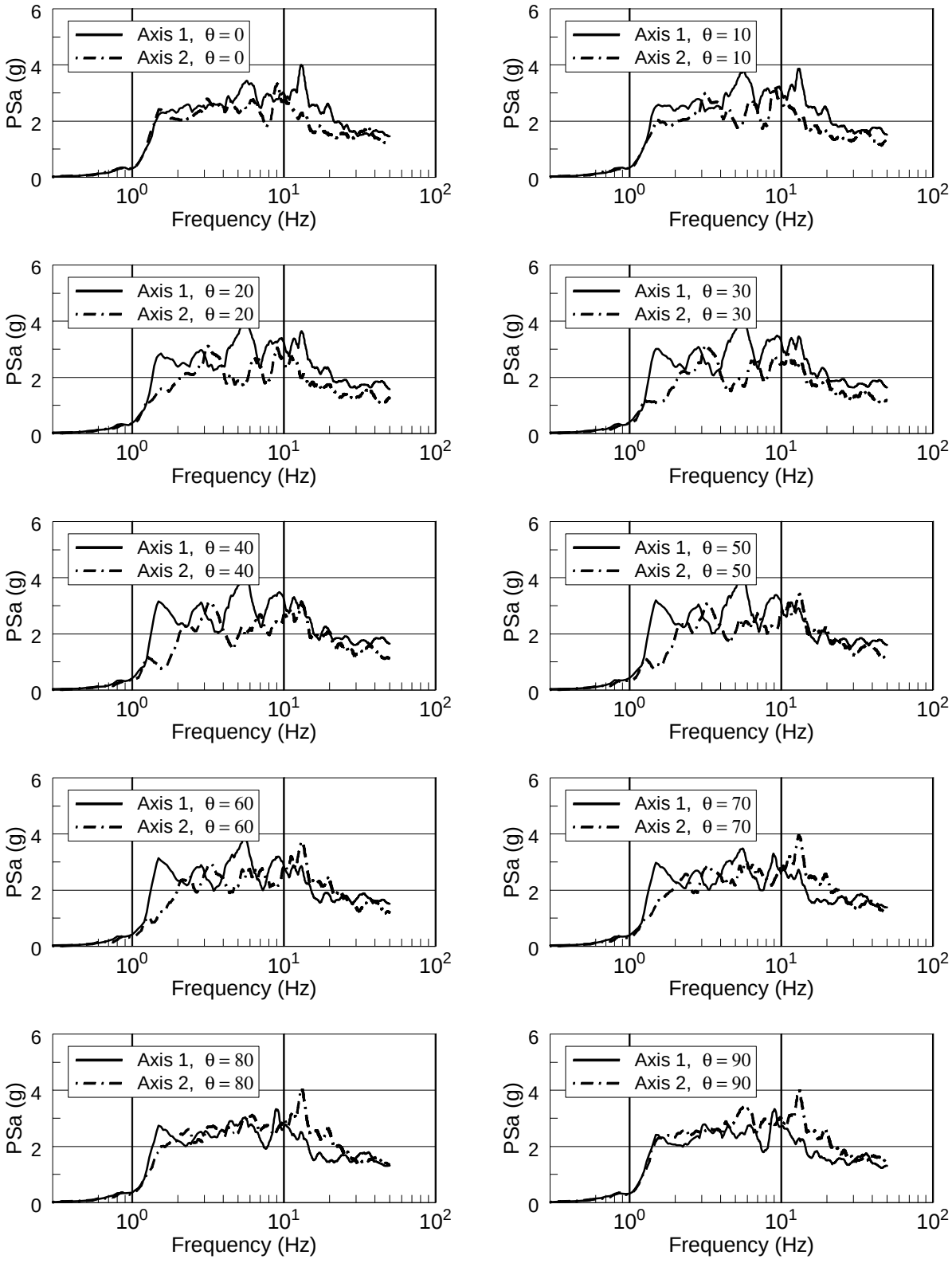

Figure 4-22 Acceleration response spectra for rotated components for Bushing-3, Tabas-A, Test Number 4

CHAPTER 5
SUMMARY AND CONCLUSIONS

5.1 Summary

5.1.1 Introduction

The reliability and safety of electrical transmission and distribution systems after an earthquake depend on the seismic response of individual substation components such as transformer bushings. Post-earthquake reconnaissance of electrical substations has identified porcelain transformer bushings as being particularly vulnerable to severe earthquake shaking.

Pacific Gas & Electric (PG&E) Company sponsored a research project to investigate the seismic response of in-service and proposed-modified 550 kV transformer bushings. The key objectives of the project were to: (1) develop earthquake ground motion records suitable for the seismic evaluation, qualification and fragility testing of bushings, (2) test three 550 kV bushings on the earthquake simulator at the Pacific Earthquake Engineering Research (PEER) Center using levels of earthquake shaking consistent with those adopted for seismic qualification and fragility testing of electrical equipment, (3) reduce and analyze the data acquired from the earthquake simulator tests, and (4) draw conclusions about the seismic performance of porcelain transformer bushings, including the likely failure modes of a bushing during severe earthquake shaking, the efficacy of the improvements in the modified bushings, and the utility of the seismic qualification and fragility testing procedures set forth in IEEE 693-1997.

5.1.2 Earthquake testing program

The earthquake testing was performed on the earthquake simulator at the Pacific Earthquake Engineering Research Center, which is headquartered at the University of California, Berkeley. The 20 ft by 20 ft (6.1 by 6.1 m) simulator can accommodate models up to 140 kips (623 kN) in weight and 40 ft (12.2 m) in height.

The three 550 kV bushings were supplied by ABB Power T&D Company, Inc., Components Division (ABB) for earthquake testing. Bushing-1 was similar to bushings that are currently in service in the United States and was designated for fragility testing. Bushing-2 and Bushing-3 were modified versions of Bushing-1 incorporating design changes intended to improve the seismic performance of 550 kv bushings. The modifications consisted of: (a) increased preload on the bushing, (b) use of a rubber-impregnated fiber gasket and an O-ring seal instead of nitrile rubber gasket at the porcelain-to-flange plate connection, and (c) increased spring travel in the bushing dome by use of multi-tiered springs. Bushing-2 was designated for fragility testing and Bushing-3 was identified for qualification testing.

For earthquake testing, the bushings were mounted on a support frame that was designed to accommodate 550 kV bushings. The mounting plate in the frame was sloped at 20 degrees measured to the vertical because a bushing qualified at this angle is deemed by IEEE 693-1997 to be qualified for all angles between vertical and 20 degrees measured to the vertical. Bushings

were attached to the support frame using 12 3/4" bolts. During the test program, there was no evidence of slip between the bushing flange plate and the mounting plate.

Earthquake simulation testing of the bushings consisted of resonant search tests (sine-sweep and white-noise) and triaxial earthquake-history tests. The resonant search tests were undertaken to establish the dynamic characteristics of the bushings. The first modal frequency of the bushing was approximately 8 Hz; this frequency corresponded to motion in the local *x-y* plane. The first mode damping ratio for Bushing-1 prior to earthquake testing was approximately 4 percent of critical. No values of modal frequency and damping ratio for response along the local z-axis or longitudinal axis of the bushing could be evaluated using the resonant search tests.

The earthquake histories used for triaxial shaking of the bushings were derived from sets of ground motion records recorded during the 1978 Tabas, Iran, earthquake. The time-domain procedures of Abrahamson were used to develop IEEE spectrum-compatible earthquake histories. Two three-component sets of IEEE spectrum-compatible motions were developed: Tabas-A for tests with peak horizontal accelerations up to 1.0g, and Tabas-B for tests with peak horizontal accelerations exceeding 1.0g.

For the Moderate Level qualification of Bushing-3, the earthquake histories were matched to the 2- and 5-percent damped IEEE spectra with peak accelerations of 1.0g (horizontal shaking) and 0.8g (vertical shaking). At this level of shaking, the porcelain stresses are required to be less than or equal to the ultimate value and the bushing must show no evidence of oil leakage. Test Number 5 met the requirements of IEEE 693-1997 for qualification at the Moderate Level. During this test, Bushing-3 leaked oil and its UPPER-1 porcelain unit slipped substantially above the gasket and flange plate. As such, Bushing-3 did not qualify at the Moderate Level.

Bushing-1 and Bushing-2 were fabricated for the purpose of fragility testing. Two limiting states of response were identified for fragility testing: oil leakage and slip of the UPPER-1 porcelain unit. For the limit state of oil leakage, the *fragility* peak accelerations of Bushing-1, Bushing-2, and Bushing-3, were 0.51g, 1.18g, and 1.32g, respectively. For the limit state of slip of the UPPER-1 porcelain unit, the *fragility* peak accelerations of Bushing-1, Bushing-2, and Bushing-3, were 0.69g, 1.18g, and 1.32g, respectively.

5.2 Conclusions and Recommendations

5.2.1 Seismic Response of 550 kV Transformer Bushings

The modified 550 kV bushing (Bushing-3) did not qualify to the Moderate Level per IEEE 693-1997 (IEEE, 1998).

Bushing-1 and Bushing-2 were built for the purpose of fragility testing. Two limiting states of response were identified for fragility testing of these bushings: oil leakage and slip of the UPPER-1 porcelain unit. Bushing-2, a modified version of Bushing-1, sustained peak accelerations approximately twice those of Bushing-1, indicating that the modifications proposed and implemented by ABB were most effective.

5.2.2 Recommendations for Future Study

Procedures for Seismic Qualification

The 550-kV bushings were installed in a *rigid* mounting frame without electrical connections and upper-tip-mounted terminals for earthquake testing. Such a configuration does not likely adequately represent the field installation and loading environment and the results of IEEE qualification must be viewed with caution.

For qualification of equipment attached to a foundation, IEEE 693-1997 specifies a response spectrum for earthquake-simulator testing. The amplitude of the input motion for qualification of bushings is doubled to account for flexibility and ground-motion amplification in the transformer or support equipment. It is not known whether the IEEE 693-1997 assumptions are reasonable, conservative, or non-conservative. Numerical (finite element) studies of transformer bushings and other turret structures should be undertaken to review the current specifications for equipment qualification. At a minimum, such studies should identify (a) the stiffness characteristics of typical bushing support structures, (b) the damping effects of the oil contained in the support structure, if any, (c) the amplification of earthquake shaking effects, if any, through the support structure to the base of a bushing, and d) the importance of rotational input to a bushing resulting from flexibility in the upper plate of the transformer to which bushings are attached. Answers to these questions will provide valuable guidance to those tasked with revising the IEEE 693-1997 *Recommended Practices for Seismic Design of Substations*.

Development of Fragility Curves for Substation Equipment

Currently adopted procedures for reporting fragility data for substation equipment such as transformer bushings are neither appropriate nor conservative. Fragility data presented in the form of peak ground (input) acceleration are of limited value because peak input acceleration is a poor descriptor of damage. Fragility data based on spectral acceleration at the frequency of the bushing provides an improved estimate of damage but cannot account for substructure flexibility and damping, both of which will profoundly affect bushing response. Mean spectral acceleration over a range of frequencies provides a means by which to account for substructure flexibility. Mean-minus-one-standard-deviation spectral acceleration *fragility* data over a range of frequencies could account for variations in spectral acceleration over a frequency range.

The fragility data presented in Chapter 4 were widely scattered. Improved, rational procedures are needed to analyze and interpret fragility test data. Such procedures must both better reflect the field installation of equipment and account for substructure flexibility, installation of terminals (for bushings), and the effects of interconnected equipment.

Interconnected Equipment

Although IEEE 693-1997 acknowledges that physical (electrical) connections between substation equipment may detrimentally affect the seismic response of individual pieces of equipment, the testing procedures described in IEEE 693-1997 do not account for the important effects of such connectivity. These physical connections can vary widely in flexibility and strength. There is substantial evidence from past earthquakes that such electrical connections may have precipitated

bushing failures because of dynamic interaction between the interconnected equipment. Analytical studies are under way to identify the important parameters affecting dynamic interaction between interconnected equipment. An experimental earthquake-simulator-testing program should be developed to investigate both the characteristics of standard interconnections and strategies to mitigate the effects of dynamic interaction.

Mathematical modeling of porcelain transformer bushings

Data on the mechanical characteristics of gaskets are needed if accurate mathematical models of bushings are to be developed. Nonlinear springs should be developed to model gaskets, and the constraint to relative lateral movement of the aluminum core and the perimeter porcelain units offered by the oil inside the bushing must be studied. Models of porcelain bushings that would be suitable for rigorous vulnerability studies could be developed with such information.

REFERENCES

Abrahamson, N. 1996. Nonstationary response-spectrum matching. Unpublished papers.

EERI. 1995. Northridge reconnaissance report. *Earthquake Spectra*, Supplement C. Oakland, Calif.: Earthquake Engineering Research Institute.

IEEE. 1998. *IEEE Std 693-1997, Recommended practices for seismic design of substations*. Piscataway, N.J.: IEEE Standards Department.

Gilani, A. S., Chavez, J. W., Fenves, G. L., and Whittaker, A. S. 1998. *Seismic evaluation of 196 kV porcelain transformer bushings*, PEER 98/02 Berkeley, Calif., Pacific Earthquake Engineering Research Center, University of California.

Lilhanand, K. and Tseng, W.S. 1988. Development and application of realistic earthquake time histories compatible with multiple-damping design spectra. *Proceedings of Ninth World Conference on Earthquake Engineering, Tokyo, Japan.*

Mathworks. 1999. *The language of technical computing*. Natick, Mass.: The Mathworks, Inc.

Shinozuka, M., ed. 1995. *The Hanshin-Awaji earthquake of January 17, 1995: Performance of lifelines*. Technical Report NCEER-95-0015 Buffalo, N.Y.: National Center for Earthquake Engineering Research, State University of New York.

APPENDIX A

IEEE PRACTICE FOR EARTHQUAKE TESTING OF TRANSFORMER BUSHINGS

A.1 Introduction

The document IEEE 693-1997 (IEEE 1998) entitled “Recommended Practices for Seismic Design of Substations” is used in the United States for the seismic qualification and fragility testing of electrical equipment such as transformer bushings. This recommended practice provides qualification requirements for substation equipment and supports manufactured from steel, aluminum, porcelain, and composites. Procedures for equipment qualification using analytical studies (static analysis, static coefficient analysis, and response-spectrum analysis) and experimental methods (response-history testing, sine-beat testing, and static pull testing) are described in the practice. The objective of the document is “... to secure equipment such that it performs acceptably under reasonably anticipated strong ground motion.”

IEEE 693-1997 identifies eleven methods for experimental testing. The most rigorous method is earthquake-response analysis using earthquake ground motion records, the spectral ordinates of which equal or exceed those of a Required Response Spectrum (RRS). Categories of earthquake simulator testing include (a) single-axis, (b) biaxial (i.e., horizontal and vertical), (c) multiaxis, and (d) triaxial.

Section 9 of IEEE 693-1997 describes seismic performance criteria for electrical substation equipment. Information on three seismic qualification levels (Low, Moderate, and High), Performance Levels, the Required Response Spectrum (RRS), the relation between PL and RRS, and acceptance criteria are provided.

The studies described in the body of this report employed triaxial earthquake simulator testing for the qualification and fragility testing of the 550 kV bushings. IEEE 693-1997 writes text on six key topics related to the seismic qualification of transformer bushings:

- Performance level and performance factor
- Performance level qualification
- Support frame and mounting configuration
- Testing procedures
- Instrumentation
- Acceptance criteria

Each of these topics are elaborated upon in the following sections. For fragility testing, the amplitude of the seismic excitation is increased in small increments to determine the level of shaking that causes damage to the bushing, thereby establishing a point on a fragility curve.

A.2 Performance Level and Performance Factor

A Performance Level (PL) for substation equipment is represented in IEEE 693-1997 by a response spectrum. The shape of this spectrum represents a broadband response that envelopes earthquake effects in different areas considering site conditions that range from soft soil to rock. Three values of equivalent viscous damping are specified: 2 percent, 5 percent, and 10 percent. IEEE 693-1997 states that very soft sites and hill sites might not be adequately covered by the PL shapes.

Three seismic performance levels are identified in IEEE 693-1997: High, Moderate, and Low. In California, the relevant performance levels are High and Moderate. Equipment that is shown to perform acceptably in ground shaking consistent with the High Seismic Performance Level (see Figure A-1) is said to be seismically qualified to the High Level. Equipment that is shown to perform acceptably in ground shaking consistent with the Moderate Seismic Performance Level (see Figure A-2) is said to be seismically qualified to the Moderate Level.

IEEE 693-1997 states that it is often impractical or not cost effective to test to the High or Moderate PL because (a) laboratory testing equipment might be unable to attain the necessary high accelerations, and/or (b) damage to ductile components at the PL, although acceptable in terms of component qualification, would result in the component being discarded following testing. For these reasons, equipment may be tested using accelerations that are one-half of the PL. The reduced level of shaking is called the Required Response Spectrum (RRS). The ratio of PL to RRS, termed the performance factor in IEEE 693-1997, is equal to 2. The High and Moderate RRSs are shown in Figures A-3 and A-4, respectively. The shapes of the RRS and the PL are identical, but the ordinates of the RRS are one-half of the PL.

Equipment tested or analyzed using the RRS is expected to have acceptable performance at the PL. This assumption is checked by measuring the stresses obtained from testing at the RRS, and a) comparing the stresses to 50 percent (equal to the inverse of the performance factor) of the ultimate strength of the porcelain (assumed to be brittle) or cast aluminum components, and b) using a lower factor of safety against yield combined with an allowance for ductility of steel and other ductile materials.

A.3 Performance Level Qualification

Procedures for selecting the appropriate seismic qualification level for a site are presented in IEEE 693-1997. Qualification levels are directly related to site-specific peak acceleration values calculated using a 2-percent probability of exceedance in 50 years. If the peak ground acceleration is less than 0.1g, the site is classified as Low. If the peak ground acceleration exceeds 0.5g, the site is classified as High. If the peak ground acceleration ranges in value between 0.1g and 0.5g, the site is classified as Moderate. Sites in California are classified as either Moderate or High.

A.4 Support Frame and Mounting Configuration

IEEE 693-1997 writes that bushings 161 kV and larger must be qualified using earthquake-simulator testing. Recognizing that it is impractical to test bushings mounted on a transformer, IEEE requires bushings to be mounted on a rigid stand during testing. To account for the amplification

of earthquake motion due to the influence of the transformer body and local flexibility of the transformer near the bushing mount, the input motion as measured at the bushing flange shall match a spectrum with ordinates twice that of the Required Response Spectrum. The resulting spectra, termed the Test Response Spectra (TRS), for Moderate Level qualification are shown in Figure A-5.

A transformer bushing must be tested at no less than its in-service slope, which is defined as the slope angle measured from the vertical. IEEE 693-1997 recommends that a bushing be tested at 20 degrees measured from the vertical. If so tested, a bushing is assumed to be qualified for use on all transformers with angles from vertical to 20 degrees. (A bushing installed at an angle greater than 20 degrees must be tested at its in-service angle.)

A.5 Testing Procedures for Transformer Bushings

Three types of earthquake-simulator testing are identified in IEEE 693-1997 for the seismic qualification of transformer bushings: (a) earthquake ground motions, (b) resonant frequency search, and (c) sine-beat testing. Earthquake ground motion tests (termed *time-history shake table tests* in IEEE 693-1997) and resonant frequency tests are mandatory; additional information on these two types of tests follow.

A.5.1 Resonant search tests

Sine-sweep or broadband white noise tests are used to establish the dynamic characteristics (natural frequencies and damping ratios) of a bushing. These so-called *resonant search* tests are undertaken using uni-directional excitation along each principal axis of the earthquake simulator platform. If broadband white noise tests are performed, the amplitude of the white noise must not be less than 0.25g.

If sine-sweep tests are used, IEEE 693-1997 specifies that the resonant search be conducted at a rate not exceeding one octave per minute in the range for which the equipment has resonant frequencies, but at least at 1 Hz; frequency searching above 33 Hz is not required. Modal damping is calculated using the half-power bandwidth method.

A.5.2 Earthquake ground motion tests

Triaxial earthquake simulator testing is mandated for the seismic qualification of 161 kV and above bushings. The Test Response Spectrum (TRS) for each horizontal earthquake motion must match or exceed the target spectrum. The TRS for the vertical earthquake motion shall be no less than 80 percent of target spectrum. Earthquake motions can be established using either synthetic or recorded histories. IEEE 693-1997 recommends that 2-percent damping be used for spectral matching and requires at least 20 seconds of strong motion shaking be present in each earthquake record.

A.6 Instrumentation of Transformer Bushings

IEEE 693-1997 states that porcelain bushings must be instrumented to record the following response quantities:

1. maximum vertical and horizontal accelerations at the top of the bushing, at the bushing flange, and at the top of the earthquake-simulator platform

2. maximum displacement of the top of the bushing relative to the flange

3. maximum porcelain stresses at the base of the bushing near the flange

A.7 Acceptance Criteria for Transformer Bushings

IEEE 693-1997 writes that a bushing is considered to have passed the qualification tests if all the criteria tabulated below related to general performance, allowable stresses, and leakage are met. The data obtained from testing using ground motions compatible with the Test Response Spectrum (see Figure A-5) are used to assess general performance and allowable stresses. Oil leakage is checked for a higher level of earthquake shaking.

General Performance	No evidence of damage such as broken, shifted, or dislodged insulators. No visible leakage of oil or broken support flanges.
Allowable Stresses	The stresses in components are below the limiting values. (See Section A.2. For example, the stresses in the porcelain components associated with earthquake shaking characterized by the spectrum presented in Figure A-5 must be less than 50 percent of the ultimate value.)
Leakage	Bushings qualified by earthquake simulator testing shall have a minimum factor of safety of two against gasket leaks for loads imposed during application of the Test Response Spectrum. IEEE 693-1997 states that an acceptable method to demonstrate this factor of safety is to have no leaks after shaking characterized by twice the Test Response Spectrum. (Such shaking corresponds to a Performance Factor equal to 1.0.)

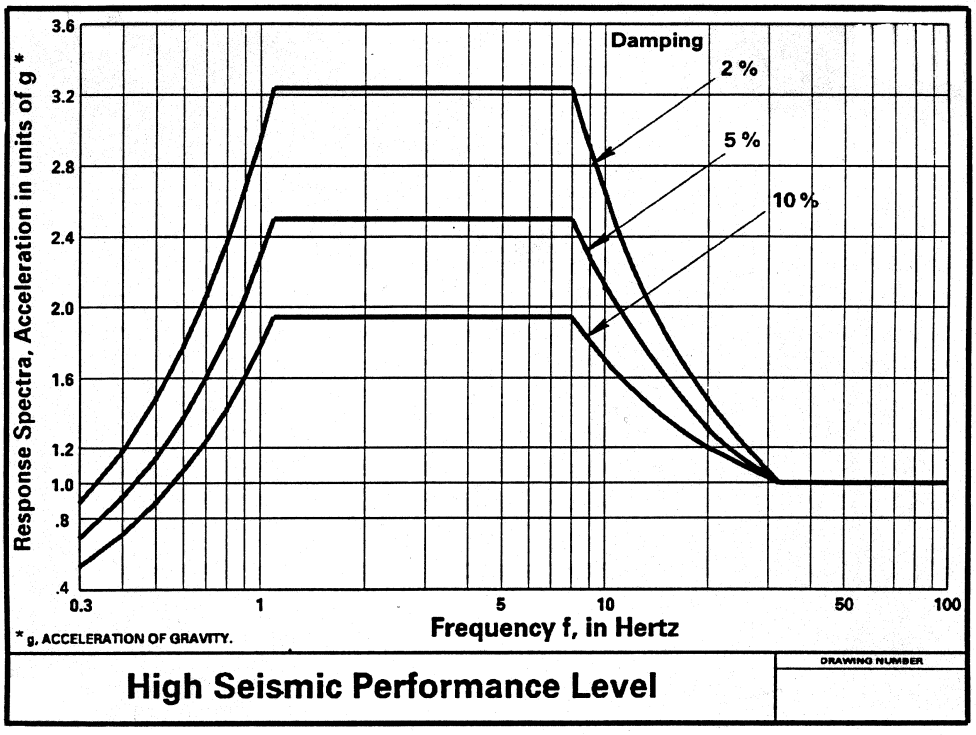

Figure A-1 Spectra for High Seismic Performance Level (IEEE, 1998)

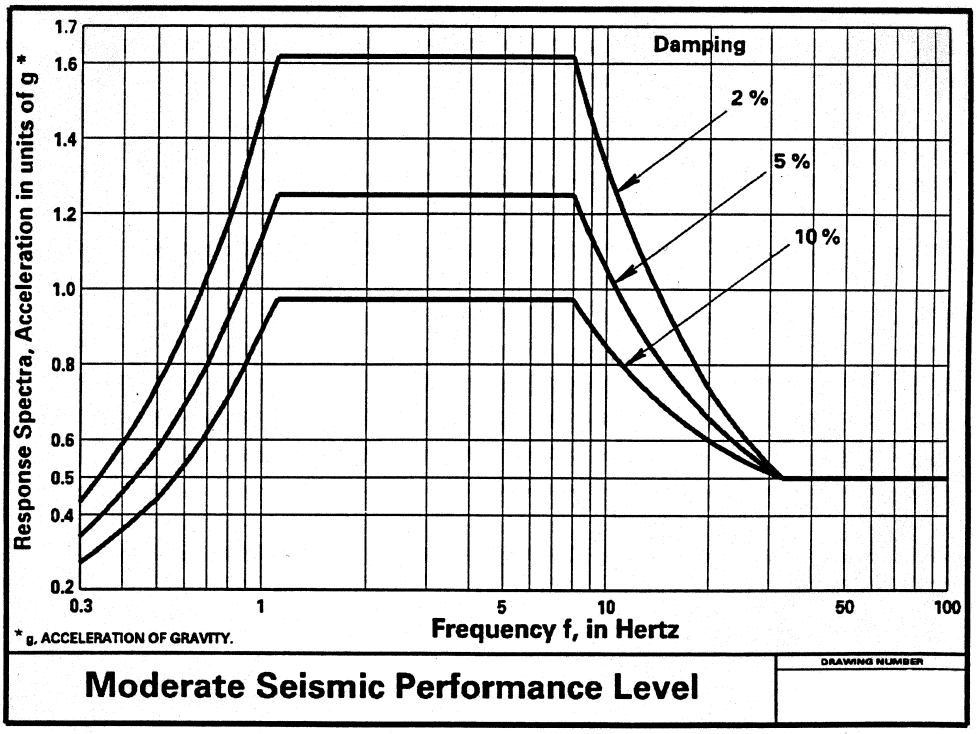

Figure A-2 Spectra for Moderate Seismic Performance Level (IEEE, 1998)

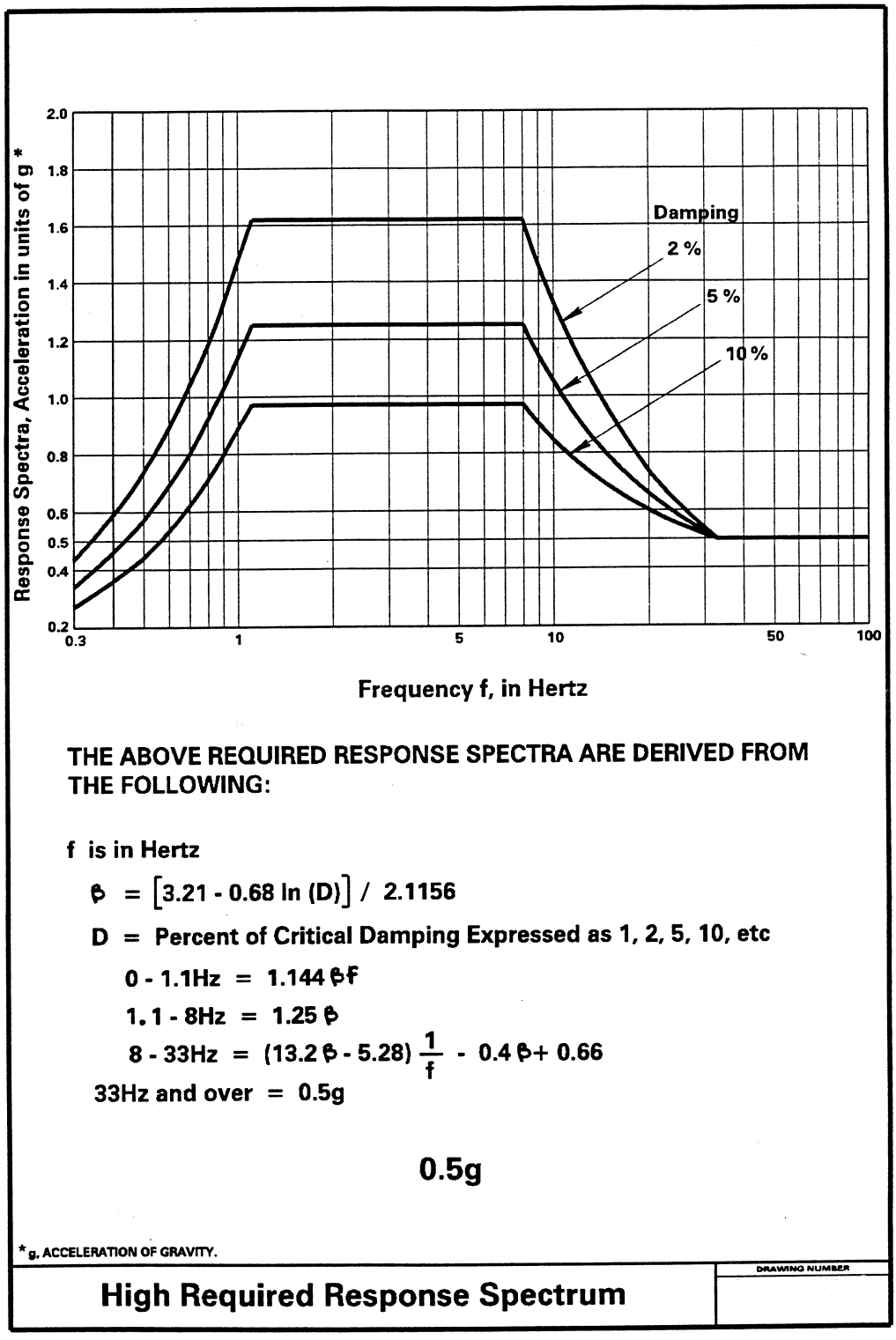

Figure A-3 Spectra for High Required Response Spectrum (IEEE, 1998)

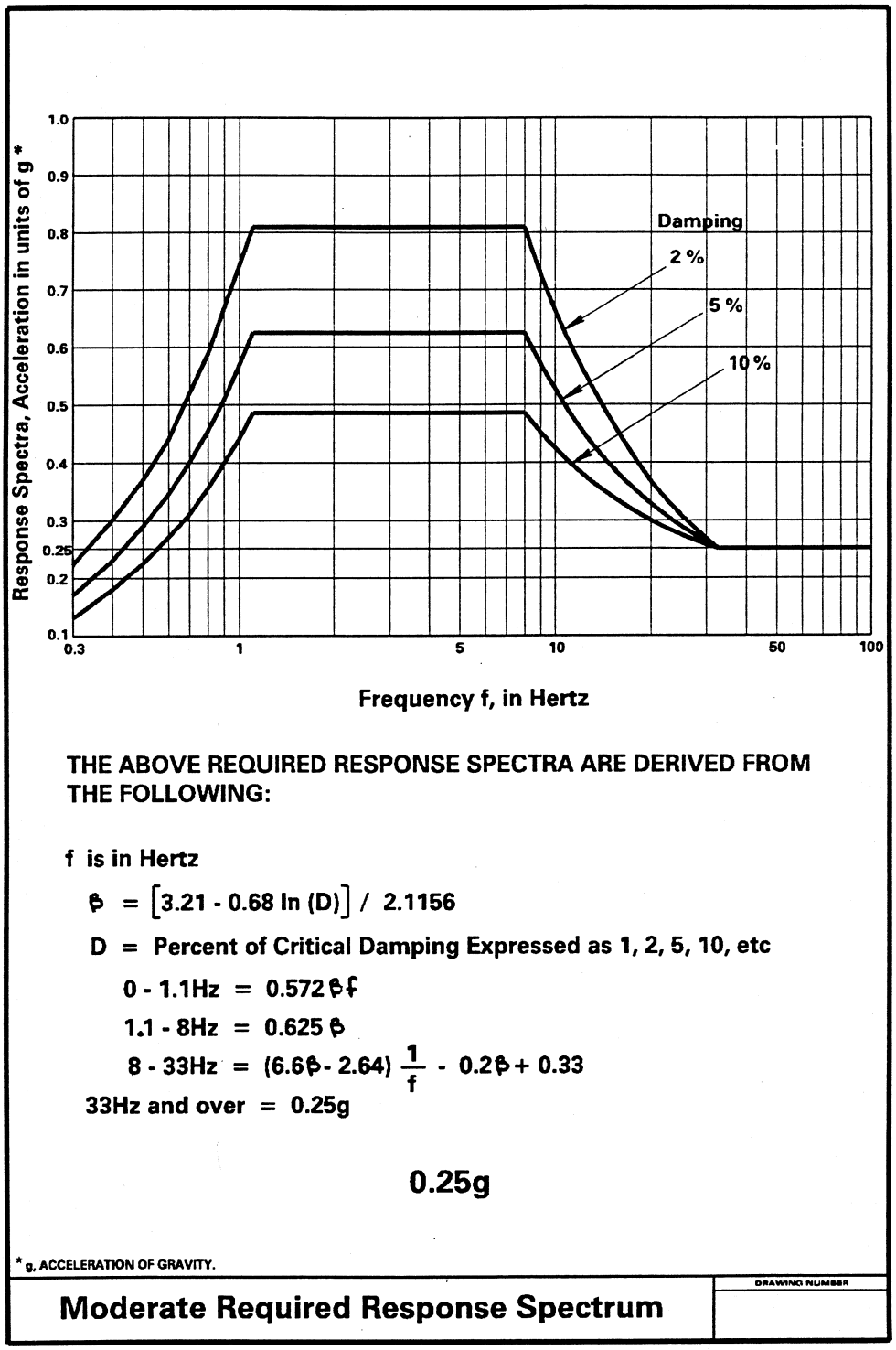

Figure A-4 Spectra for Moderate Required Response Spectrum (IEEE, 1998)

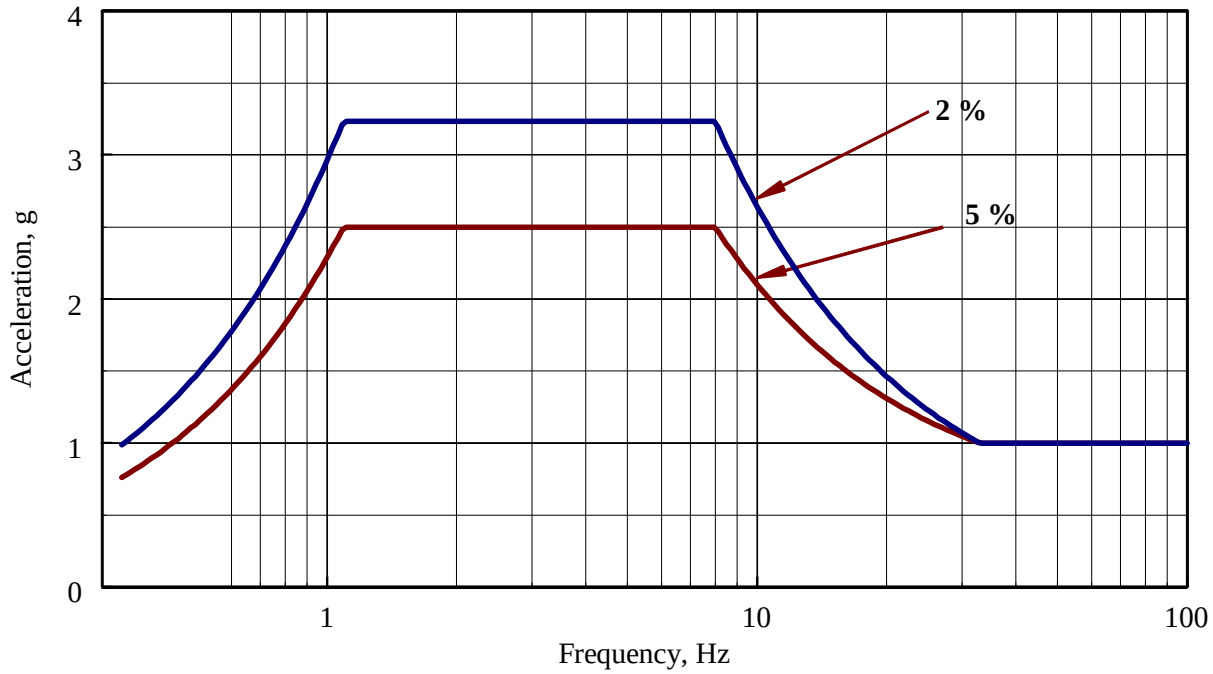

Figure A-5 Test Response Spectra for Moderate Level qualification of a transformer-mounted bushing

PEER REPORTS

PEER reports are available from the National Information Service for Earthquake Engineering (NISEE). To order PEER reports, please contact the Pacific Earthquake Engineering Research Center, 1301 South 46th Street, Richmond, California 94804-4698. Tel.: (510) 231-9468; Fax: (510) 231-9461.

PEER 2001/09 *Ground Motion Evaluation Procedures for Performance-Based Design.* Jonathan P. Stewart, Shyh-Jeng Chiou, Jonathan D. Bray, Robert W. Graves, Paul G. Somerville, and Norman A. Abrahamson. September 2001. $26.00

PEER 2001/07 *The Rocking Spectrum and the Shortcomings of Design Guidelines.* Nicos Makris and Dimitrios Konstantinidis. August 2001. $15.00

PEER 2001/06 *Development of an Electrical Substation Equipment Performance Database for Evaluation of Equipment Fragilities*. Thalia Agnanos. April 1999. $15.00

PEER 2001/05 *Stiffness Analysis of Fiber-Reinforced Elastomeric Isolators.* Hsiang-Chuan Tsai and James M. Kelly. May 2001. $20.00

PEER 2001/04 *Organizational and Societal Considerations for Performance-Based Earthquake Engineering.* Peter J. May. April 2001. $15.00

PEER 2001/03 *A Modal Pushover Analysis Procedure to Estimate Seismic Demands for Buildings: Theory and Preliminary Evaluation.* Anil K. Chopra and Rakesh K. Goel. January 2001. $15.00

PEER 2001/02 *Seismic Response Analysis of Highway Overcrossings Including Soil-Structure Interaction.* Jian Zhang and Nicos Makris. March 2001. $20.00

PEER 2001/01 *Experimental Study of Large Seismic Steel Beam-to-Column Connections.* Egor P. Popov and Shakhzod M. Takhirov. November 2000. $15.00

PEER 2000/10 *The Second U.S.-Japan Workshop on Performance-Based Earthquake Engineering Methodology for Reinforced Concrete Building Structures.* March 2000. $39.00

PEER 2000/09 *Structural Engineering Reconnaissance of the August 17, 1999 Earthquake: Kocaeli (Izmit), Turkey.* Halil Sezen, Kenneth J. Elwood, Andrew S. Whittaker, Khalid Mosalam, John J. Wallace, and John F. Stanton. December 2000. $20.00

PEER 2000/08 *Behavior of Reinforced Concrete Bridge Columns Having Varying Aspect Ratios and Varying Lengths of Confinement.* Anthony J. Calderone, Dawn E. Lehman, and Jack P. Moehle. January 2001. $20.00

PEER 2000/07 *Cover-Plate and Flange-Plate Reinforced Steel Moment-Resisting Connections.* Taejin Kim, Andrew S. Whittaker, Amir S. Gilani, Vitelmo V. Bertero, and Shakhzod M. Takhirov. September 2000. $33.00

PEER 2000/06 *Seismic Evaluation and Analysis of 230-kV Disconnect Switches.* Amir S. J. Gilani, Andrew S. Whittaker, Gregory L. Fenves, Chun-Hao Chen, Henry Ho, and Eric Fujisaki. July 2000. $26.00

PEER 2000/05 *Performance-Based Evaluation of Exterior Reinforced Concrete Building Joints for Seismic Excitation.* Chandra Clyde, Chris P. Pantelides, and Lawrence D. Reaveley. July 2000. $15.00

PEER 2000/04 *An Evaluation of Seismic Energy Demand: An Attenuation Approach.* Chung-Che Chou and Chia-Ming Uang. July 1999. $20.00

PEER 2000/03 *Framing Earthquake Retrofitting Decisions: The Case of Hillside Homes in Los Angeles.* Detlof von Winterfeldt, Nels Roselund, and Alicia Kitsuse. March 2000. $13.00

PEER 2000/02 *U.S.-Japan Workshop on the Effects of Near-Field Earthquake Shaking.* Andrew Whittaker, ed. July 2000. $20.00

PEER 2000/01 *Further Studies on Seismic Interaction in Interconnected Electrical Substation Equipment.* Armen Der Kiureghian, Kee-Jeung Hong, and Jerome L. Sackman. November 1999. $20.00

PEER 1999/14 *Seismic Evaluation and Retrofit of 230-kV Porcelain Transformer Bushings*. Amir S. Gilani, Andrew S. Whittaker, Gregory L. Fenves, and Eric Fujisaki. December 1999. $26.00

PEER 1999/12 *Rehabilitation of Nonductile RC Frame Building Using Encasement Plates and Energy-Dissipating Devices.* Mehrdad Sasani, Vitelmo V. Bertero, James C. Anderson. December 1999. $26.00

PEER 1999/11 *Performance Evaluation Database for Concrete Bridge Components and Systems under Simulated Seismic Loads.* Yael D. Hose and Frieder Seible. November 1999. $20.00

PEER 1999/10 *U.S.-Japan Workshop on Performance-Based Earthquake Engineering Methodology for Reinforced Concrete Building Structures.* December 1999. $33.00

PEER 1999/09 *Performance Improvement of Long Period Building Structures Subjected to Severe Pulse-Type Ground Motions*. James C. Anderson, Vitelmo V. Bertero, and Raul Bertero. October 1999. $26.00

PEER 1999/08 *Envelopes for Seismic Response Vectors.* Charles Menun and Armen Der Kiureghian. July 1999. $26.00

PEER 1999/07 *Documentation of Strengths and Weaknesses of Current Computer Analysis Methods for Seismic Performance of Reinforced Concrete Members.* William F. Cofer. November 1999. $15.00

PEER 1999/06 *Rocking Response and Overturning of Anchored Equipment under Seismic Excitations.* Nicos Makris and Jian Zhang. November 1999. $15.00

PEER 1999/05 *Seismic Evaluation of 550 kV Porcelain Transformer Bushings.* Amir S. Gilani, Andrew S. Whittaker, Gregory L. Fenves, and Eric Fujisaki. October 1999. $15.00

PEER 1999/04 *Adoption and Enforcement of Earthquake Risk-Reduction Measures.* Peter J. May, Raymond J. Burby, T. Jens Feeley, and Robert Wood. $15.00

PEER 1999/03 *Task 3 Characterization of Site Response General Site Categories*. Adrian Rodriguez-Marek, Jonathan D. Bray, and Norman Abrahamson. February 1999. $20.00

PEER 1999/02 *Capacity-Demand-Diagram Methods for Estimating Seismic Deformation of Inelastic Structures: SDF Systems*. Anil K. Chopra and Rakesh Goel. April 1999. $15.00

PEER 1999/01 *Interaction in Interconnected Electrical Substation Equipment Subjected to Earthquake Ground Motions.* Armen Der Kiureghian, Jerome L. Sackman, and Kee-Jeung Hong. February 1999. $20.00

PEER 1998/08 *Behavior and Failure Analysis of a Multiple-Frame Highway Bridge in the 1994 Northridge Earthquake.* Gregory L. Fenves and Michael Ellery. December 1998. $20.00

PEER 1998/07 *Empirical Evaluation of Inertial Soil-Structure Interaction Effects.* Jonathan P. Stewart, Raymond B. Seed, and Gregory L. Fenves. November 1998. $26.00

PEER 1998/06 *Effect of Damping Mechanisms on the Response of Seismic Isolated Structures.* Nicos Makris and Shih-Po Chang. November 1998. $15.00

PEER 1998/05 *Rocking Response and Overturning of Equipment under Horizontal Pulse-Type Motions.* Nicos Makris and Yiannis Roussos. October 1998. $15.00

PEER 1998/04 *Pacific Earthquake Engineering Research Invitational Workshop Proceedings, May 14–15, 1998: Defining the Links between Planning, Policy Analysis, Economics and Earthquake Engineering.* Mary Comerio and Peter Gordon. September 1998. $15.00

PEER 1998/03 *Repair/Upgrade Procedures for Welded Beam to Column Connections.* James C. Anderson and Xiaojing Duan. May 1998. $33.00

PEER 1998/02 *Seismic Evaluation of 196 kV Porcelain Transformer Bushings.* Amir S. Gilani, Juan W. Chavez, Gregory L. Fenves, and Andrew S. Whittaker. May 1998. $20.00

PEER 1998/01 *Seismic Performance of Well-Confined Concrete Bridge Columns.* Dawn E. Lehman and Jack P. Moehle. December 2000. $33.00